ETABLISSEMENT DE SOUTENANCE

ECOLE DOCTORALE 352 - Physique et sciences de la matière

Inserm U1067 / CNRS UMR 7333

Laboratoire Adhésion et Inflammation

Thèse présentée pour obtenir le grade universitaire de docteur

Discipline : Physique et sciences de la matière
Spécialité : Biophysique

Alexander HORNUNG

Two-dimensional migration of human effector T-cells : Integrin-dependent motility studies under shear stress

Soutenue le 29/09/2016 devant le jury :

Sylvain GABRIELE	Mechanobiology and Soft Matter Group (Université de Mons)
Jean-Paul RIEU	ILM (Université Claude Bernard Lyon 1)
Giovanni CAPPELLO	Laboratoire Interdisciplinaire de Physique (Université Grenoble Alpes)
Olivier THEODOLY	LAI (Aix-Marseille université)
Marie-Pierre VALIGNAT	LAI (Aix-Marseille université)

I always keep my mind open. For me, a mind has to work like like a parachute, works only if it's open.

-Rickson Gracie

(I hope you have read the quote with a brazilian accent)

Acknowledgements

First of all I want to thank my thesis supervisor Marie-Pierre Valignat for guiding, motivating, teaching and helping me through my thesis.
Olivier Théodoly for knowing everything everytime in group meetings and therefore being able to answer any questions in group meetings or surprise attacked with questions.
Pierre Bongrand, for challenging questions and his ability to always provide input.
Pierre-Henri Puech the only person in the world mastering AFM, statistics, conversation and grappling.
Philippe Robert who shows human greatness by proof-reading a physicists approach to immunology and awesome sense of humour.
Laurent Limozin and Cyrille Mionnet for help, advice and being nice human beings.
Thomas Sbarrato, the only person coming from a country smaller than mine, who might be one of the most friendly and helpful human beings I have ever met. Laurene Aoun, Paulin Nègre and Xuan Luo for help, support and input.
Anaïs Sadoun for being an exceptional human being in and out of the lab, giving me the most support(ch) without even knowing it.
Kamel Khelloufi who made me feel very welcome in France and being a genuinely good human being, oida.
Cristina "lab fairy" Gonzalez. No matter how grumpy you come in the lab, Cristina can make you smile.
Everybody who once had a workplace in the PhD student's office especially (future) Doctor Wu. This is a velociraptor-free workplace!
Martine Pélicot and Adeline Querdray for laughter, cytometry and technical support.

So the co-workers are done...
All of this wouldn't have been possible without my loving family, especially my parents Renate and Andreas who supported me through all the years, as well as my grand parents to whom I dedicate this work.
Herbert and Jürgen, my Bandmates and constants over the last years.
All the wonderful people from all the walks of live I met here doing Brazilian Jiu Jitsu
Another special salute goes to the Orden der offenen Hosentürl who brought a piece

of Austria to Marseille and made me laugh a lot during office hours. Philippe Seil, my oldest friend, who even finishes his PhD at the same time like me, and Gert, Nina and Victor and the entire austrian crew!

To my grandparents

Abstract

Migration and homing of cells is fundamental to a wide variety of physiological procedures including the underlying mechanisms of immune responses as well as processes like tissue arrangement. Although the qualitative and phenomenological description of cellular migration in context of the adaptive immune system is already quite sophisticated in its holistic approach, some long known and basic procedures have not yet been investigated from a quantitative, bottom-up point of view.
One example for this is the migrational behavior of human effector T-cells in 2 dimensions. While their behavior in vivo is already long known and described in a qualitative way, a quantitative, modular in-vitro approach offers insight to various, not yet examined relations between the adhesion molecules on the substrate and cellular integrins, which are one of the key players for understanding T-cell function. It is already known that the interactions between the integrins LFA-1 (αLβ1) and VLA-4 (α1β4) with their corresponding adhesion molecules ICAM-1 and VCAM-1 are the main responsibles for two dimensional effector T-cell migration. In their responsibility for organizing immune cell motility, those two proteins were the main targets of examination in this thesis. Understanding integrin function and henceforth the basic mechanisms of lymphocyte migration opens the door to understanding various pathologies related to a malfunctioning immune response and inflammatory diseases.
Nearly all of these previous findings were made by examining T-cells on living tissue whose composition and density of adhesion molecules can neither be determined nor tuned in a precise manner. We have recreated artificial substrates which emulate these conditions to link and examine physical cellular properties like speed, forward migrational index etc. to a direct response to the substrate composition and to concatenate specific movement patterns with specific integrin-adhesion molecule interactions. Going a step further we also modulated and re-analyzed the conformational state of the integrins to alter their affinity which changes the properties described above.

Resumé

La migration et l'adressage ou "homing" sont fondamentales dans de nombreux procédés physiologiques tels que la réponse immunitaire ou le réarrangement tissulaire. Bien que la description qualitative et phénoménologique de la migration cellulaire soient décrites de façon minutieuse dans son approche holistique, des mécanismes de base et connus depuis longtemps n'ont pas encore été explorés quantitativement avec une approche "bottom-up".
Un de ces exemples est le comportement migratoire en deux dimensions des lymphocytes T effecteurs humains. Alors que leur comportement in vivo est déjà connu depuis longtemps et décrit qualitativement, une approche quantitative in vitro offre de nombreuses perspectives, notamment au niveau des interactions entre les molécules d'adhésion d'un substrat et les intégrines présentes à la surface de ces cellules. Ces dernières sont primordiales pour la compréhension du fonctionnement du lymphocyte T. Les interactions des intégrines LFA-1 (αLβ1) et VLA-4 (α1β4) avec leurs ligands respectifs ICAM-1 et VCAM-1 ont déjà été étudiées et sont les principales molécules impliquées dans la migration des lymphocytes T effecteurs en 2D. Du fait de leur importance dans l'organisation de la mobilité des cellules immunitaires, ces deux protéines sont les principaux objets d'étude de cette thèse. La caractérisation du fonctionnement des intégrines et donc des principes élémentaires de migration des lymphocytes ouvre la voie à une meilleure compréhension des maladies inflammatoires et de nombreuses pathologies liées à un dysfonctionnement de la réponse immunitaire. La majorité des travaux précédents ont été réalisés en observant les lymphocytes T dans des tissus vivants dont la composition et la densité des molécules d'adhésion ne peuvent ni être déterminées ni contrôlées de façon précise. Nous avons developpés des substrats artificiels permettant d'imiter et de contrôler ces caractéristiques adhésives afin d'examiner et de relier les propriétés physiques des cellules tels que la vitesse ou l'index de migration orientée, avec une réponse cellulaire donnée ainsi que d'associer un type de mouvement avec des interactions intégrines-ligands spécifiques. Pour aller plus loin, nous avons à nouveau analysé la conformation des intégrines puis l'avons modulé pour altérer leur affinité et changer les propriétés précédemment décrites.

Motivation

Cell motility is one of the most fundamental biological processes providing functions like tissue differentiation, gastrulation and cell trafficking as well as the key features for the human adaptive immune response like homing and defense against intruding pathogens. Especially the ability of T-lymphocytes to migrate to sites of inflammation towards all different types of tissues based on the interplay between biochemical and mechanical signaling is unique among human cells and underlines the importance of their complex motility apparatus relying on multiple stimuli like cytokines, shear stress and integrin-surface interactions.

A crucial part within the leukocyte adhesion cascade, which describes the guidance mechanisms of leukocytes from the blood flow to the pathogen, is the firm attachment of the immune cell to the inner wall of the blood vessel and the subsequent migration along its surface until crossing the endothelial cell barrier. These migrational steps are guided not only by the shear stress to which the cell is exposed to by the flow of blood, but also by chemokines and expression of adhesion molecules, the most important among them are ICAM-1 and VCAM-1 who are a part of the venule's extracellular matrix, and their integrin counterparts LFA-1 and VLA-4, expressed by the immune cell. These involved proteins are crucial not only in a mechanically anchoring sense, but they also play a part in an intracellular signaling process leading to a change in migrational direction, overall cell affinity and phenotype. Few is known about how all components shape the movement behaviour on a quantitative level, raising questions about hierarchy, affinity and density of the involved proteins. Besides enhancing the general knowledge of the mechanisms of T-cell migration, the role of ICAM-1 and VCAM-1 in diseases like vasculitis, artherosclerosis, lupus, etc., makes this study a promising endeavour. The approach taken in this thesis is to dissect and recompose the important adhesion molecules on a laminal flow chamber to link the cell's response to them to specific movement properties and answer the questions addressed above.

Contents

Chapter 1

Introduction

1.1 T-lymphocytes

1.1.1 Developement and maturation of T-lymphocytes

T-lymphocytes (T-cells) are cells of the adaptive immune system. After undergoing maturation including presentation of antigen as described in this chapter, they differentiate into one of different functional types of effector T-lymphocytes like cytotoxic T-cells, who kill infected cells or helper T-cells, who are responsible for additional signaling to increase the efficiency of killing pathogens by other cells. Regulatory T-cells suppress other lymphocyte activity and memory T-cells have the ability to transform to effector T-cells in case of a second infection with the same antigen. Their motility, which depends on the interplay of complex mechanisms of cytoskeleton-dependent movement, adhesion molecules, migrational cues and cytosolic messenging, is one of their key attributes, necessary to immunosurveillance and immune response. They have the ability to move, sustain themselves and enter any tissue in the body. They derive from hematopoietic stem cells in the bone marrow and migrate to the thymus where they mature. Upon encounter with a dendritic cell, which carries the corresponding antigen fragment that is able to bind with the lymphocytes specific T-cell receptor, it gets activated and proliferates. Eventually it exits the lymphatic tissue to enter the blood circulation. In case of infection it may exit the vascular system, migrate into inflamed tissue and fight infection.
The most distinctive feature of T-cells is the recognition of foreign antigen from self antigen. In tissues, if a cell is infected by an intracellular pathogen, major histocompatibility complex (MHC) molecules deliver peptides cut from pathogen proteins to the surface of the infected cell. Dendritic cells also capture and present pathogen peptides to the lymphocytes within the lymphatic system as part of T-cell activation. The molecular assembly of the lymphocyte responsible for scanning and recognizing foreign peptides is

called the T-cell receptor. In its function of antigen recognition, the TCR works together with other surface proteic assemblies like the CD3 complex to form the TCR-complex and, more specific, with either CD4 (helper T-cells) or CD8 (cytotoxic T-cells).

T-lymphocytes develop out of hematopoietic stem cells which are proliferating in the bone marrow and are multipotent, i.e. they are able to differentiate into several type of blood cells. As a first step, they become progenitors of T-cells which is the only part in their development that is happening in the bone marrow. Afterwards they migrate via the blood to the thymus (hence the name T(hymus-dependent)cell) where they undergo maturation and selection. The developing T-cell, also called thymocyte, undergoes several differentiation steps separated by checkpoints like principally rearrangement of T-cell receptor genes to produce a new variant, selection of cells producing a functional new (so-called "positive selection") and elimination of cells producing a self reactive new receptor (so-called "negative selection"). Selected newly formed T cells leave the thymus as "naïve T-cells" that will need activation prior to participate in forthcoming adaptive immune responses.

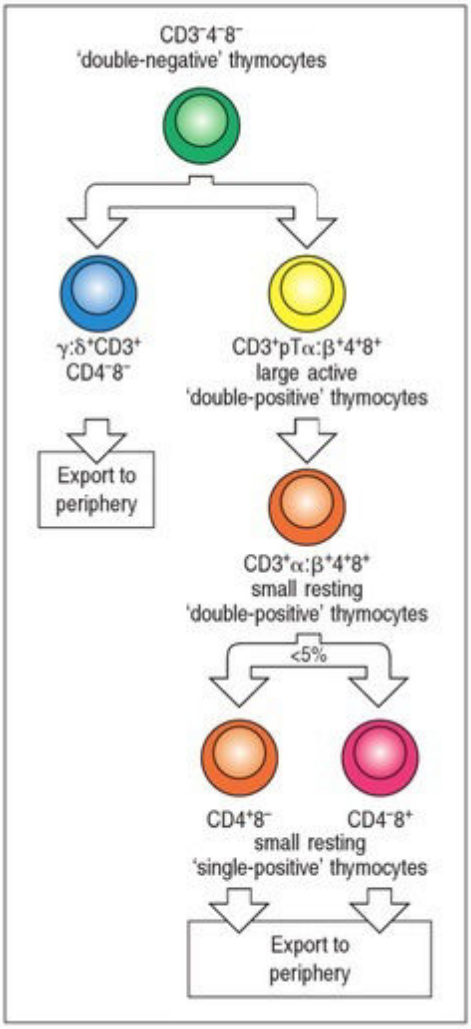

Figure 1.1: principal stages of thymocyte differentiation (*1*).

After arriving in the thymus, the progenitor cell receives a signal via the Notch1 receptor which activates the genes responsible for developing into a T-cell instead of a B-cell. The source of that signal is a network of epithelial cells called the thymic stroma. Differentiation happens through various stages where each stage includes modification of the status of T-cell receptor genes, but also of the expression of cell surface receptors,which are used as a marker of the current stage of thymocyte developement. This differentiation period can last up to one week, followed by a phase of proliferation. Interestingly (in a mouse model) only about 2% (around 1-2x10^6 out of 5x10^7) of the generated thymocytes leave the thymus per day to enter into the bloodstream. The remaining 98% die of apoptosis and get phagocytosed by macrophages. What looks inefficient at first glance is a consequence of an intensive testing period where the ongoing immune cells get reviewed

for their ability to fulfill their tasks. T-cells may express either $\alpha : \beta$ or $\gamma : \delta$ - TCR. We will focus on the more frequent $\alpha : \beta$-subset, as only these cells will be relevant for the following work and as both subsets developments in thymus are similar.
Thymocytes follow the developmental process that can be seen in figure 1.1. They initially lack surface proteins implied in TCR signaling, the so-called co-stimulatory molecules CD4 and CD8, which are present in mature lymphocytes. The cells of this subset are called 'double negative thymocytes' (the green cell type in figure 1.1). The first step of differentiation is the assembly of a pre-T-cell-receptor which is expressed on the cellular surface together with CD3, and formed of a newly recombined α- chain and an invariant pre-β chain. Once the pre-TCR starts to emerge, the cell induces proliferation and both CD4 and CD8 are expressed, while further recombination of the α-chain locus is stopped (the yellow cell type in figure 1.1). Thymocytes then cease to proliferate (orange in figure 1.1) and their β -chain locus rearranges, upon which a new TCR is expressed. If this new TCR is able to detect pMHC and transmit signals either through CD4 or CD8, the cell survives and keeps expressing the co-stimulatory molecule that participated in signaling, whereas non-reactive cells undergo apoptosis. This step is called 'positive selection' and ensures the production of functional TCR. Thymocytes are at this stage single-positive thymocytes (orange and pink cells in figure 1.1) and form a huge variety of T-cells, each able to bind one specific antigen (*1*). Thymocytes then undergo the so-called 'negative selection', where they are presented with self peptide-bearing HLA molecules. Cells that are able to activate in response to self undergo apoptosis, this step ensures that remaining thymocytes are not self-reactive. On the whole, thymocytes able to produce a functional but non self-reactive form 2% of the initial thymocyte, and may then join the blood stream.

1.1.2 Effector T-cells

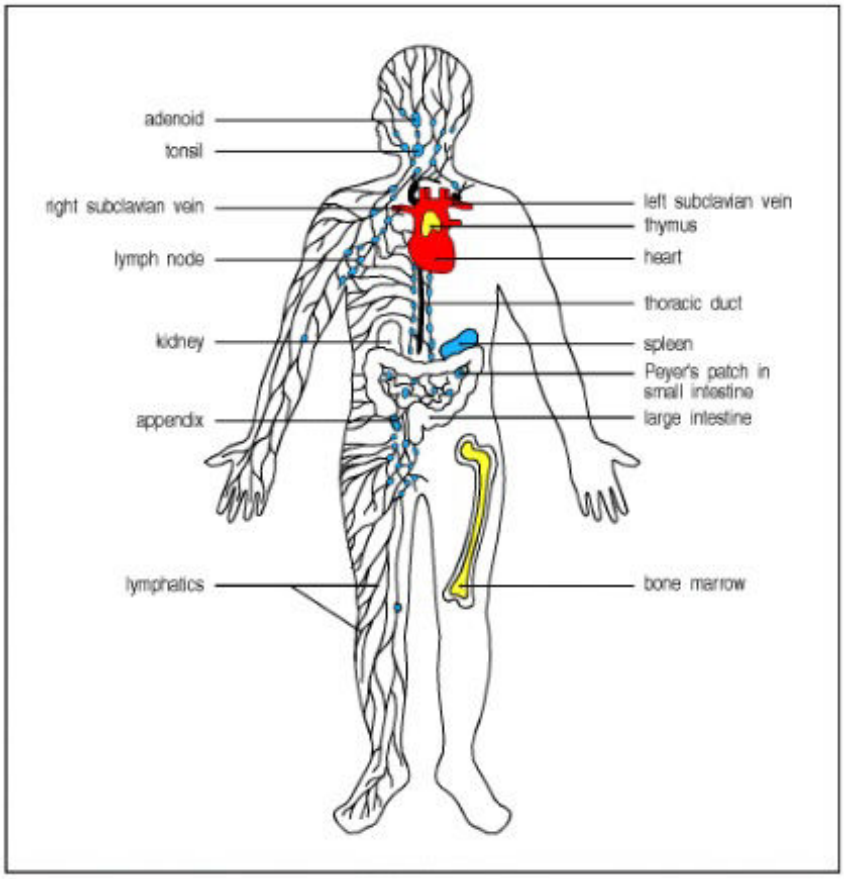

Figure 1.2: T-Lymphocytes are built in the bone marrow from stem cells and start to differentiate in the thymus(yellow), afterwards they migrate via the blood to the peripheral lymphoid organs (blue) (*1*).

Up to now, all the lymphocytes generated in the thymus are considered naive T-cells, meaning that although their development is already advanced and their TCR is tuned to a certain antigen, they have not yet been activated. For this, they would have to encounter their specific, fitting antigen presented by a 'professional' antigen presenting cell with proper accompanying signals. Starting where we left in 1.1.1, the naive cell exits the thymus and gets carried away by the blood stream until it reaches the peripheral lymphoid organs like the spleen, the lymph nodes and mucosal lymphoid tissues. Once they reach these organs, specialized blood vessels called high endothelial venules (HEV) secrete chemokines that signal the naive cells to attach and transmigrate out of the vessel into the lymphatic organs (fig. 1.3). These organs are highly differentiated, consisting of stromal tissue similar to the thymus which build up the structural framework of the organ and interact with the lymphocytes to give them survival signals and

sustain life. T-cells as well as B-cells develop in the lymph nodes although they are spatially separated and mature at different places called the paracortical area for T-cells where they encounter dendritic cells, and the primary lymphoid follicle for B-cells. If no infection occurs, non-activated cells enter the blood stream again and recirculate until they eventually meet their antigen in the next secondary immune organ or die, refraining from further development and proliferation. In case of an infection, local dendritic cells whose purpose is to capture pathogens and present their antigens on their cellular surface, detect pathogens or tissue damage and change their phenotype from a static one to an activated state that is mobile, highly endocytic and highly antigen-presenting. They capture pathogens, reach the tissue lymphatic vessels and are transported to the downstream lymph node, where the same chemokines that induce the homing for T-cells also attract activated dendritic cells to enter and meet the naive T-cells.

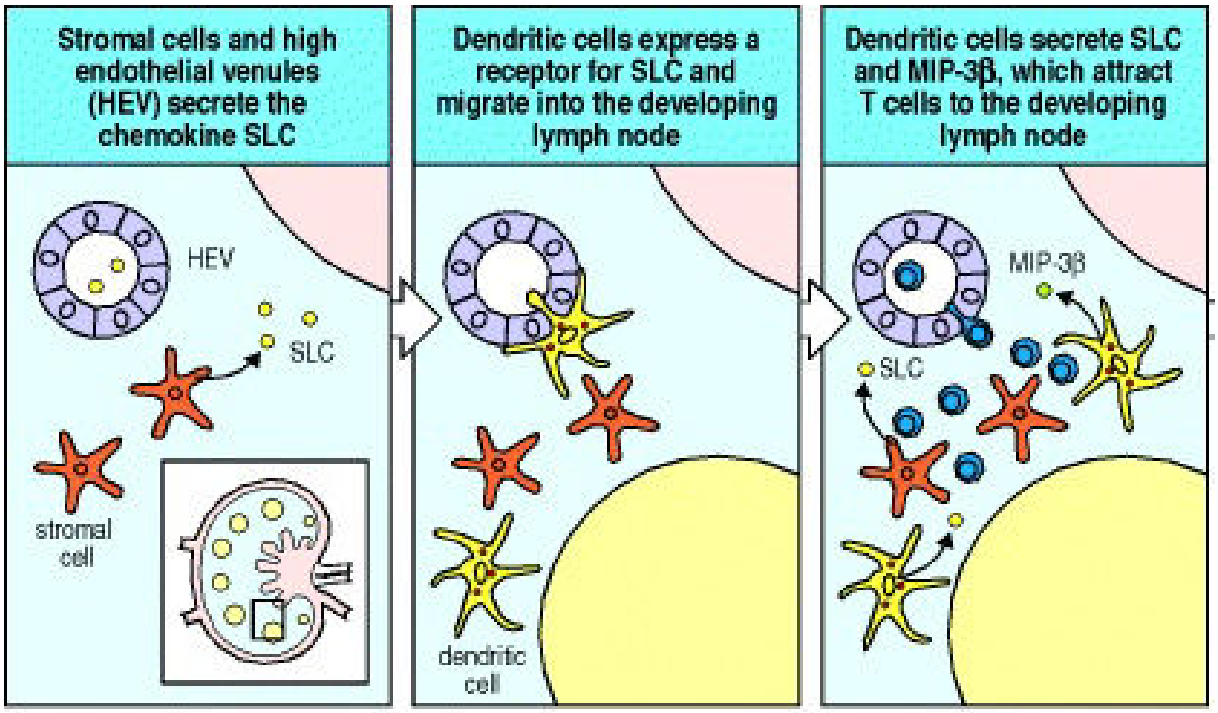

Figure 1.3: Processes leading to T-cll maturation in the lymph nodes are induced by chemokines (*1*).

As a matter of probability, only a few resident lymphocytes will be able to recognize presented pathogens and these low quantities would not be able to effectively eliminate the pathogen. If an activated dendritic cell presents its antigen to a naive T-cell whose T-cell receptor matches the pathogen, the final stages of transformation into an effector T-cell are initiated: Together with the initial contact of antigen and corresponding TCR, the dendrite delivers a 'danger' signal via so called co-stimulatory molecules on

its cellular surface. Both signals are necessary to induce T lymphocytes activation. If that second signal is not granted, cells would undergo clonal deletion or become inactive. The need for a 'danger' signal, produced by activated dendritic cells in response to tissue damage of typical pathogen patterns detection, permits to avoid T-lymphocyte activation in response to non-pathogenic non-self molecules. This avoids inflammation in response to common non-threatening environment molecules such as found in pollen or food. Eventually, the activated T-lymphocyte stops migrating and changes its phenotype by increases in cytoplasm and nucleus volume and starts synthesizing new proteins, then enters mitosis and is now called lymphoblast. After this phase of proliferation, every lymphoblast can create around 1000 daughter cells. This grants the effectivity of the adaptive immune system to first generate a sufficient amount of defensive cells who subsequently differentiate into effector T-cells of either cytotoxic T-cell class (characterized by expression of CD8 with the TCR) which destroy pathogen-infected cells, or helper cells (expressing CD4 with the TCR) which activate other cells of the immune system. This is how the adaptive immune system grants a dynamic, variable ever changing pool of possible responding cells without constantly maintaining a huge amount of different lymphocytes in number, sufficient for an immune response that would be at very high energetic and organizational costs. From this point on the recirculatory migration that is characteristic of naive T-cells stops: chemokine receptors and adhesion molecules expression change to allow entering inflamed tissues and avoid lymph nodes. T-cells (helper and cytotoxic) migrate into the blood to enter inflamed tissues while some helper-T-cells stay in the lymphoid tissues to activate B-cells.(*1*).

1.2 Integrins

The ability to migrate with rather high speed (depending on the environment from 10 to 30 μm/min) (*2*) is probably the most basic and crucial attribute of leukocytes and fundamental to provide immune response. As soon as the cell establishes contact with any substrate, either two or three dimensional, the actin polymerization of the cytoskeleton triggers the movement. When the cell is exposed to a dense three dimensional matrix, the sheer pushing forces of the cells might be responsible for advancement due to the confinement (*3*). In two dimensions however, T-cells undergo brownian motion without necessarily being adhesive just by sliding along the substrate.

Integrins are a family of transmembrane proteins expressed by all mammalian cells (except erythrocytes). They provide adhesion binding to extracellular matrix ligands or cell-surface ligands, therefore the cellular repertoire of integrins a cell can express, which act as receptors, determines the type of substrate (ligating adhesion molecules)

it can interact with. One of their main functions is to provide a clutch for the cellular driving forces to transmit friction to the surface (*3*, *4*) which makes them necessary for two-dimensional migration in general and especially for effector T-lymphocytes exposed to shear stress like in this work. Apart from the mechanical view as a force transduction clutch, integrins have more attributes like serving various signalling purposes: Outside-in, as well as inside-out like, for example, their ability to alter their affinity to their corresponding adhesion molecule (*5*), oftentimes differently over the cell-substrate interface, to alter their migrational attributes (*6*) and induce transmigration. The substrate-selective integrin repertoire mentioned above can also already be described as a form of signaling since it determines the pathways a cell can go for homing and trafficking.

A key attribute linking the signaling and the force transduction attributes of the integrins is the changeable affinity to the ligand. Low-, intermediate-, and high-affinity states exist, each corresponding to a structural and spatial change of the subunits as can be seen in figure 1.4.

1.2.1 LFA-1

Concerning the following work, leukocyte function-associated antigen-1 (LFA-1; (αLβ2 / CD18 CD11a) is the most important integrin. It is important in antigen-specific responses and is expressed in all leukocytes to mediate firm adhesion, homing and extravasation, and it contributes to the immunological synapse between the immune cell and the antigen presenting cell. Its ligands are expressed by the endothelium, which upregulates their expression after stimulation by cytokines (*7*, *8*) as well as on antigen-presenting cells(*9*). The corresponding ligand with the highest affinity to the I-domain of the αL subunit is intercellular adhesion molecule (ICAM)-1, although it also binds to ICAM-2,ICAM-3 and ICAM-5, and only this I-domain is involved in ligand binding, despite the big extracellular component of the integrin (*10*).

Outside-in signaling of LFA-1 includes polarization of the leukocyte after binding to ICAM-1 by rearrangements of the cytoskeleton (*11*)

The signalling procedures happening in the cytosol between the intracellular parts of the subunits are incomparably more complex, involving additional proteins like talin, kindlin, α-actinin and so forth who establish, or help to establish a bond between the cytoskeleton and the transmembrane protein. Inside-out signaling events include the activation of the integrin by a process of intracellular signaling pathways induced by other receptors. These events can happen on a timescale of $<$1s which enables the immune cell to react fast to changes in their immediate environment like cytokine concentration changes, or general environmental influence induced by antigen-presenting

cells and therefore induce changes in its migrational behaviour (*12*).

1.2.2 VLA-4

Besides LFA-1, the most important integrin regarding homing and motility along the vascular cell wall is the very late antigen 4 (VLA-4, $\alpha 4\beta 1$ / CD49d CD29), a homing receptor very similar to LFA-1, whose purpose is to bind to its corresponding ligand vascular cell adhesion molecule 1 (VCAM-1) to mediate adhesion, rolling and tight adhesion (*13*). The level of its expression is directly related to the development stage and purpose of T-cells. While naive lymphocytes are high in L-selectin to induce recirculation through the lymphatic system, effector T-cells, who patrol in the blood, express much lower levels. In case of inflammation, endothelial cells increase their expression of VCAM-1 (besides ICAM-1 and E-selectin) upon stimulation by tumor necrosis factor alpha (TNF-α), which then binds to mature effector T-cell's VLA-4 and facilitates transmigration to the site of infection (*1*). The interplay between VLA-4 and VCAM-1 alone is also enough to induce the rolling of leukocytes under shear flow neglecting the presence of selectins, a phenomenon described in 1.2.4.

1.2.3 Structure, I-domains and states of affinity

Integrins are heterodimeric transmembrane proteins with an α and a β subunit which are totally distinct and which have no detectable homology between each other. In humans there are at least 18 α and 8 β known subunits, resulting in 24 combinations. Both subunits contribute to extracellular binding of the ligand (*14*). The extracellular part of the integrin once more consists of several domains like for example the $\alpha 7$-helix, whose locking at various positions induces the closed, intermediate or high affinity state for ICAM-1 (*9*).

The I-(insertion)domain very similar to the von Willebrand factor A domain, is a special part within half of the closely related α-type subunits. If present, it is the main ligand-binding site of the respective integrin. It contains a metal-ion dependent adhesion site (MIDAS) crowned with a Mg^{2+} which obtains a key role in conformational change between states of different affinity due to the binding of divalent cations (*9*). The increase in affinity between the closed and the open conformation, shown by introducing a disulphide bond between the $\alpha 6$ and $\beta 6$ loop is 9000 times higher, a clear evidence that this conformational change is the trigger for the affinity change. Henceforth, the state of the integrin is not only characterized by an open or closed state (which would correspond to an "on" and "off" switch), but there also exists an intermediate state, whose affinity is 500 times higher as the closed state (*9*) as also shown in

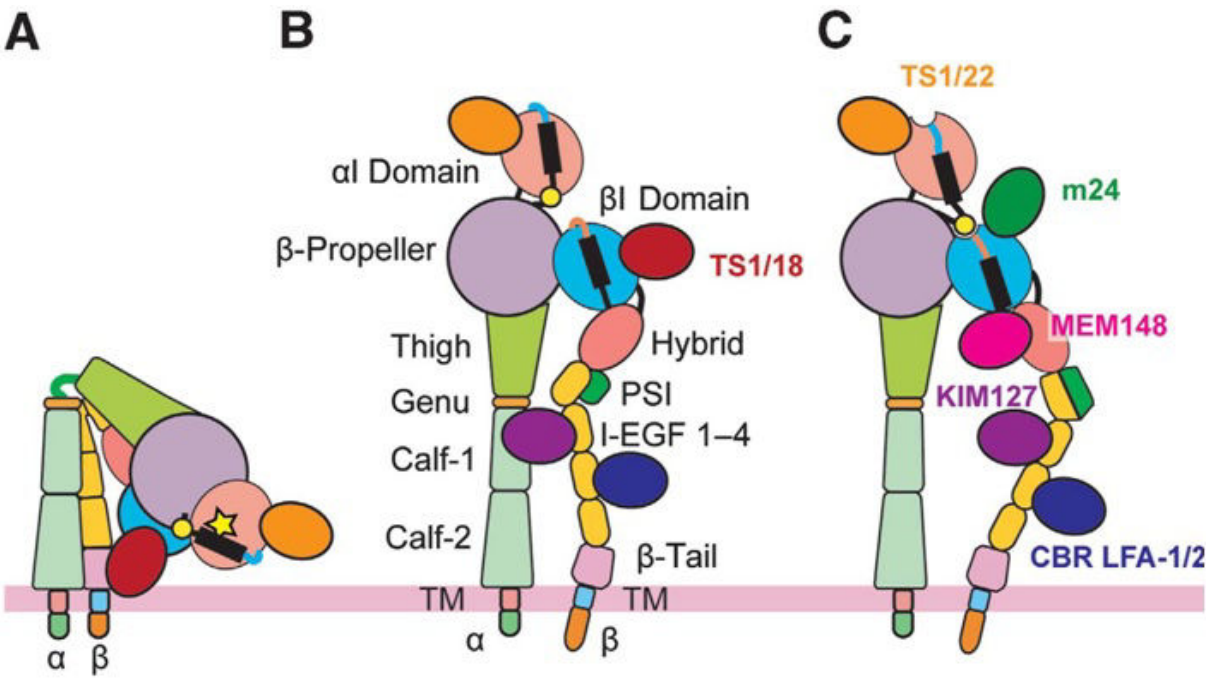

Figure 1.4: Integrins can exist in low-(A), intermediate-(B) or high-affinity (C) conformations. (*8*)

this work.

Each spatial orientation and subunit rearrangement in the integrin from low-, to intermediate- or high-affinity state and back corresponds to a change of affinity. How cells regulate the state of adhesiveness is still controversial. Still polarization and adhesion is granted in all cases, implying that only intra-lymphocyte signaling is responsible or the cells themselves release the responsible chemokines. Here, the complex intracellular signaling pathways related to LFA-1 might come into play. One model suggests that binding of Talin, a protein responsible in the coupling of the integrins with the cytoskeleton, between the short, cytoplasmic parts of the β-chain allows separation, spreading or spatial change of the two transmembrane parts of the heterodimer inducing an intermediate- or high–affinity state without the need for any more involved components (*16*, *17*). Another option includes the movement of the proteins in the cell wall, coupled with their binding to the cytoskeleton with proteins who attach to the β-subunit. In this case, lateral forces induced by the cytoskeleton would be responsible for pulling apart the two subunits although the headpiece would still remain closed and affinity would remain intermediate. If the ligand is soluble, the state of the integrin does not change. If though the ligand is also presented in an immobilzed state, as a part of another cell wall or bound to a surface, it would act as an anchor and the lateral force applied by the cytoskeleton would increase, finally inducing the opening of

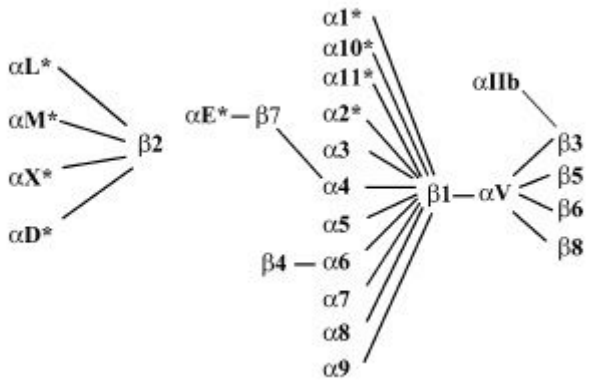

Figure 1.5: possible subunit combinations, asterisks indicate the presence of an I-domain. Figure adapted from (*15*)

the headpiece and integrin extension, which goes along with an increase of affinity and adhesion as shown in figure 1.6 (*8*, *18*) It should be mentioned though, that both these models have been proposed by examining the $\alpha IIb\beta 3$ integrins, not on LFA-1 (αLβ1)

Increasing LFA-1 affinity with manganese

To observe any influence of LFA-1 affinity on migrational properties of lymphocytes it is necessary to switch and lock the integrin conformation in a specific desired state. As already mentioned in 1.2.1, only the metal-ion dependent adhesion site of the I-domain of the α-subunit of LFA-1 is involved in the binding of ICAM-1. The working principle behind adding manganese is straight forward: Its property as divalent cation acts directly on the MIDAS to initiate the high-affinity state . The Ion stabilizes an otherwise spacially and energetically unfavourable and hydrophobic ridge which acts as binding site for ICAM-1 (*8*, *19*)

1.2.4 The leukocyte adhesion cascade

As explained previously, one of the most distinguished features of leukocytes is their motility and unique ability to migrate into practically any part of the body. Modes of movement, intra- and extracellular signalling, as well as intracellular communication are closely linked together: The involvement of cytokines and adhesion molecules allow specific recruitment of immune cells and lead to various distinct types of cellular behaviour at the various steps from floating passively in the blood stream until actively moving towards the antigen.

The process of recruiting T-cells from the blood stream to the source of infection including the description of involved factors is called leukocyte adhesion cascade, illus-

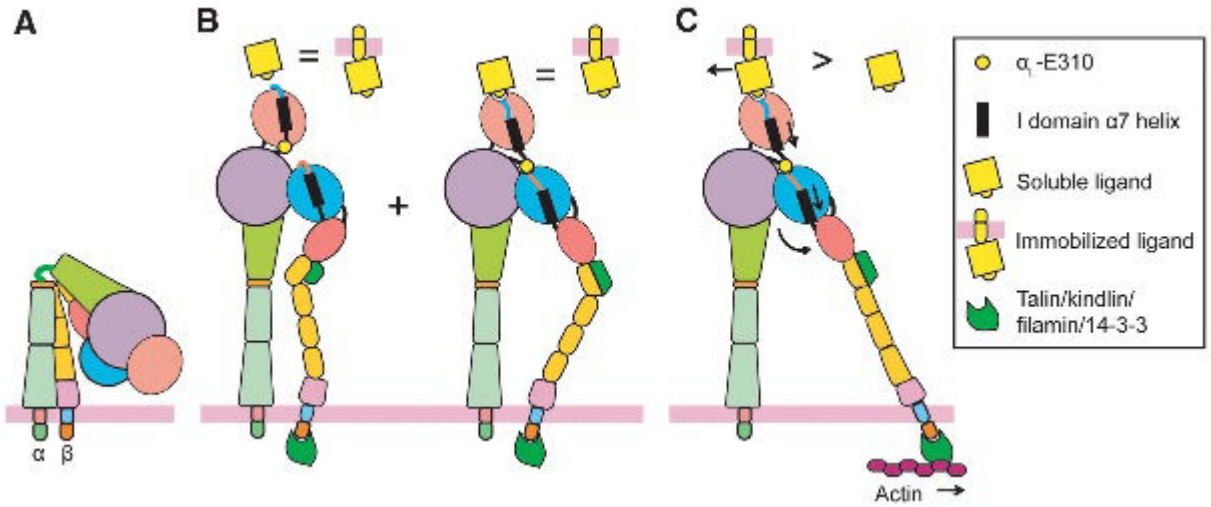

Figure 1.6: Correlation of integrin affinity to models proposed in 1.2.3: (A) Shows the integrin in the inactive and bent conformation. (B) shows the activation induced by cytosolic binding of Talin to the β-subunit, changing the sterical orientation of the two transmembrane domains and opening the headpiece. Affinity for soluble and immobilized ligand are the same. In (C) the cytoskeleton, whose components are in constant flow, exerts lateral force on the cytosolic β-domain which is again transduced to the integrin by coupling proteins (*8*).

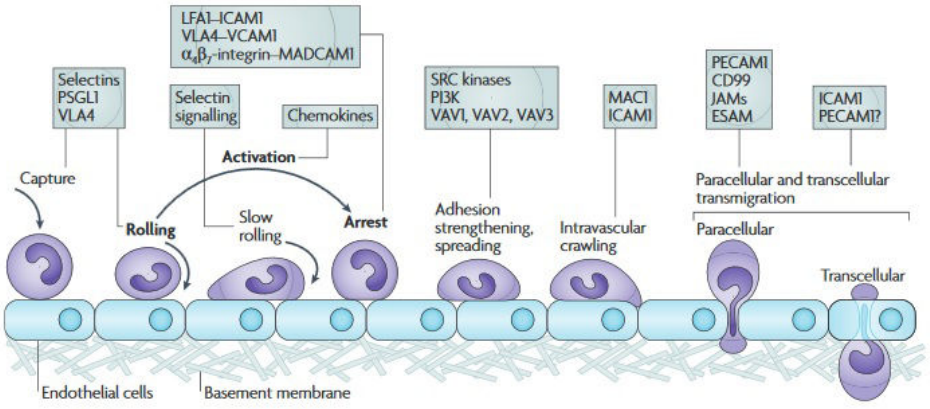

Figure 1.7: Schematic view of the various stages of the leukocyte adhesion cascade including the essential proteins for each step (*17*)

trated in figure 1.7. Briefly described, the immune cell undergoes three main phases after being recruited: rolling, activation and firm adhesion. This, followed by transmigration has been known since the nineteenth century, delivering a qualitative description of the process. Only the discovery of integrins and selectins made it possible to explain the disctinct phases of recruitment and now a more detailed and current view reveals additional important phases of slow rolling, adhesion strenghtening, intraluminal crawling and paracellular and transcellular migration.

Capture and rolling

The first established adhesive contact between a floating leukocyte in the blood stream and the inner vessel wall is established by the family of selectins: P-,E- and L-selectin are all expressed by endothelial cells and interact with the P-selectin glycoprotein ligand 1 (PSGL1). Despite its name it can ligate all three of the aforementioned ligands and the bond induces a tethering of the immune cell on the endothelium, characterized by high on and off rates, leading to a rolling type of movement in direction of the blood flow. Interestingly, shear stress is required to form bonds, if the flow is stopped, the selectin unbinds. Also the opposite is true: the bond becomes increasingly stronger the higher the applied drag becomes. Although PSGL1 as ligand seems not to be particularly specific because of its ability to bind all three types, specific selectin subtypes are only expressed by certain cells under specific conditions: L-selectin mostly by leukocytes, E- and P- selectin by inflamed endothelial cells (in case of P-selectins also by activated platelets). While the purpose of expression for inflamed endothelial cells is obvious, i.e. recruiting immune cells, the purpose of L-selectins is to initiate leukocyte-leukocyte interactions to further recruit other leukocytes by tethering to already attached cells of the same type, which is important to recruit immune cells who don't express P- or E-selectin ligands.

Although selectins are an important part in the cascade, lymphocyte do not necessarily need them to undergo rolling behaviour as can also be seen in this work. A certain surface concentration of VCAM-1 is also enough to induce rolling, also because of higher on and off rates than for the equally well researched and important adhesion molecule ICAM-1, which needs additional selectins (*17*, *20*).

Activation and subsequent arrest

When inflamed, the endothelium is upregulating the expression of certain adhesion molecules and chemokines to constantly attach lymphocytes on the venule wall locally and shut down rolling. In this phase, ICAM-1 and VCAM-1 are expressed by the endothelial cells and become the main acting adhesion molecules together with their in-

tegrin counterparts LFA-1 and VLA-4. These integrins of the $\beta 1$ and $\beta 2$ families are the most relevant integrins in the two mentioned phases, which made them target of most research. Although not used in the research of this work, chemokines also have an important role in regulating the affinity state of the integrins which enables dynamic arrest under flow in the first place, an inside-out signaling event which happens at almost instantaneous speed. However, all this does not happen in a "all or nothing" manner. Neither the three states of integrin conformation (bent, intermediate and open) are discrete steps, but rather continuous transitions. The affinity increase does not happen all over the plasma membrane for all expressed integrins, but always affects only subsets of the same integrin type, but still increasing the overall adhesion of the cell. Outside-in signaling, which is responsible for this effect, is involved in various cellular processes besides adhesion, like apoptosis or proliferation (*21*) and is induced by spatial phenomena like integrin clustering upon binding adhesion molecules, as well as allosterical changes are prerequisites for the formation of signalosomes, protein complexes which induce and are responsible for intracellular signaling leading to cellular arrest (*17*).

After arrest on the endothelium, T-cells have move at the chosen site of extravasation, on the extracellular matrix provided by the endothelium. Although the adhesion forces of the cell are an order of magnitude higher (*22*), the hemodynamic shear stress exerted on the cells is still significant for influencing processes involving integrin engagement and cytoskeletal dynamics like formation of pseudopodia and activating the guidance mechanism resulting in alignment of the cell with the flow. Physiological shear stresses in capillaries range from average 3-10 dyn/cm^2 (*23*) but can reach up to 25-30 dyn/cm^2. In the frame of this work, shear stresses up to 12 dyn/cm^2 were applied, with the relevant data acquired at maximum shear rates of 8 dyn/cm^2.

Due to the fact that the subsequent planar migration of lymphocytes is the main topic of this work, it will be covered more extensively in an own chapter in 1.3.

Extravasation

The final phase of the cascade, the penetration of the endothelial barrier and three dimensional migration into the tissue, starts after establishing firm adhesion between leukocyte and endothelium and triggering by chemokines requiring additional shear stress. Additionally different subpopulations of leukocytes have different requirements in beforementioned conditions to undergo extravasation. This attachment is prerequisite for crawling along the cell wall, which is described in particular in chapter1.3

and is highly dependent on ICAM-1. In context of extravasation, its purpose is to find a proper place for entering the tissue in close proximity of certain cues provided by the environment and it can happen either through a single cell (transcellular) or between cells (paracellular) of the endothelial barrier. In any case, three layers have to be crossed: the endothelial cells themselves, followed by the basement membrane, which serves as a extracellular matrix barrier between underlying tissue and the endothelium, and finally the pericyte sheath. Pericytes are cells who build up an additional layer by wrapping up around cells beneath the endothelium and are involved in tissue organisation. Another important part of the interplay between both types of cells is the induction of clustering of ICAM-1, VCAM-1 and ERM-proteins as well as proteins that interact with the cytoskeleton after establishing adhesion which creates preferred loci of transmigration. If initial crawling is disabled, extravasation is significantly reduced and the transcellular pathway is preferred (*24*).

Transcellular migration makes the leukocyte go through one single endothelial cell itself very rapidly (<1 min (*25*)) in specific scenarios: *in vitro*, in the central nervous system and during inflammation (*26*). This specificity and also the fact that transcellular extravasation is the less common pathway (5-20% in cytokine activated T-cells on HUVEC (*27*)) might be the reason why the discovery of this phenomenon is rather recent. As a prerequisite, the leukocyte chooses locations where the distance between the top and the bottom membrane is shorter than usual making the migrational distance shorter. Thereupon, it starts forming pseudopods and probes the endothelial cell. Also here ligation of ICAM-1 by the leukocyte is the initializing trigger, especially in regions of high ICAM expression, as already mentioned. The endothelial cell contains ICAM-1 filled caveolae, small special organelles maintained by the protein caveolin, who, after ligation, aggregate along the anticipated pathway forming an intracellular channel to facilitate penetration by the leukocyte. These pseudochannels,so called vesiculo-vacuolar organelles, form in regions where the endothelial cell agglomerates ICAM and actin fibers to provide an adhesion gradient as cue. ERM-protein density around these structures is also higher which helps to maintain structural integrity for the cell by involving the cytoskeleton's actin and vimentin and therefore the integrity of the endothelium is only minimally disrupted and the cell avoids damage during the migration to the basal membrane.

Paracellular migration happens after ligation of the leukocytes own macrophage antigen-1 (MAC1) with the ICAM-1 expressed by the endothelium, a signaling pathway induces endothelial cell contraction by activating intracellular myosin. This tightening up of the tissue creates gaps between the cells through which the leukocyte can pass. Interestingly cells can actively redistribute junctional molecules to open up migrational

pathways: They remove intracellular vascular endothelial cadherin bonds who connect adjacent cells, and increase the local concentration of adhesion molecules that might ligate to leukocytes and actively induce extravasation like platelet/endothelial-cell adhesion molecule 1 (PECAM1) or junctional adhesion molecule A (JAM-A) to create a gradient leading the cell along the way and stabilizing the whole procedure.

Interestingly both pathways make use of the same principles, like haptotactic gradients and also many types of proteins, like PECAM1 used for leukocyte engulfment in transcellular and as extravasation inducing protein in paracellular migration, are involved either way.

The basement membrane is made up of two layers of different kinds of protein: vascular laminin and collagen type IV. One of the purposes of the pericytes is to contribute in building up the membrane, and since the density distribution of pericytes is not isotrope, the protein density of the membrane also corresponds with gaps between pericytes. As already stated, leukocytes cross the barriers at the points of shortest distance and lowest protein density, therefore the congruency in density turns out to be favourable for transmigration pathways. Including chemoattractants to the equation, the low density-effect is amplified, since those gaps are also easier permeable for soluble molecules, which creates a chemotactic gradient and eventually a cue for leukocytes which is even more feasible considering that components of the membrane can bind and therfor store chemokines. Also here PECAM1 plays an important role since its binding increases the expression of $\alpha 6\beta 1$-integrins who bind the membranes own laminin. Crossing the basement membrane and the pericyte layer is again common for both migrational paths. The former is crossed at areas of low protein density and the latter in gaps between single cells with the help of other integrins, the ERM proteins and proteases. While crossing the endothelial cells takes $<$5 min, getting through the basement membrane takes $>$5-15min (*17*).

1.3 How do T-cells move in two dimensions?

Cell migration in general is a crucial feature of cellular organization, may it be single cells like those of the immune system as well as a prerequisite for multiple cells, for example fibroblasts or vascular endothelial cells for wound healing, as well as in forming tissues like in embryogenesis, developement of the nervous system or gastrulation. Finally, besides tissue engineering, cancer research is also closely linked to the same underlying principles, as understanding the cellular mechanics of migration means understanding propagation of cancer metastasis by tumor cells.

Fast cellular movement mechanics based on manipulation of the actin cytoskeleton,

as viewed with human effector T-lymphocytes, are called 'amoeboid' migration, who are also characterized by rather weak adhesion to the substrate which is prerequisite for its high movement speed, as well as the affected cell constantly changing its shape due to their protrusions ('amoeboid' from the greek *amoibe* for 'change'). Their highly explorative behaviour and necessity to being able to migrate all over the body makes their amoeboid motility one of their most important attributes. On the contrary, mesenchymal cells migrate slower due to their higher dependence on adhesive forces.

The directed migration towards certain organs or sites of inflammation (homing) is one of the most interesting properties of effector T-cells and a key prerequisite for their role within the adaptive immune response. In general, their movement can be passive, as a part of the blood, exposed to the shear stress within the blood vessels, or active by propulsion induced by cytoskeletal rearrangements with and without coupling to the endothelium or extracellular matrix by integrins. The direction and homing is dependent on all of the mentioned factors additionally to other migratory cues like cytokines. These chemoattractants are also responsible for diverse changes in phenotype like cytoskeleton rearrangements as well as attachment in the front and detachment in the back of the cell as prerequisite for directed migration. The more coordinated and synchronized this attachment and detachment is executed, the more the cell shape is conserved during locomotion. Numerous papers have already been published on the two-dimensional migration of lymphocytes (*28*, *29*) in vivo who confirmed the model of T-cells preferentially migrating against the direction of shear stress *in vitro* with no further directional guidance mechanisms involved on ICAM-1 substrates(*23*). Indeed, shear stress is even contributing to induce LFA-1 dependent adhesions (*30*). In general, migrational direction of white blood cells is crucially dependent on integrin-surface interactions and integrin involved signaling (*31*).

Up to now, nearly all of these experiments except (*23*), amongst few others, have been performed with endothelial cells as a substrate, either inflamed or not. This poses a serious problem, since the intra- and extracellular factors involved in directed migration are interlinked and integrated among cytokines, cell - surface interactions and shear stress or other environmental influences, and since it is virtually impossible to exactly control or modulate the surface conditions regarding extracellular matrix interactions, integrin and adhesion molecule expression and involvement of cytokines of any kind on a cellular substrate model, it is also impossible to focus on distinct contributions of beforementioned factors. So single properties of lymphocyte migration can not be properly attributed to their specific cause. The big advantage of an in-vitro model, as used in this work, is that the components of the substrate, which can influence cellular move-

ment, can be inserted and modulated nearly at will, since involved adhesion molecules can be quantified, shear stress can be precisely controlled. The only remaining parameter, cytokines, can be neglected, because none are added to the substrate or the bulk solution and autocrine factors influencing migration on a global scale (an example is described in (*32*)) are not relevant.

1.3.1 Polarization and cell shape

One of the first and most basic prerequisites to induce migration, is that cells have to undergo polarization. Initially, effector T-cells in suspension are round and spatially isotropic and polarize upon adhesion to the surface. If the cells remain unpolarized, they hardly move, and do not reach the characteristically high speeds one can usually observe in lymphocyte migration. Interestingly also cells who do not engage their adhesion molecule receptors upon contact with the surface mostly polarize, which means that no signaling process triggered by binding is necessary to rearrange cell shape, the same holds true for migration: Although no external signaling, let alone integrin engagement, is provided, cells start to move spontaneously in a swimming manner as observed in this work. Since most research was done on substrates composed of endothelial cells (*28*, *29*, *33*, *34*), most publications assume signaling as prerequisite for every step involved in migration although not implicitely necessary. The initial orientation and reshaping of the cellular outline is observed virtually all the time as cells start to run their migrational apparatus, with leukocytes displaying very distinct phenotypes characterized by a flat, sheet-like and extensive lamellipodium at the front, probing the cellular surroundings in the direction of movement as well as laterally. It is an important maintaining component of cellular polarity and, even if the outlines may undergo a constant change, its overall shape and purpose is always maintained. On the contrary, cells also probe their immediate neighbourhood with filopodia, which are thin and needle-shaped and may exist only for short periods of time. Furthermore there exists a (compared to the lamellipodium) smaller protruding uropod in the back, usually erect, resembling a small cellular antenna. Interestingly, the

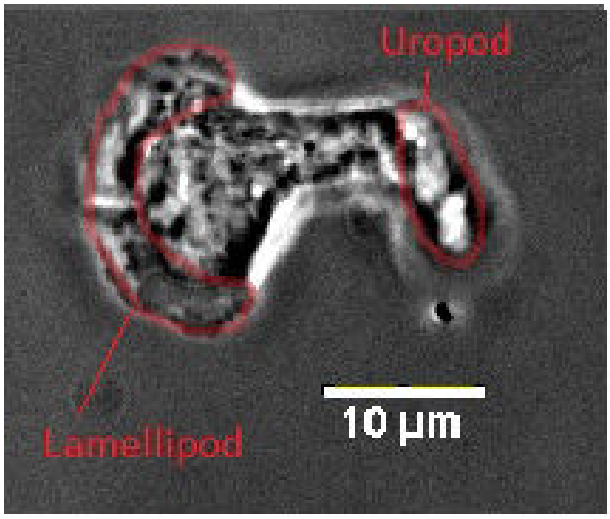

Figure 1.8: Effector T-cells on 10μg/ml ICAM-1 substrate under 4 dyn/cm^2. The uropod is erect and aligned with the flow. Both the thin and broad lamellipod and the uropod are clearly distinguishable.

uropod is not present in other migrating eukaryotic cells. Various reasons favour this polarised cell shape over a round phenotype, among them the spatially heterogenous distribution of mechanical or chemical sensors for movement cues as directional pacemakers. The distribution of receptors, is a distinctive case: Imagining a gradient of any soluble cue may it be two- or three dimensional, an unpolarized cell with a homogenic distribution of receptors could still detect the source of the signal just by the difference of ligation events at different edges of the cell. The actual internal mechanisms involved in polarization and migration are complex involving numerous pathways and as well as molecules involved in signaling (for example tyrosine kinases, lipid kinases, Rho GTPases and second messengers).

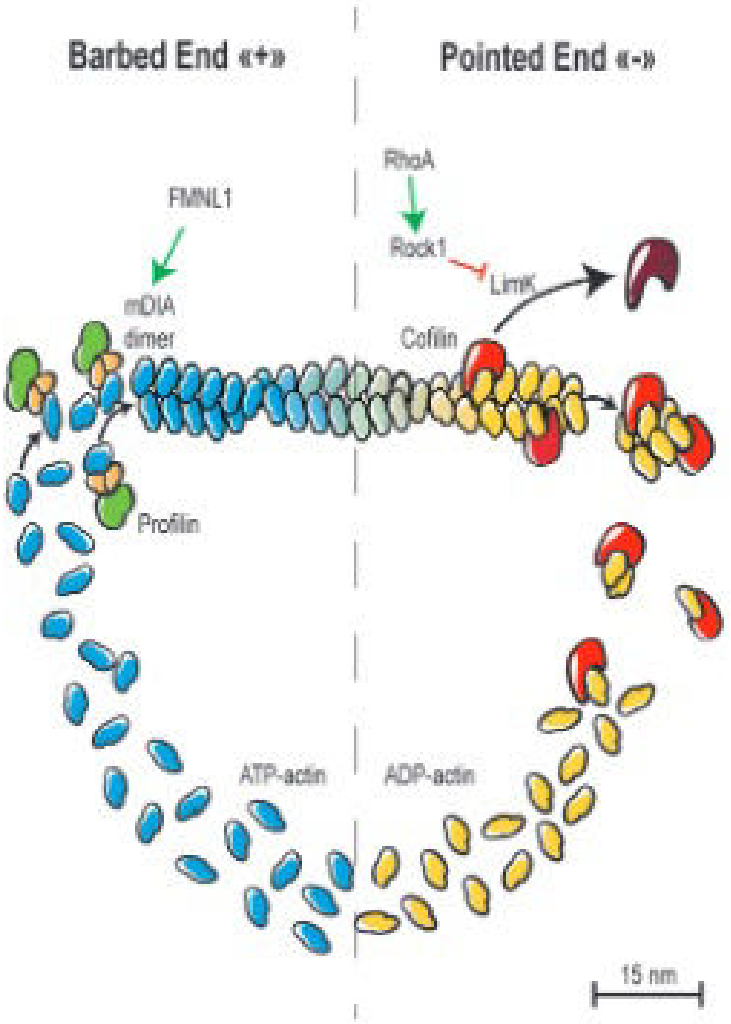

Figure 1.9: Dynamics of actin polymerization and involved actors (thoroughly described in 1.3.2)(35).

It is known that force transduction happens via integrins and that the necessary force

is generated by the polymerization of the actin cytoskeleton. However, these interactions between actins and the membrane proteins are, like the signaling, in most of the cases indirectly involving various proteins like ERM (ezrin, radixin and moesin)-proteins who bind actin at their C-termini, cluster up at the inner membrane surface and bind the cytosolic part of the integrins with their N-termini, giving them a purpose as linkers or force transducers (*36*). They are unique in their capability of not only binding to integrins, but also to antigen- and chemokine receptors (*37*). A graphic overview of the involved components is shown in figure 1.12. Compared to, for example, endothelial cells, effector T-cells have a high migrational speed (up to 20 $\mu m/min$). This is proportional to the elusive nature of these cells, who never fully develop focal adhesions to the substrate, whose binding dynamics would slow down cellular migration significantly (*38*). As a matter of fact, the constant dynamic remodeling of the cytoskeleton provide and form distinct cellular parts like uropod, lamellipod and other podia equiping the cell for a wide variety of tasks not limited to force transduction and movement in two and three dimensions but also probing of the surroundings and contributing to form the immunological synapse. Chemoattractants leading to cellular polarization are responsible for a rearrangement of cellular f-actin: Whereas it is arranged in a radial pattern in unpolarized cells, it concentrates in particular regions and amasses at contact zones (*39*) and at the leading edge in the lamellipod to form 70° branches using the arp 2/3 complex when polarised. Myosin-induced contractions of the actin meshwork give the cell its particular shape: broad lamellipodia and filopodia at the front, which are attached to the substrate and a narrow uropod at the back (*40*).

Even though chemoattractants play a huge role in internal cellular signaling as well as in migration, the uropod with its antenna-like shape might overtake their usual role as migrational cue: Recent studies on lymphocytes have shown that their uropod acts as a sensor for the direction of applied shear stress in two-dimensional *in vitro* migrational studies. This would describe a simpler and more direct mechanism of feedback to blood flow, although it has to be mentioned that lymphocytes crawl upstream but for example neutrophils downstream, which makes it difficult to deduce a general passive signaling cue (*22*).

1.3.2 The role of the actin cytoskeleton

The actin cytoskeleton

Lymphocytes, like cells of all domains of life, have a cytoskeleton, a highly organised network of filaments who provide structure and cellular shape whose complexity depends on branching and crosslinking of existing fibers. As can be seen in figure 1.11 this

three-dimensional network is shaped differently in different parts of the cell. However there is another underlying structure called cortical actin, which coats the inner part of the plasma membrane to sustain cell shape. It is formed of actin proteins, which are found in two distinct states whose names already describe their condition: g(lobular)-actin and f(ilamentous)-actin.

If a critical concentration of ATP-bound g-actin is reached, the polarization of a double-helical and polar f-actin filament starts. Polarity of the actin strand is characterized by a barbed (plus) end, which is more dynamic than the counterpart, the pointed (minus) end, polymerizing ten times slower. Various proteins control the propagation of the filament as well as the assembly and the disassembly of actin:

1. formins, which act as nucleators and help to prolong the barbed end
2. profilin, which inhibits the buildup of oligomers and prevents further self-nucleation of globular actin
3. capping proteins which cover the barbed ends of the strands to inhibit further prolongation or depolymerization
4. cofilin, which promotes depolymerization of ADP-bound actin at the pointed end
5. Lim Kinase, which gets activated by phosphorylation by the Rho-associated protein kinase (Rock)(*35*), controls this depolymerization

Actin structures are also responsible for the formation of the various distinct sectors of the cell like lamellipodia, uropodia and filopodia which are created by a locally different polymerization behaviour like growth rate and branching causing different spatial expansion.

Actin-driven force generation and motility

Also the levels of calcium vary within different regions of the cell: Whereas the concentration is low at the frontal lamellipodia, they are high in the back indicating a connection to the myosin II activity in the uropod leading to contraction and detaching the protein complexes responsible for cell-substrate attachment. Adhesive protein complexes, who link the cytoskeleton to the substrate will move backward as the cell protrudes forward. Since cells reuse these adhesion proteins, a transportation mechanism to the front is required which also seems to be linked to internal concentrations of free calcium; like for example an endocytotic cycle or forward diffusion (*41*). The basic principles of two-dimensional lymphocyte movement is based on actin polymerization.

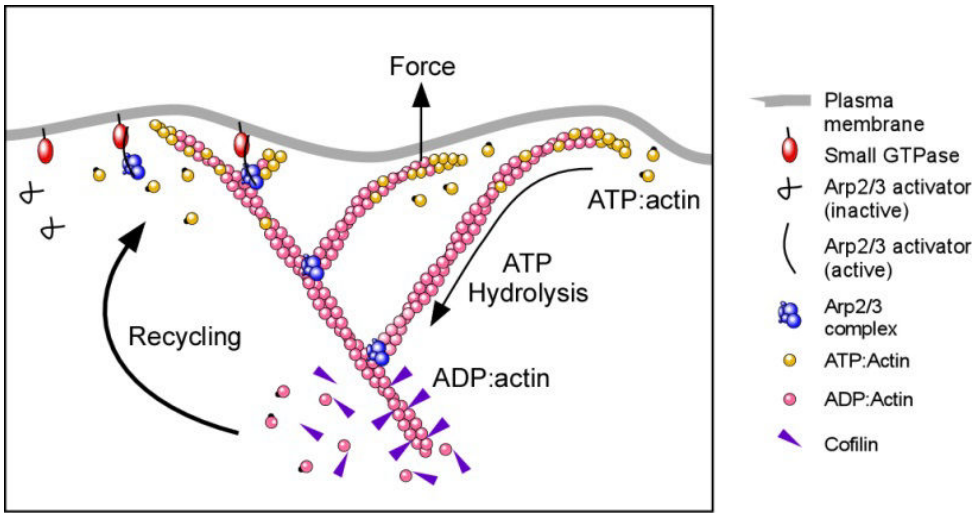

Figure 1.10: Actin-treadmilling: G-actin attaches to F-actin fibers at the cell front and dissociates at the end of the polymer. The fiber is not attached to the substrate or cell wall, so the net force of the prolonged fiber pushes the membrane forward at the leading edge and itself back, generating cell locomotion (*43*).

If actin polymerizes on one end and depolymerizes on the opposing end, a net movement of the cytoskeleton is generated, membrane-parallel and against the direction of locomotion. However, the moving cytoskeleton has to transmit the force generated by this process to the surrounding cell and does this by two mechanisms: The simpler one is just the pushing force of polymerizing actin at the leading edge of the cellular membrane generating filopodia and lamellipodia (*42*).

Actin-polymerization-driven membrane extension

Due to the important fact that the cytoskeleton is a highly dynamic, permanently rearranging meshwork, g-actin constantly associates to existing, polymerized actin filaments (f-actin) at the leading edge in direction of migration and dissociates at the trailing edge, a phenomenon called actin-treadmilling (figure 1.10): The assembling, growing fiber exerts physical force on the forward part of the membrane just by the pressure the newly attached actins apply to the bilayer. If the cytoskeleton is not bound to any proteins acting as force clutch, the force applied to the membrane equals an opposing force pushing the polymerizing fibers backwards, inducing a retrograde flow. Different association and dissociation rates at different locations help the cell to sustain shape, interaction with other cells and persistence of migrational direction. These cytoskeletal rearrangements are well regulated and dynamic, as can be demonstrated by a look at the speed of the involved process: It has been shown that the polymerization of actin at the barbed end can be as fast as 3000 subunits per second, this would mean growth in the length scale of a lymphocyte (10μm) in <2s (*44*) proving that polymerization

is definetely not the limiting factor in achievable cell speed. From an energetic point of view, this big discrepancy between polymerization speed and net cell locomotion makes sense: excess energy from the actin network expansion is transmitted to the cell wall and dissipates via deformation of the membrane which helps to rupture adhesion molecule bonds at the plasma membrane-substrate interface, one of the reasons why mesenchymal cells are slower than amoeboid cells.

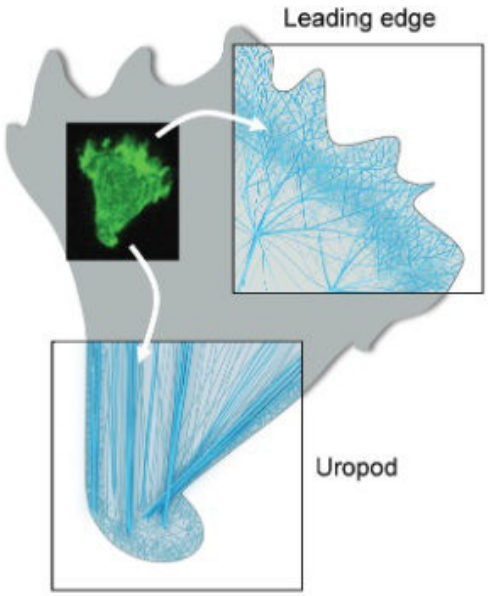

Figure 1.11: Strongly branched filaments at the leading edge to support filopodia and lamellipodia. The meshwork in the uropod is parallel allowing myosin II motorproteins to generate locomotive forces by contraction (*35*).

This methods works without any active binding of the cell to the substrate, since forces are generated and transduced completely in the cytosol by pushing the actins backward. The second method is more complex and relevant to this work: The cytoskeleton is additionaly coupled to transmembrane proteins, in our case integrins, who bind their extracellular ligands and therefore provide a temporary anchoring and force transduction. Additionally to the two already described methods of propulsion (the pure protrusion of the cytoskeleton and the transduction of forces via transmembrane proteins) a third one, slightly more complex, has to be added: contraction

Actomyosin contraction

Myosin II is a double-headed abundantly available motorprotein which binds on actin and associates with the myosin II-counterpart bound on another filament. In this arrangement, the proteins pull their fibers antiparallel under conversion of adenosine triphosphate (ATP) to adenosine diphosphate (ADP), the same procedure that is also happening during muscular contraction. This is the only mechanism that can actively shrink the cytoskeleton which generates hydrostatic pressure within the cytosol, which subsequently generates movement force. If this hydrostatical pressure detaches a part of the cytoskeleton from the plasma membrane, the force leads to formation of a so called 'bleb', a bubble-like cellular protrusion initially lacking structure-building actin or other components. Once the generation of the bleb equilibrates the hydrostatic pressure pulse, f-actin is recruited into the new protrusion (*45*).

All three described methods work synergistically although interestingly, T-lymphocytes are able to move only relating on the polymerization strategy, excluding contractile and adhesive components. This can be shown by blocking myosin II, which disables the other two movement options (*46*). The cooperation of the involved mechanisms is also present in the cytoskeleton - integrin interactions who have to be dynamically regulated: Attached transmembrane proteins have to be spatially modulated in their affinity so that bound integrins detach once they reach the cell rear to avoid slowing down the cell or interfering with actin depolymerization and be ready for re-usage at the cell front. Since all this comes at an energetic cost, the cytoskeleton actively helps in detaching the integrins and amoeboid cells can maintain a faster pace because of two reasons: The proportion of adhesive forces is lower than in mesenchymal cells, so less energy is used for releasing the binding and velocity can be kept high(*3*). Secondly due to the fact that the plasma membranes elasticity is low, stress applied at the cell front by protruding actin fibers is quickly equilibrated over the cellular surface and the pushing force at the front is translated as well to a pulling force in the back helping retraction (*47*). Force transduction although, is only possible by actively pulling on actin fibers connected to integrins, not by protrusion alone. This has been shown by inhibiting myosin II or its regulator Rho kinase in dendritic cells, which lead to a still protruding cell front, while the back not only lost its ability to contract but also was not able to release adhesion at the cell back leading to massively elongated cells, showing that the contraction and protrusion modes are spatiotemporally disconnected, meaning that the trailing edge, if not contributing to movement by actin fiber contraction, is just pulled ahead by the protruding cell front (*46*) and that active pulling work by motor proteins is necessary to disassemble adhesion molecules (*48*) showing that there is an asymetry in traction. The applied force on the substrate is >1000 pN, compared to the exposed shear stress in blood vessels which is 100 pN and the negligible friction between 'pure' plasma membrane and substrate, it is clear that external physical influences play a small part regarding normal movement conditions and that overcoming the adhesive bonds is the main part in energy expenditure.

Connecting integrins with the cytoskeleton

As briefly described in 1.2.1 and 1.3, actin filaments do not bind directly to integrins, therefore the propulsion generated by the cytoskeleton needs additional proteins involved to transduce force from the actin network to the substrate via bound integrins. Not only is this connection purely mechanical, it also involves inside-out signaling which leads to a complex interplay of proteins interacting and modulating each other. The complex synergy of so many proteins might be necessary to sustain the high dynam-

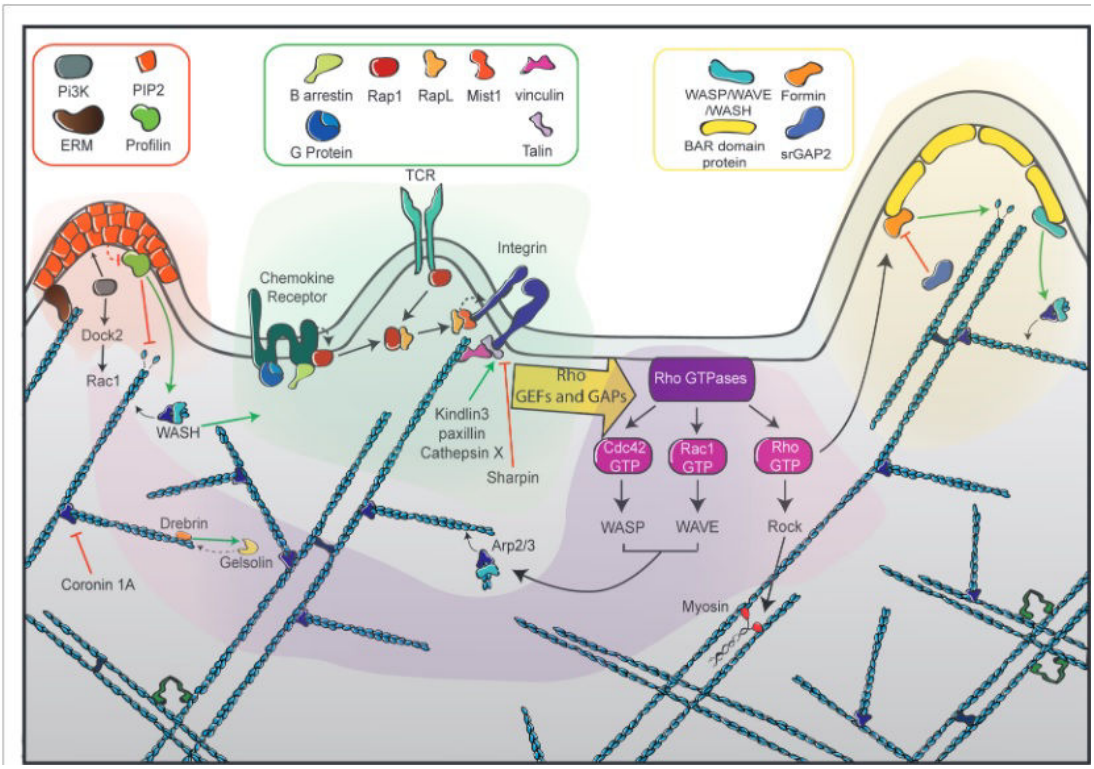

Figure 1.12: The complex interplay between intracellular signaling and the cytoskeleton. Green area: affinity regulation and coupling of actin fibers and integrins by talin and vinculin, modulated by kindlin-3, paxillin and cathepsin X. Protein functions described in 1.3.2 (*35*).

ics of the cytoskeleton in time and space. Talin is one of the most important coupling proteins due to its attribute as driving force of integrin activation. It binds to the short cytosolic part of the β2-chain of LFA-1 and induces an opening of the extracellular headpiece to high affinity (*6*). Once established, kindlin-3 also strengthens the cell-substrate bond by also binding to the same chain. Another regulator who comes then into play is paxillin, binding to the intracellular β2-chain as well and controlling adhesion assembly (*35*), interestingly it also affects the second most important integrin in this work: VLA-4 inducing its adhesiveness under flow (*49*) due to its role of mechanical regulator of VCAM-1 bonds in absence of chemokines. It interacts as well with proteins like vinculin, also linking the intracellular subunits of the integrin to the cytoskeleton by binding to already-bound talin. Whereas these proteins are used as signalling and linking proteins all over the cell, α-actinin is found in the leading edge of the cell to induce new adhesions and is required for directional migration, also acting with the cytoplasmic β2-domain of LFA-1 (*50*). To induce the interaction of integrin with α-actinin and talin, a cleavage of the β2-cytoplasmic tail is induced by cathepsin X another modulator towards high-affinity state LFA-1 (*51*). For better understanding, some of these interactions are graphically visualized in figure 1.12

1.4 How do T-cells move in three dimensions?

With integrin-independent movement in three dimensions like in a collagen matrix, the $\beta 1$-integrins, who are parts of VLA-4 and VLA-5 integrins, are transported towards the uropod (*52*). The role of the uropod seems to change after the cell induces transmigration and moves through a three dimensional matrix: it might attach to the ECM and induce binding and interaction with other cells as well as inducing the transendothelial migration (*53*). Structurally the uropod gets a new purpose: The MTOC retracts into it, increasing microtubule density and therefore increasing mechanical stiffness (*54*). The Rho-GTPases who are responsible for polarity in two dimensions induce the contraction of the actin filaments in the uropod in a three dimensional matrix, making the uropod the location of force generation for contractile movement. In lymphocytes, the various protrusions at the leading edge are used as a probing tool for suitable locations for transendothelial migration. A task which requires frequent adaptations of cell shape provided by the dynamic nature of the actin filaments which are densely packed in those structures (*30*). This displacement of the integrins in combination with the spatial surroundings leads to an entirely different situation: the tightly packed three-dimensional matrix surrounding the cell reduces the role of adhesion molecules significantly. A cell pushing against its tight surroundings just by protrusion of its cytoskeleton might be enough to migrate, similar to a climber pushing against the walls of a tight natural chimney (*55*). Also contractile forces are used by T-cells showing the utilization of hydrostatical forces in confined environments. Here, Myosin II induced pulling on dense parallel actin strands in the uropod pushed cytosolical matter to the cell's leading edge, generating pressure that leads subsequently to movement. This was shown by inhibiting of myosin II and therefore eliminating contraction, demonstrating that T-cells are able to utilize the synergy of diverse forms of propulsion while not solely relating on one in particular (*56*).

1.5 Preliminary findings and state of the art

The experiments and procedures used in this work, the *in vitro* analysis of T-cell migration on artificial substrates, are for the most part based on (*23*). Using very similar experimental setups, like IBIDI flow chambers, that work analyses and quantifies properties of effector T-cell motility on pure ICAM-1 coated substrates exposed to shear stress. It is shown that T-cells, as opposed to neutrophils or HSB-2 (a T-cell line derived from T accute lymphoblastic leukemia), migrate against the direction of flow whereas only directionality but not speed are influenced by the level of shear. Further elaborat-

ing on the underlying guidance mechanisms of this phenomenon, the role of the uropod was examined in (*22*), showing that the orientation against the direction of flow is induced by the alignment of the erect uropod, which acts as a wind vane to sense flow and induce a change in migrational orientation.
Both works show that directed effector lymphocyte migration is a phenomenon which requires only minimal external physical stimulus, showing a robust and fast response to flow without the need of biochemical signaling or external chemical cues.
The following work tries to compare the findings described above with modified substrate conditions to see if and how the density and type of adhesion molecules influences the migrational behaviour of effector T-cells under flow. Further we try to integrate the state of cellular integrins to the existing model to explain the effects of adhesion on various substrate compositions under flow.

Chapter 2

Materials and methods

2.1 Cells and reagents

Whole blood from healthy donors was obtained from the Etablissement Français du Sang. Peripheral mononuclear cells (PBMCs) were extracted by

1. putting 15ml Ficoll-Pague PLUS (GE Healthcare, USA) in a 50ml Falcon tube
2. adding 30 ml whole blood
3. centrifuge for 20-30 min at 840g without braking at 22°C
4. pipette out the PBMC band carefully to avoid contamination with neighboring bands
5. wash 3x with Roswell Park Memorial Institute medium 1640 (RPMI; Gibco, USA)

The obtained PBMCs were stimulated with 10 mg/ml or 40mg/ml phytohemagglutinin-L (PHA-L; Roche Diagnostics, USA). Afterwards, the cells were cultivated at 37°C at 5% CO2 in RPMI to which 25mM GlutaMax (Gibco, USA) and 10% fetal calf serum (FCS, Lonza, CH) were added. For stimulation 50ng/ml Interleukin-2 (IL-2, Miltenyi Biotec, USA) is added. Cells were used after 7-11 days after stimulation.

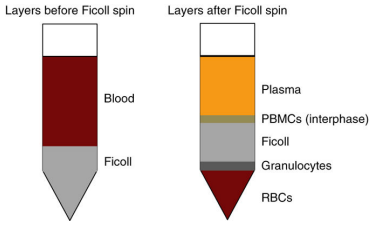

Figure 2.1: Separation of the various components in human whole blood by centrifugation with ficoll (*57*).

2.2 Microscopy

A Zeiss Observer Z1 (Zeiss, Germany) operated by μ-Manager (*58*) was used. The microscope is equipped with a CoolSnap HQ CCD camera

(Photometrics, USA). Depending on the purpose different objectives (all by Zeiss) and lenses were in use: X10 objective / x0.5 lens for migrational tracking of lymphocytes X63 objective / x1 lens for fluorescence and RICM measurements

2.2.1 Reflection interference contrast microscopy

Reflection interference contrast microscopy (RICM) is a method for examination of thin layers. Although the resolution of conventional types of light microscopy is limited by the wavelength of used light, RICM enables longitudinal resolutions in the nanometer range using interference patterns who can be displayed as color differences. The described spatial and temporal resolution in the millisecond range as well as its viability to work in liquid environment make this method a preferred tool for analysing cellular adhesion on transparent surfaces, especially because it does not require labeling of the sample. In this work, the special properties of RICM were excellently suited to analyse the attachment areas distributed among the plasma membrane of adhering, migrating cells under flow in real time.

The working principle of RICM is based on interference of adjacent beams caused by a change of refraction index: Polarized light is focussed on a sample on a glass coverslide. While a part of this beam will be reflected on the interface between glass and liquid medium (and acting as a "reference beam B_r") another part will get transmitted and hits the sample B_s. Here, it will also get reflected and therefore interfering with B_r. As the phase difference between B_s and B_r is a function of the distance between the two loci of refraction, the beam resulting of the interference yields information about the distance between glass slide and object causing refraction, a distance that can be less than the wavelength of the used light and can be visualized by the interference patterns. Furthermore a second polarizer is used before obtaining the resulting signal to block out scattered light.

The resulting intensity of the final beam created by interference is

$$I_{\text{final}} = I_r + I_s + 2\sqrt{I_r I_s}cos(2kh(x,y) + \Phi) \tag{2.1}$$

with $k = 2\pi/\lambda$ and $h(x,y)$ is the height difference between sample and coverslide at the lateral coordinates (x,y). Φ is a phase shift, usually π. The intensities I_r and I_s in formula 2.1 are only dependent on the intensity of the initially emitted beam, but additionaly the second part of the formula is dependent on h and therefore modulates the intensity of the final beam. Fresnel's formulas also say that the intensity of the refracted beams is dependent on the refractive indices of the two media. Hence, the expected intensity will be low for biological samples in watery solutions, so any scattered light

might seriously impact the signal-to- noise-ratio and should be blocked out. A method to discriminate between light from the sample and stray light is the Antiflex technique, which is the difference to interference reflection microscopes (IRM): The polarized light focussed on the sample additionaly passes a $\lambda/4$ plate which circularily polarizes the initial beam. When hitting an interface between two different refractive indices fresnel's formulas come into play again as the following cases may occur:

1. decreasing refractive index: The parallel component of the reflected beam is shifted by π, the perpendicular component remains as it was.

2. increasing refractive index: The perpendicular component of the reflected beam is shifted by π, the parallel component remains as it was.

The reflected beam passes the $\lambda/4$ plate again, this time shifted in orientation by $\pi/2$ and can pass through. Light that did not undergo this orientation shift is blocked out by the crossed polarizer before the analyzer (*59*).

2.2.2 Traction force microscopy

Looking at the integrin-surface interactions who are the driving force underneath cellular migration can also be interesting from a mechanical outside perspective. The migrational properties of cells, from a mechanistic point of view, are depending on surface density, local distribution and affinity of integrins, their role as a force clutch between actin and substrate and the contractile properties of the cytoskeleton. Especially in the context of the random walking model for the cell, where the diffusion coefficient measured is dependent on the interplay of the substrate composition and integrin states traction force microscopy is a convenient tool to examine the force exerted by the cell on its substrate depending on the properties described above:

Polyacrylamide gel containing fluorescent beads, mostly made of latex, is spread as a thin layer and subsequently functionalized with extracellular matrix proteins like fibronectin to enable cellular locomotion. Knowing the young's modulus of the hydrogel and using fluorescence microscopy, the displacement of the beads, which is a direct consequence of the contractile forces of the cellular motility apparatus, is measured and can be translated into a spatial force map translating bead movement into local, contractile forces generated by the cell. As this protocol is already established for attaching fibronectin to the polycrylamide (*60*), a modification of the existing protocols was made to use ICAM-1 and VCAM-1 instead in the frame of this work. Unfortunately no used linking protocol (UV activation, polylysine linking, etc.) provided a functional status of the surface and although binding of the proteins was proven by fluorescence microscopy, no cells kept adhering on the surface yielding no further insight.

2.3 Software

The statistical analysis and MSD related fitting of all data was done with the program GraphPad Prism6 for Windows (GraphPad Software, USA). If not otherwise stated, all averaged data is displayed in the form are mean± S.E.M.. To determine statistical significance, also Graphpad was used to perform two-way ANOVA tests combined with Tukey's multiple comparisons test with $P<0.05$. Only statistically significant comparisons were marked as such in the graph. No marking means therefore no statistical significance.
Custom-developped MATLAB (The Math- Works, USA) software was used for cell tracking. Simlpified, the program registers the two dimensional positions of all cells within a frame and compares it to the subsequent frame to do its calculations. Especially important for statistics are the amount of cells the program counts in the first image and the tracked cells, which are defined by cells who move a minimum defined distance for a certain amount of frames. As a consequence, not moving cells are not included in statistics regarding mobility and only taken into account for adhesion measurements. To suit the more sophisticated modes of movement observed in this work, the programs used in (*23*) were slighty modified and updated to implement the algorithms described in 4.1.1. The most important parameters given as output include:

1. **Cell speed**

   defined by

   $$v_{cell} = \frac{\sum_{n=2}^{N}[P(x_n, y_n) - P(x_{n-1}, y_{n-1})]}{\#_{tracked frames} \; framerate} \tag{2.2}$$

   The enumerator describes the total distance the cell travelled, with N as the sequence number of the frame and $P(x_n, y_n)$ as position of the cell in two dimensions in the n-th frame; the denominator defines the total time the cell could be tracked: The amount of frames multiplied by the framerate, typically 10s. Used unit is μm/min.

2. **Adhesion**

   is dependent on the interactions between integrins, surface and shear stress. Cells who do not bind to the surface, and therefore do not show adhesion, might still be polarized and move in a gliding or swimming manner which is difficult to distinguish from attached, integrin-dependent movement. Although such cells will get washed away as soon as shear stress is applied. That is why all definitions of adhesion presented here are time- and shear stress dependent. '#' represents the number of cells under described conditions with applied shear stress:

(a) *adhesion vs. fix* is defined by $\frac{\#_{last\ image}}{\#_{first\ image}}$

(b) *adhesion vs. track* is defined by $\frac{\#_{tracked\ under\ x\ dyn/cm^2}}{\#_{tracked\ at\ 0\ dyn/cm^2}}$

(c) *track vs. nb image 1* is defined by $\frac{\#_{tracked\ under\ x dyn/cm^2}}{\#_{first\ image\ at\ 0\ dyn/cm^2}}$

(d) *adh fix* is defined by $\frac{\#_{(first\ image-tracked)\ under\ x\ dyn/cm^2}}{\#_{(first\ image-tracked)\ at\ 0\ dyn/cm^2}}$ which delivers the ratio of not moving cells under shear stress compared to no shear.

(e) *l4/l0* is defined by $\frac{\#_{last\ image(4dyn)}}{\#_{last\ image(0dyn)}}$

The resulting ratio is displayed in percent in the results and discussions section and therefore multiplied by 100. Due to the nature of the definitions, the values are always set 100% in absence of shear stress,except for track vs. nb image 1 which is calculated as described above.

3. **yFMI**

   One of the most distinctive attributes of t-lymphocyte migration is their orientation against the flow (*23*). To quantify this, the y-forward migration index (yFMI) is used, which is simply

$$\frac{y-component\ of\ distance\ travelled\ against\ the\ flow}{total\ distance\ travelled} \tag{2.3}$$

   which gives a value between ±1 (completely straight, upright cellular migration against(1) or with (-1) the flow as extremes)

4. **Distinction between movement types**

   This is done by implying the models descibed in 4.1.1, especially pointed out in 4.3 to make the program distinguish between rolling and firmly adhesive cells. Not moving, or stuck, cells are simply calculated by taking the difference between cells in the first respective image and the tracked cells.

2.4 Flow chamber

For all experiments an uncoated μ-Slide VI 0.4 flow chamber connected to an IBIDI pump with a white perfusion set (both IBIDI, Germany) was used.

2.4.1 sample preparation

First, protein A is adsorbed on the uncoated, hydrophobic surface of the flow chamber. Basically it just serves as a linker to optimize adhesion molecule adsorption.Additional reasons why protein A was used as a first incubation step are described in 2.6.7. To passivate the remainder of the surface, Bovine seralbumine (BSA) is used, and as a final step for functionalizing, FC-ICAM (R&D Systems, USA) or FC-VCAM (R&D Systems, USA) is adsorbed. The added Fc-residue of the ICAM and VCAM has a high affinity to protein A and grants adsorption of the protein while sustaining a functional state.

The exact incubation protocol used for the chamber is the following:

At 37°C 5% CO2:

1. 100μg/ml Protein A (Sigma Aldrich, USA) for 2 hours
2. rinsing with 1xDPBS (Gibco, USA),
3. 5% Bovine seralbumin (IDBio, France) for 30 min
4. rinsing with 1x DPBS(Gibco, USA)

at 4°C :

5. Adhesion molecules of diverse compositions and concentrations overnight

First, protein A is adsorbed on the surface of the uncoated flow chamber.Basically it just serves as a linker between the uncoated, hydrophobic surface of the flow chamber and the added adhesion molecules. The attached Fc-fragment of the used ICAM-1 molecule has a high affinity for protein A, improving the spatial orientation of the binding site for the integrins providing a higher functional density of adhesion moelcule. Additional reasons why protein A was used as a first incubation step are described in 2.6.7.

2.4.2 Preparation of lipid bilayers

The next step to approach *in vivo* conditions is to reconstitute funtional adhesion molecules on a lipid bilayer. This results in mobile ligand and possibly different migrational behaviour of the T-cells. For this, 1,2-Dioleoyl-sn-glycero-3-phosphocholine (DOPC; Avanti Polar Lipids, USA) and biotinylated Phosphatidylethanolamine (Bio-PE; Avanti Polar

Lipids, USA) were mixed in the relation 98% DOPC to 2% Bio-PE. The biotin on the PE provides binding sites for streptavidin (Sigma Aldrich, USA) on which biotinylated protein A (Sigma Aldrich, USA) and subsequently Fc-ICAM-1 (R&D Systems, USA) is adsorbed.

Due to the volatile nature of the chloroform based solution some additional steps had to be taken care of during lipid preparation. Following steps of the mixing process are performed under hood: Since the Bio-PE comes in a break-open bottle that can't be closed again some additional steps are necessary before first using the lipids:

1. Wash a glass bottle of appropriate size with chloroform and dry with N2.
2. Wash glass pipette with chloroform.
3. Crack open container with the Bio-PE and immediately transfer whole content as fast as possible with the glass pipette to the washed glass bottle.
4. Flood with N2 and close bottle, seal with parafilm

These steps were necessary for the initial transfer of the lipid dissolved in chloroform to aliquotes. To prepare the proper mixtures of lipid the following protocol was used:
Under the hood:

1. Wash a small glass container of appropriate size with chloroform
2. Open bio-PE bottle, and transfer 29μl of DOPC into glass container (for this step it is necessary, although not ideal, to use plastic pipette tips to transfer the correct amount of lipid) as fast as possible.
3. Flood DOPC bottle with N2, close and seal with parafilm.
4. Open Bio-PE bottle, and transfer 2μl of Bio-PE into glass container (for this step it is necessary, although not ideal, to use plastic pipette tips to transfer the correct amount of lipid) as fast as possible.
5. Flood Bio-PE bottle with N2, close and seal with parafilm.
6. Put glass bottle with the lipid mixture in 38°C heat reservoir and expose it to a continuous stream of N2 for at least 30 min or until dried.
7. Make sure all chloroform is evaporated so only a dried film of lipid remains at the bottom of the glass bottle.

From here on, the hood is not necessary anymore to prepare the aliquotes:

1. Add 1.85ml of 1xPBS to the glass bottle to resuspend the dried lipid film and reach a final concentration of 0.4mg/ml.
2. Vortex the solution repeatedly for 10s with 10s break in between to ensure proper resuspension, the solution should look milky now.
3. Sonicate lipid solution for around 2 minutes at medium intensity (25-30% power) using a tip sonicator.
4. Aliquote solution to desired portions (100 μl).

To prepare the sample surfaces we procede:

1. Deposit the vesicles on a hydrophilic substrate (plasma treated glass device) and leave at room temperature for 30min
2. Wash 5-10x with milliQ water to burst out the vesicles onto the surface. Equilibrate with 1x wash with PBS
3. (Optional) Block the surface with BSA/PBS at room temperature for 30 min.
4. Incubate the Streptavidin at room temperature for 30min.
5. Incubate the ProtA btwn 50-100 μg/ml at room temperature for 1h.
6. Incubate the ICAM-1 at room temperature for 1h.

2.5 Substrate rigidity dependent measurements

As described in 2.2.2 experiments on custom made polyacrylamide gels did not work. The results presented in 5.1 were obtained with commercially available products, namely μ-Dish 35 mm, high ESS dishes (IBIDI, Germany) of 1.5, 15 or 28 kPa rigidity. To functionalize the surfaces, a small PDMS mask was used to optimize the active area of the gel. This mask was plasma cleaned on low intensity for 2 min before putting it on the sterile surface. The incubation protocol afterwards is similar to the flow chamber: At 37°C 5% CO2:

1. 100μg/ml Protein A (Sigma Aldrich, USA) for 2 hours
2. rinsing with 1xDPBS (Gibco, USA),
3. 5% Bovine seralbumin (IDBio, France) for 30 min

4. rinsing with 1x DPBS(Gibco, USA)

at 4°C :

5. 10μg/ml ICAM
   overnight

2.6 Fluorescence quantification of adhesion molecules

To quantify the amount of incubated ICAM that binds to the IBIDI fluorescence measurements are used. To make measurements easily comparable, for both ICAM and also VCAM the same staining on the specific antibody is used (anti-human-ICAM-1-PE / anti-human-VCAM-1-PE; Affymetix, USA) and also the same light intensity is always chosen. To determine the amount of bound ICAM alone a mixture of ICAM and human IgG was used to have a binding competitor for ICAM and to maintain the same overall protein concentration in volume. For all measurements including VCAM, a mixture of ICAM and VCAM was used (see below). All measurement and preparation steps are the same for ICAM and VCAM unless otherwise noted. Due to an early stage of the experiments, a non-linear binding dynamics of ICAM and VCAM was noticed and rectified by using Protein A. In this report only the measurements on ICAM are described, VCAM works the same way.

2.6.1 Sample preparation

1. 50μl Protein A (100μg/ml) per IBIDI channel for 2h
2. Wash 3x100μL PBS
3. 100μl BSA 2.5% weight BSA in 97.5
4. Wash 3x100μl PBS
5. ICAM/VCAM mixture 30μl per channel (10μg/ml in total), overnight

All incubation steps are done at 37°C at 5% CO2 except the last one, which is done overnight at 4°C. Previously only step 5 was done, with no surface modification by Protein A, this lead to an extreme imbalance of Protein adsorbtion in favor of VCAM.

2.6.2 ICAM/IgG mixtures

ICAM and IgG are diluted to 10μg/ml with PBS. For the IgG it is important to use the theoretical weight (76kDa) for calculation, not the experimental (100kDa) (The experimental weight is due to polarity generated by protein folding. This makes the protein run faster through a gel, so the determined weight is too high).
5 Different ratios are incubated

1. 100% ICAM / 0% IgG (30μl ICAM)
2. 75% ICAM / 25% IgG (22.5μl ICAM / 7.5μL IgG)
3. 50% ICAM / 50% IgG (15 μl ICAM / 15 μL IgG)
4. 25% ICAM / 75% IgG (7.5μl ICAM / 22.5μL IgG)
5. 0% ICAM / 100% IgG (30 μL IgG)

It is important, that both Proteins are mixed before incubation and not subsequently incubated on the same channel, because of possible different association constants.

2.6.3 ICAM/VCAM mixtures

ICAM has a molecular weight of 76kDa and VCAM (101.6kDa), which means the weight ratio VCAM/ICAM is 1.34. This means we prepare the ICAM solution with 10μg/ml with PBS and the VCAM to 13.5μg/ml. Stock of both ICAM and VCAM is 500μg/ml: ICAM: 3μl stock in 147μl PBS VCAM: 3μ stock in 108μl PBS 5 Different ratios are incubated

1. 100% ICAM / 0% VCAM(30μl ICAM)
2. 75% ICAM / 25% VCAM (22.5μl ICAM / 7.5μL VCAM)
3. 50% ICAM / 50% VCAM (15 μl ICAM / 15 μL VCAM)
4. 25% ICAM / 75% VCAM (7.5μl ICAM / 22.5μL VCAM)
5. 0% ICAM / 100% VCAM (30 μL VCAM)

It is important, that both Proteins are mixed before incubation and not subsequently incubated on the same channel, because of possible different association constants.

2.6.4 Fluorescent antibody incubation

40μl of pure AB* is mixed with 160μl PBS to receive a AB* concentration of 10 μg/ml. After washing the channels with PBS (3x100μl) 30μl of the AB* dilution is pipette into each channel.

1. Remaining liquid on IBIDI channel was removed. Thin film has to remain, to avoid bubbles and drying out.
2. Wash 3x100μl PBS
3. Incubate with 30μl AB* dilution with 10μg/ml ON at 4°C in aluminium foil (to avoid bleaching of fluorophores by daylight)
4. Wash 3x100μl PBS

2.6.5 Calibration

To calibrate the obtained fluorescence data and transform them into a surface density, various dilutions of the fluorescent antibody (called AB* from now on) are prepared (mostly 7/5/3/1.5/0 μg/ml. In general the range of calibration dilutions should be chosen after measuring the sample) . The concentrations have to be chosen in a way to cover the range of fluorescence of the sample in a proper way. It is important to slightly vortex the AB* stock solution before preparing the dilutions. These dilutions are filled into a PDMS microfluidics channel of 30μm height and subsequently the fluorescence signal of each channel is obtained. Here a low intensity and longer illumination time is chosen to avoid photobleaching of the used fluorophore. Repeatedly measuring the calibration signals revealed, that this method is very stable and extremely linear. Another method to improve the stability and robustness of the measurement is to rinse the channels with PBS after obtaining the signal and measuring the fluorescence signal of the rinsed channels again. This signal serves as background for each channel and is thereforee subtracted from the initial signal. This is valid since a lot of fluorophore is unspecifically adsorbed on the walls of the porous channel. This adsorbed fluorophore does not change the concentration in the bulk, but adds additional “false” fluorescence to the obtained signal and should thereforee be subtracted. Plotting the measured fluorescence of diverse solutions over their concentration in volume provides a calibration curve like in figure 2.2)

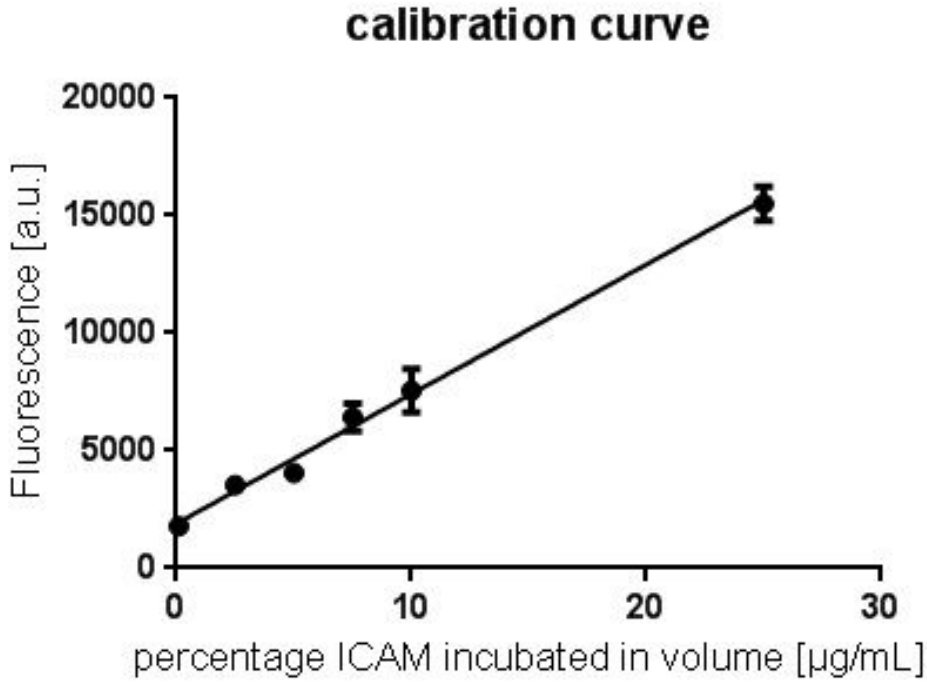

Figure 2.2: Calibration curves for ICAM for 400ms illumination time (fluorescence signal over theoretical surface density of AB*). Mean + standard deviation. 5 different spots on sample were evaluated. Data from 151109

2.6.6 Fluorescence calibration measurement procedure

As general rule to avoid photobleaching the illumination intensity should be kept low and only the excitation time should be used as adjustment for optimum yield. Optimum time for a given excitation intensity is characterized by being close to the saturation level of the camera when measuring the substrate with the highest fluorescence. This improves the stability of the signal as well as sensitivity, although there should remain a little 'top space' between sample signal and saturation to adjust the calibration spectrum optimally. In all cases several images should be made to average their intensity and check homogenous coverage of the substrate. In the calibration solutions the exact positioning of the focal plane is not important since the fluorophor distribution is homogenous in bulk. On the other hand it is important when measuring the sample, to be focused on the surface where the adhesion and signal should be maximal. The exact plane is easily found due to formation of fluorophor clusters, on which to focus.

2.6.7 Conversion

To obtain a surface concentration of the AB* in desired units [molecules/μm^2] the following estimation is used: If a certain amount of fluorophores F in a channel with the

height of 30 μm yields a fluorescence signal x, and the same concentration of fluorophores is adsorbed on a surface (due to the high specificity and adsorbtion coefficient of the antibody), one can multiply the height of the channel with the concentration of the AB* to convert it into a surface density. The underlying principle can be seen in figure 2.3

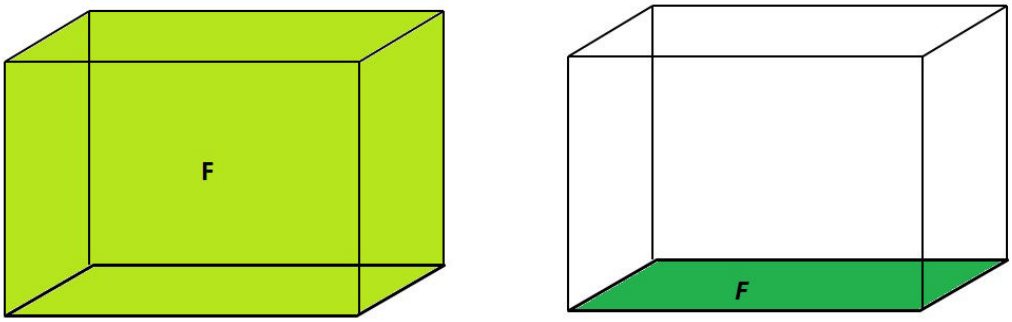

Figure 2.3: The same amount of fluorophores F distributed in a volume (left) and adsorbed on a surface (right)

So the conversion factor k (μg/ml to molecules/μm^2) can be calculated:

$$k = \frac{C\left[\frac{\mu g}{ml}\right] * height\,of\,channel * \mu g\,to\,ng * cm^2\,to\,\mu m^2 * ng\,to\,kDa}{weight\,of\,AB[kDa]} \tag{2.4}$$

The used channel had a height of 30μm which leads to following coefficient:

$$k = \frac{C\left[\frac{\mu g}{ml}\right] * 30 * 10^4 * 10^3 * 10^{-8} * 6.022 * 10^{11}}{150} \tag{2.5}$$

or

$$k = C\left[\frac{\mu g}{ml}\right] * 120.44 = C\left[\frac{molecules}{\mu m^2}\right] \tag{2.6}$$

The channel height is to be chosen freely within certain constraints: too thin channels were difficult to fill and the required pressure may lead to detachment of the PDMS

from the glass and inhomogenous distribution of the solution, while the signal of too high channels may not be fully recorded by the limited focal depth of the microscope. Applying this calculated theoretical surface density as new unit of the x-axis in calibrationsee (see figure 2.4), the resulting gradient can be used to determine the surface density of the AB* (and therefore the ICAM/VCAM) by simply dividing the resulting fluorescence signal obtained by the sample of interest by the gradient.

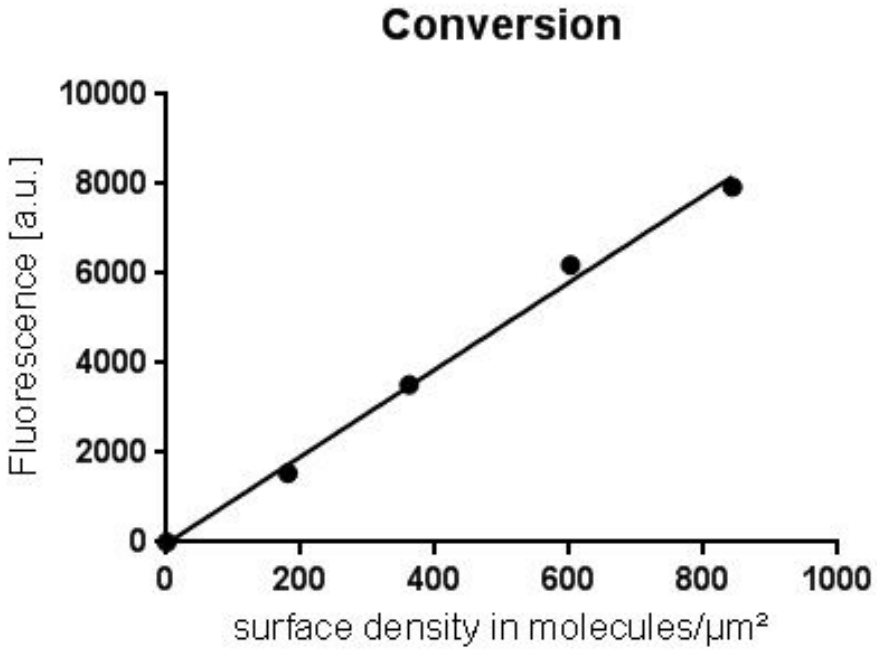

Figure 2.4: Calibration curve minus individual channel background (fluorescence signal over calculated surface density of AB*) for 400ms illumination time. Mean + standard deviation (too small to be visible).5 different spots on sample were evaluated. Data from 151109

Repeated experiments and applying methods described above deliver the relation between incubated concentration in bulk and surface density of adsorbed antibodies, see figure 2.5:

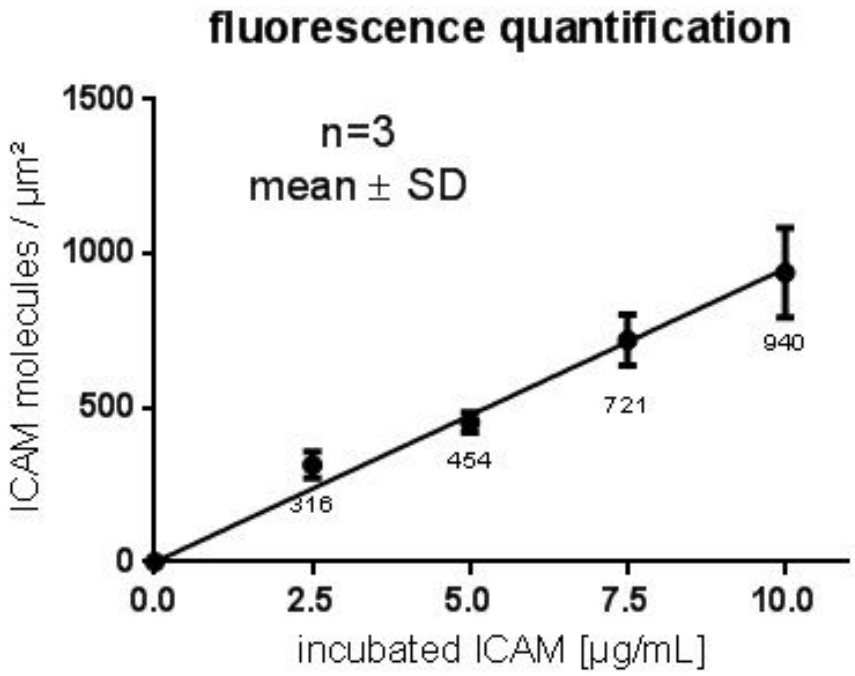

Figure 2.5: surface density of ICAM and linear fit. Actual values (rounded) underneath data points

This protocol is highly robust and reproducible as can be seen on the error bars. To show that the substrate protocol Protein A-BSA*-ICAM is efficient, a comparison to previously used protocols was done. Although the increase in fluorescence for 44-66-100% ICAM is not linear as expected, it shows, that the values are still in the same range as seen in figure 2.6

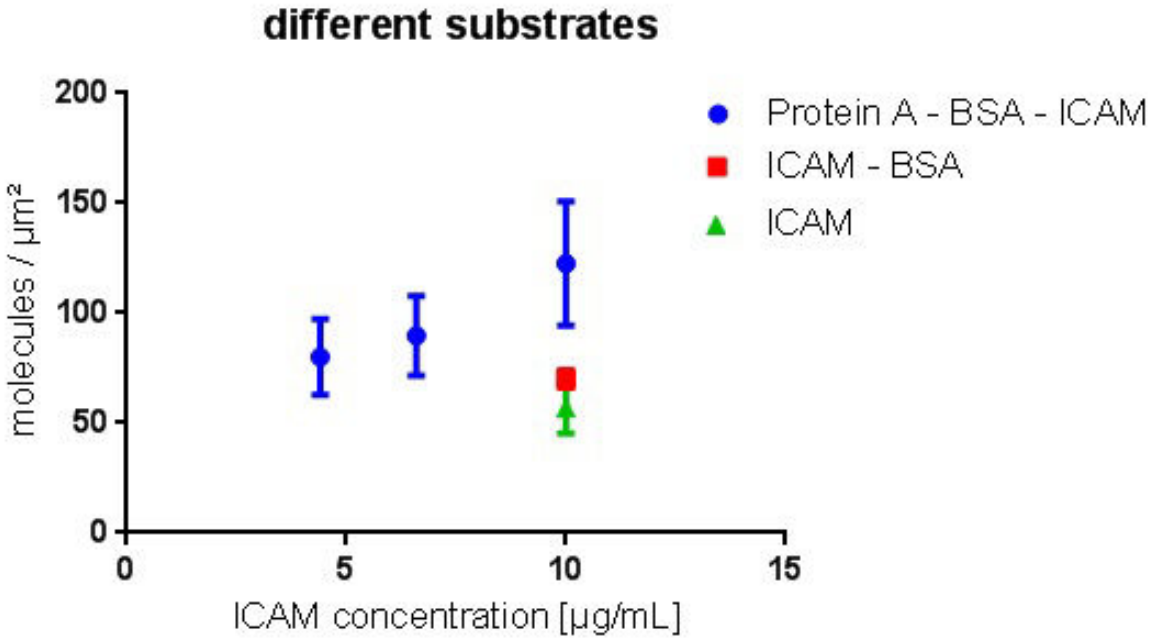

Figure 2.6: Comparison of different substrate preparations using the calibration method. Mean+SD, 3 different spots on the sample were averaged. illumination time 200ms. Data from 141124

Results without protein A

Initial experiments were done without the use of a bottom Protein A layer which resulted in an extreme imbalance between ICAM and VCAM. This might be due to the fact that, on our given substrate, VCAM adsorbs sterically more favourable or simply faster than ICAM. The underlying mechanisms are although unclear, especially regarding the very similar structure and weight of the proteins. A graphic representation can be seen in figure 2.7. Both proteins were labelled with the same fluorophore (and therefore measured on separated surfaces) to have a similar yield in fluorescence. The non-visible error bar for the datapoints is because of the high reproducability of the measurement. The following two graphs describe the adsorption behaviour of ICAM-1 and VCAM-1 examined via fluorescence measurements. The x-axis describes only the concentration of ICAM-1, the VCAM-1 concentration is complementary to 10μg/ml meaning $C_{VCAM}[\mu g/ml] = (10 - C_{ICAM})[\mu g/ml]$

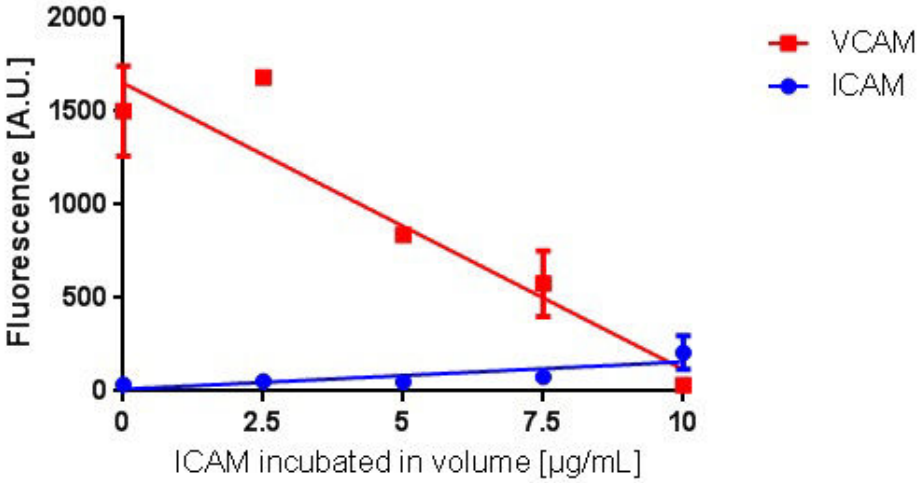

Figure 2.7: Calibrated image showing the extreme imbalance between adsorbed ICAM and VCAM (arbitrary units over incubated concentration of ICAM, plotted are the means with SEM, n=2).

Results with Protein A

However adding protein A ensured a more balanced distribution of both adhesion proteins (see figure 2.8

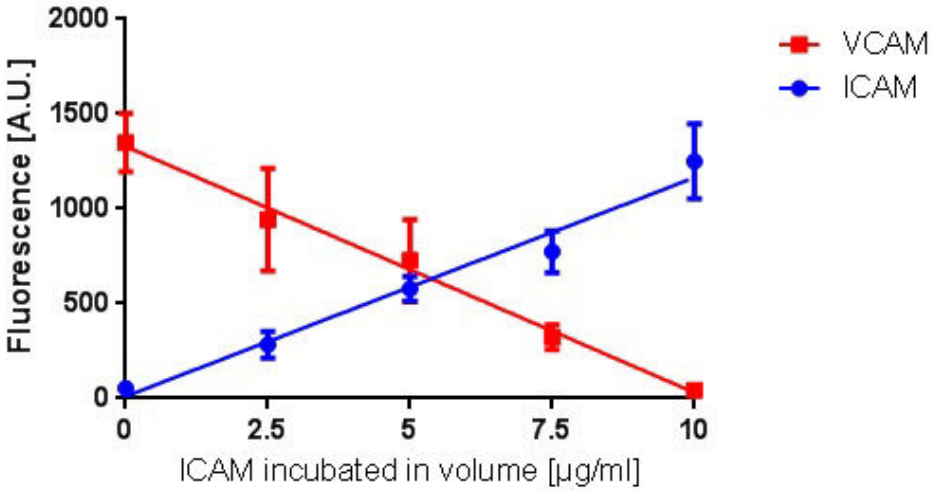

Figure 2.8: Calibrated image of ICAM and VCAM on protein A surface including linear fit (plotted are the means with SEM, n=4).

As can be seen, protein A does not only equalize the adsorption of both adhesion molecules in terms of quantity but also in terms of linearity.

2.7 Cell seeding and incubation procedure on the IBIDI flow chamber

This is the standard protocol for setting up a measurement on analysing cell motility, used for every experiment regarding cell tracking unless stated otherwise:

1. Heat the microscopy chamber to 37°C
2. Fill up the IBIDI pump reservoirs with medium (RPMI), connect the tubing without attaching any sample, start the circulation of the buffer to equilibrate and get rid of air bubbles in the medium for around 10 min.
3. Wash functionalized IBIDI channel once with buffer, remove as much liquid from the channel as possible without generating air bubbles within the chamber. A thin film of liquid has to be maintained at the surface at any time.
4. Seed cells, 50-100μl at a concentration of 1.5 million cells/cm^3
5. Let incubated channel rest under 37°C at 5% CO2 for around 10 min
6. Fill up both ports of the channel with medium up until the point where a dome of medium generated by surface tension is emerging.
7. plug both ports to the IBIDI pump while avoiding bubbles within the system. During plugging and de-plugging, the tubing has to be clamped to avoid spill of medium.
8. rinse channel at 1 dyn/cm^2 for approx. 1 minute to wash away non-adherent cells

2.8 Measurement procedures and data analysis

After preparing the samples for the migration experiments as described in 2.7 the plugged IBIDI-chip with the flow chambers is set up for measurements in the isolation chamber of the microscope at 37°C . Optionally, one image is taken of the seeded cells before washing to compare pre- and postwash images to measure adhesion. Individual measurements can be compared regarding adhesion, since the cells in suspension are prepared during cell culture at homogenous concentration of 1.5 million/ml. Supposing uniform seeding behaviour, the resulting surface concentration of cells should be also equal among various channels and also dates. If not stated otherwise, each channel, after washing, is used three times: first measurements are done in the absence of

flow, to reduce residual flow coming from the tubing system of the pump, the tubes are clamped. Additionally, one image of the background is taken (usually next to the incubated channel) and substracted afterwards from each frame. After this, the clamp is removed and the pump is set to a flow of 4 (second experiment) or 8 (third experiment) dyn/cm^2. Each of these three experiments are performed for 100 frames with a sampling rate of 10s/frame, which corresponds to 16min 41s. Pauses between these three data sets are kept to a minimum so it is essentially possible to examine the same set of cells for 3 different shear stresses (unless cells move in or out of the field of view). The genereated movies for each shear stress are then imported to the custom MATLAB software, where the position of the cells on each image are located and their trajectories taken. Various cells are sorted out during this whole process, mechanically, by washing away non-adherent cells, and also by the software, since only cells are taken into account, who move for a minimum of 30μm since only functionally migrating cells are of interest. This point is important and has to be taken into consideration when looking at data like speed or yFMI, because it intentionally includes inert cells.
The trajectories of the selected cells are then furthermore processed by the MATLAB programs to evaluate their yFMI, distance travelled, speed and directionality (a more generalized version of the yFMI where the distance between first and last image is divided by the total distance travelled by the cell).
Fluorescence experiments are performed at room temperature and without shear stress. For calibration in volume, one focal plane within the channel is chosen at will. At least three images are taken for each concentration at different locations to avoid photobleaching. When measuring fluorescence at the actual sample, it is imoprtant to set the focal plane as exactly as possible on the actual sample surface by focussing at impurities or clusters of fluorophores on the sample to provide optimal sample signal. Again, several different locations on the sample should be measured and afterwards averaged.

2.8.1 The cell as a random walker

Applying the movement analysis shown in figure 4.2 and in the absence of any shear force, it can be clearly seen that all cells, independent of their integrin expression and the composition of their underlying substrate, migrate at a constant speed. Henceforth, in absence of any other (anisotropic) cues or obstacles, chemical or mechanical, their movement could be described as a random walker following two-dimensional brownian motion. therefore the only variable we would need to describe this type of cellular movement could be described by the diffusion coefficient D [$\mu m^2/min$] and Einstein's formula (*61*)

$$MSD = 2n_{\text{dim}}Dt \tag{2.7}$$

with MSD as the mean square displacement, n_{dim} as the number of dimensions (in our case 2, since we only consider planar movements) and T as the absolute temperature. Out of reasons of completion it should be mentioned that in Einstein's theory D is defined from a fluid- and thermodynamical point of view :

$$D = k_{\text{b}}T/\gamma_0 \tag{2.8}$$

where k_{b} is Boltzmann's constant and $\gamma_0 = 6\pi\eta a$ is Stokes drag coefficient for a rigid sphere with radius a moving with constant speed through a resting fluid with the dynamic viscosity η. In our experimental setup this model is too simplistic and has to be expanded, because we are not in the realm of pure thermodynamics and brownian motion. The model implicates continuous random movement over the surface and does not consider discrete steps or changes in direction. In our case this has to be considered because of integrin-adhesion molecule interactions. These provide not only bindings that eliminate completely stochastic behaviour due to non-zero on- and off-rates but also introduce cellular signaling which makes cell movement less random. Since this receptor-ligand expansion of the model is the only significant change (the remaining experimental setup as medium, substrate etc. stays the same) it is possible to link the diffusion related parameters to aspects of the cell-surface interactions like integrin density and overall affinity.

Rearrangements of the cytoskeleton who are responsible for directional switches as described in 1.3 do not happen in zero-time so a change in movement always implies a change of polarity. This requires an additional temporal parameter, persistence time P [s], which describes the discrete time steps a cell undergoes before it is able to change direction by managing these rearrangements. Another way of explaining this is to consider persistence as "remembering" movement direction (by the spatial structure of the actin network and polarity) and preferring to take a step in the same direction as the previous one (*62*). If the cell moves with continuous speed v_{cell}, as in our case, this persistence time correlates with persistence length L

$$L = v_{\text{cell}} * P \tag{2.9}$$

analogous to a worm-like chain model. It has already been shown that there is a direct relation between cell speed and persistence length/time and that high speeds stabilize upkeep of cytoskeleton polarity (*63*). Including the new parameter P to include directional stability by polarity upkeep integrin-surface interactions we can now use Fürth's

equation to describe our cell trajectories (*64*)

$$MSD = 2n_{\text{dim}}D(t - P(1 - e^{-t/P}) \tag{2.10}$$

this formula is a consequence of the Langevin equation (*65*)

$$m\ddot{\vec{x}}(t) = -\gamma_0\dot{\vec{x}}(t) + \vec{F}_{\text{thermal}} \tag{2.11}$$

which describes the speed of a brownian particle with the inertial mass m in a liquid exposed to Stokes friction force $-\gamma_0\dot{\vec{x}}(t)$ and a random thermal force $\vec{F}_{\text{thermal}} = (2k_{\text{b}}T/\gamma_0)^{1/2}\eta(t)$. So we can rewrite formula 2.10 into the following form

$$P\frac{d\vec{v}}{dt} = -\vec{v} + (2D)^{1/2}\eta \tag{2.12}$$

simply by setting $P \simeq m/\gamma_0$ and inserting 2.8 which gives as a rephrased form of the Langevin equation with our parameters D and P, the *Ornstein-Uhlenbeck process* (OU-process) (*66*) although it has to be stated that this description should be handled in mathematical and not in physical terms, since the inertial mass of a cell, regarding its velocity, is irrelevant for its motion as well as friction in surrounding medium need not be considered because of the firm attachment to the substrate, described above (*62*).

Going back using formula 2.10, we now have a convenient tool for fitting cellular migration to obtain diffusive parameters. This would deliver values for both D and P although one can reduce the system to one variable which results in an even better fit. For this we have to introduce the concept of intrinsic speed: First of all we have to expand the basic formula for linear translation

$$s = vt \tag{2.13}$$

into square form, so that the distance becomes an area that we can identify with the mean squared displacement of the cell.

$$MSD = s^2 = v^2{}_{\text{intrinsic}}t^2 \tag{2.14}$$

and further

$$v_{\text{intrinsic}} = \sqrt{\frac{MSD}{t^2}} \tag{2.15}$$

By definition, our cells follow a linear regime within a certain, small timeframe, smaller than P, so a linearization by a Taylor-approximation for t 0 makes sense. Developping the Taylor-series of formula 2.10 to the first non-zero term at the second degree

$$T = f(0) + f'(0)t + \frac{f''(0)}{2}t^2 \tag{2.16}$$

gives us the Taylor-linearization of MSD, MSD^*

$$MSD^* = \frac{2D}{P}t^2 \tag{2.17}$$

which already looks like formula 2.14 and the term $\frac{2D}{P}$ can be identified with v^2 which leads to the final form of the intrinsic speed $v_{\text{intrinsic}}$ (*67*)

$$v_{\text{intrinsic}} = \sqrt{\frac{2D}{P}} \tag{2.18}$$

First this seems to be a rather theoretical value derived by a mathematical approach, but our cells are always migrating at a constant speed over the whole time frame, with hardly any fluctuations. therefore it is allowed to use the measured mean speed of the cells of one data set and use it as $v_{\text{intrinsic}}$ and furthermore reduce the amount of unknowns to 1 by reformulating formula 2.18 to

$$D = \frac{Pv^2}{2} \tag{2.19}$$

And then inserting in formula 2.10 which is reduced to one unknown parameter P to which we can fit. Out of convenience reasons, we divide Fürth's formula (2.10) by t. In this form, the function converges to 4D for $t >> P$ so a quick look at the graph is enough to check the robustness of the data. Finally this provides a convincing way to determine diffusion coefficient and persistence time out of the collected trajectories to look for correlations with integrin expression and surface interaction .

Results and discussion

To obtain quantifiable data on the motility properties of effector T-cells, several parameters have to be controlled to identify cause and effect of cell migration. While previous publications on which this work is based were only working on one specific substrate (*22*, *23*), the first task in the frame of this thesis was to develop a method with which it is possible to quantify and control the amount of adhesion molecules on the substrate. To analyze the connections between cellular movement and substrate density, the initial aim was to develop a method with which one can grant a direct and robust protocol to transfer incubated densities of ligand in volume to adsorbed densities on an area. Although the method which was developed for that could be counted as a result, it is described in the materials and methods section and only briefly summarized in 3.1.
Having created these tools, we developed a protocol to be able to create substrates with adjustable densities. The main challenge therein lies to grant a linear correlation between the concentrations of the incubated solutions of adhesion molecules and the final concentrations on the substrate, a problem that could be solved by first covering the flow chamber with soluble protein A and subsequent use of adhesion molecules with an Fc-terminus. This antibody part, added to both used adhesion molecules, granted uniform binding behaviour to the surface, an aim that could not be realized without the use of protein A (see also 2.4.1). No matter what molecules are used for the substrate, ICAM-1, VCAM-1 or IgG, all involved components have the same reactive group and bind with the same properties. ICAM-1 and VCAM-1 are used as functional adhesion molecules, their importance for leukocyte migration is explained in the introductional part of this work, whereas human IgG is only used to maintain the same amount of surface binding molecules in solution to grant unchanged binding kinetics.
Now, able to control substrate composition in a stable and reproducible manner, the migrational properties under flow in which we are interested in, can be examined and linked to the quantifiable properties of the substrate. Attributes like adhesion, directionality, speed or amount of cells can be observed, quantified and set in context to the cell's reaction to its ligands. For only ICAM-1 first, then expanded and complexified for added VCAM-1, to add various degrees of freedom like cell movement type, subpopulations, etc.. All described experiments are performed as in the description given in 2.8

Chapter 3

Quantification of lymphocyte migration on ICAM/IgG substrates

3.1 Surface density analysis of adhesion molecules on IBIDI flow chambers

As a necessary preliminary step to justify the legitimacy of the results of this work it was important to first establish a protocol which allows the measurement of the surface density of the incubated adhesion molecule. Out of reasons of structure, this procedure is in general already described in 2.6 in the materials and methods section, although it can also be considered as a result of this work. Insofar only additional practical considerations in applying this method are mentioned here.
Rectangular PDMS channels usually used for microfluidics measurements were used for calibration due to their small adjustable incubation volume and especially channel height. These small volumes provide several benefits: First of all the small amount of reagents that is necessary and second the ability to use channel heights which are of similar size as the focal depth of the microscope.
The increase of channel height also increases the fluorescence yield, since more fluorophores are contributing in z-axis. On the other hand the focal volume, fluorescent solution that can be illuminated and therefore contributes to the obtained signal, is, amongst other parameters, defined by the z-axis component of illumination. If the channel exceeds this z-axis, the underlying assumption of the calibration does not apply anymore which is the following: If a given volume and a given surface deliver the same fluorescence intensity, the amount of particles in volume equals the amount of particles on the surface. If although the (z-component of the) measurable volume is lower than the channel volume, the calibration strategy would deliver too low density results since it would neglect the contribution of the molecules in the height difference.

Performing the calibration, various factors had to be considered, such as illumination time: Where too long exposition leads to photobleaching of the fluorophore, too little time does not yield enough signal, so the whole spectrum of the camera cannot be used for optimum results. Second, a reasonably big span of fluorophor concentrations have to be used to cover all possible sample densities, etc. Testing various channel heights, 30μm turned out to be the optimum balance between the previously described parameters. Bigger channels turned out to be less feasable for bigger incubation volumes are needed, whereas small channels turned out to be difficult to fill and often collapsed. The used channels delivered the following results (already shown in 2.6.7):

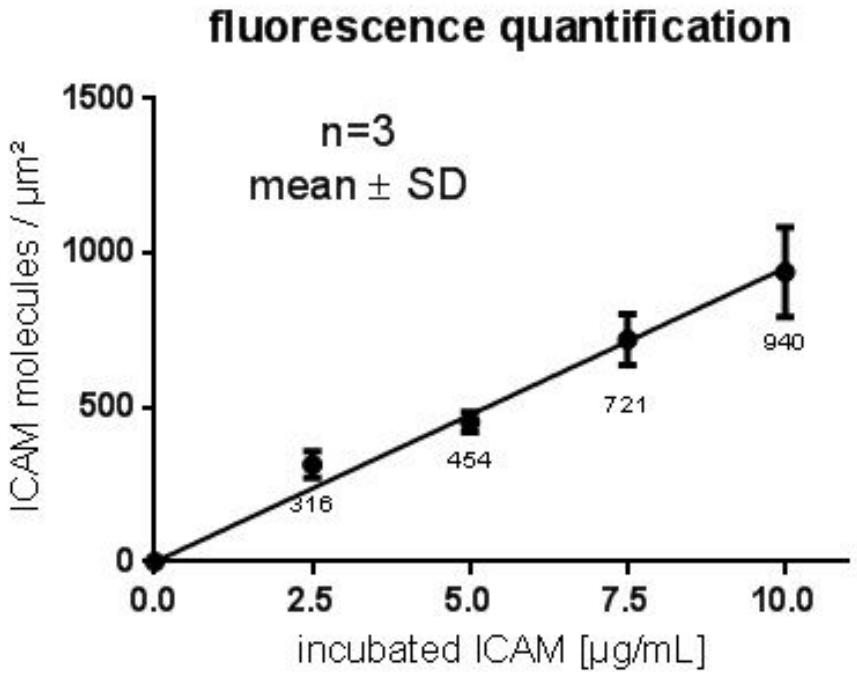

Figure 3.1: surface density of ICAM and linear fit. Actual values (rounded) underneath data points

Considering the expression level of ICAM-1 , which reachs from 100 molecules/μm^2 for non-inflamed and 1000 molecules/μm^2 for inflamed human endothelial cells (*33*), the used concentrations cover well the physiological spectrum and validate the obtained results regarding cell migration.That is why these concentrations were used in the following experiments. Further experiments have shown, that for concentrations bigger than 10 μg/ml the linearity in figure 3.1 collapses and a saturation effect occurs.

3.2 Quantification of lymphocyte migration on ICAM/IgG substrates

Considering the involved components in lymphocyte cell migration, these primary findings presented here represent a minimum setup of experiments: Only one type of adhesion molecule is involved and, on the cellular side, no external influence on the integrins was exercised. A surface only consisting of ICAM-1 as active component was prepared according to the protocol in 2.4.1 to determine cellular migrational behaviour depending only on shear stress and surface density of ligand as tunable variables. Flow chambers of various surface densities were fabricated, and initially tested using the developed protocol described in 2.6 to ensure that the proportion of functional ligand to competing IgG was granted in volume as well as at surface.

3.2.1 Ligand density

Speed

Previous findings show that the speed of the cells is independent of the shear stress they are exposed to (*22*, *23*), although these measurements were only made on one defined substrate density. As quoted in the introduction, this is due to the significantly larger force generated by the motility apparatus of the cell compared to the effectively acting shear forces on the cellular cross section.

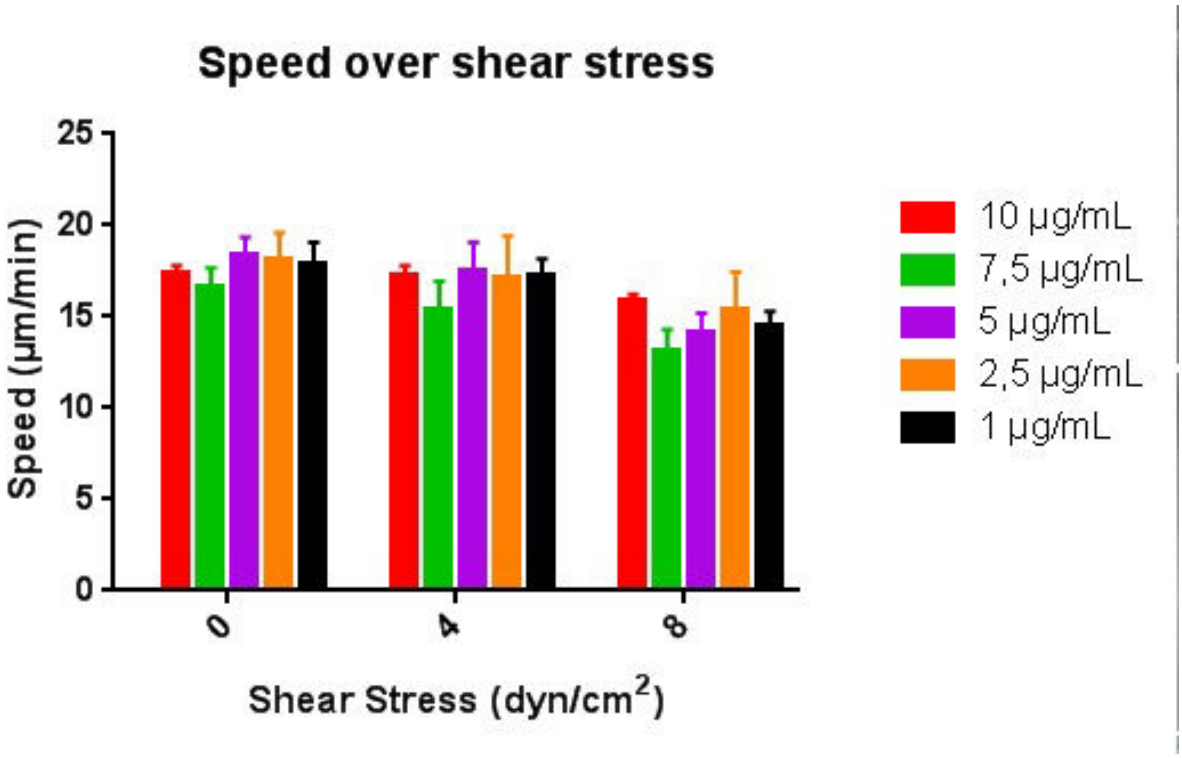

Figure 3.2: Average cell speed (n=3) dependent on shear stress and adhesion molecule surface density. All concentrations given are for ICAM-1

A two-way ANOVA test run on the data shows no statistical significant influence of substrate density on cell speed. A finding which can be seen in context with 1.3.2: Additionally to the rate of actin-polymerization, availability of binding partners for integrins is not the limiting factor for cell speed. Also the energy used to break up bonds to the surface, which derives from polymerization, seems to be negligible as can be seen in fig 3.2: Although there is a 25-fold surface density decrease in ligands for potential binding between the highest and the lowest tested substrate, the theoretical energy saving is not converted into higher cell speeds.
Looking at the speeds for each shear stress, it might imply that general cell speed is slightly decreasing. This is only partially true due to cell selection. The variety of adhesion strength depending solely on cellular attributes like amount of integrins, conformation and distribution leads to the fact that a non-negligible subgroup of cells, which are functionally adherent and migrating under absence of flow, might not be able to remain attached and get washed away by the current, therefore not contributing to the average cell speed calculations anymore. Even though this effect is visible and common, it does not have statistical influence on the result.

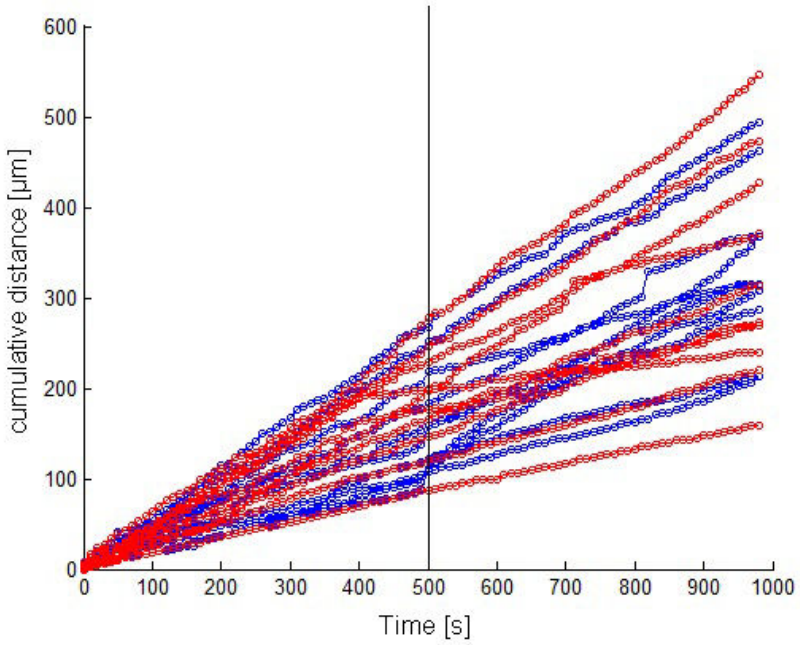

Figure 3.3: Cumulative distance over time for individual T-cells on ICAM-1. The first 500 seconds the cells are not exposed to flow (left), then immediately 4 dyn/cm^2 shear stress are applied (right). Blue lines represent cells with a positive yFMI, red lines represent cells with a negative yFMI

.

To prove that speeds do not change with shear stress, cumulative distances of the cells can be seen in 3.3. The speed is constant, both without and with shear stress (areas split with the line), so the slope of these functions does not change as a function of flow.

Adhesion

As already mentioned in 3.2.1, application of shear stress imposes a mechanism of selection, where cells with lower adhesive properties are not able to sustain migration. To explore a possible relation between adhesion molecule density and adhesion, the definitions in 2.3 were used:

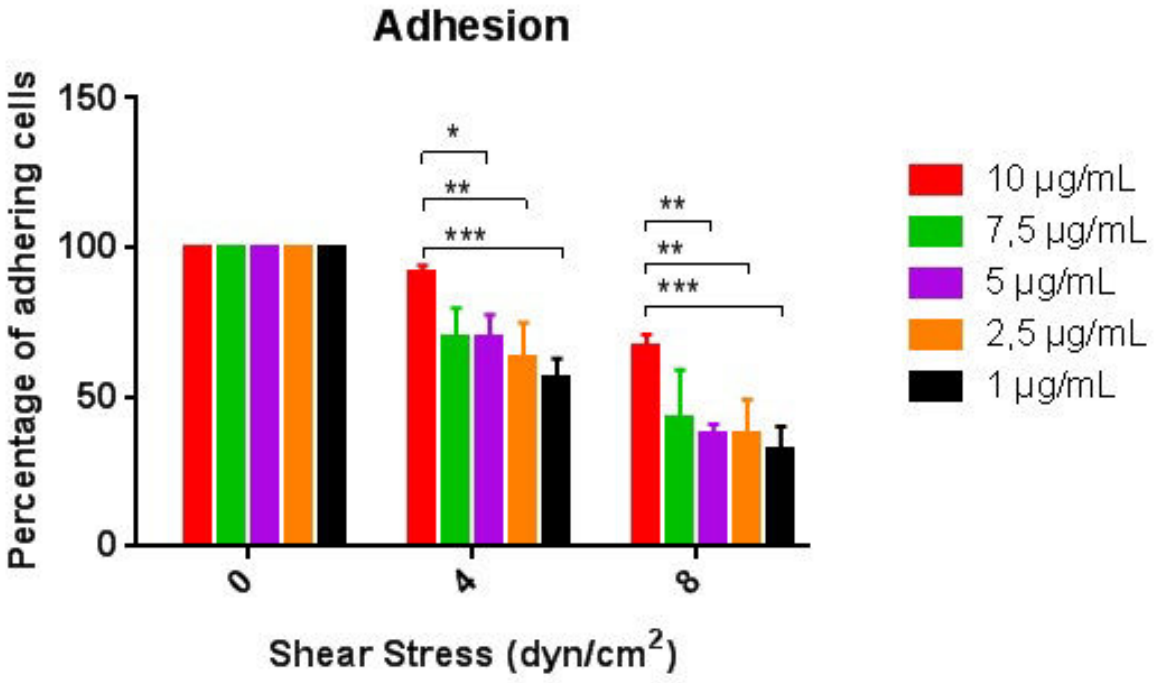

Figure 3.4: Adhesion (n=3) dependent on shear stress and adhesion molecule surface density. All concentrations given are for ICAM-1.

Unless otherwise stated, in all figures concerning adhesion the adhesion vs track definition is used: Per definition, 0 dyn/cm^2 is the reference value and after discarding all non-adherent or immobile cells by rinsing the sample with 1 dyn/cm^2, the statistics are valid for adherent, moving cells only. Here the adhesion clearly drops of with decreasing surface density, nearly linear for 4, and even stronger for 8 dyn/cm^2.

yFMI

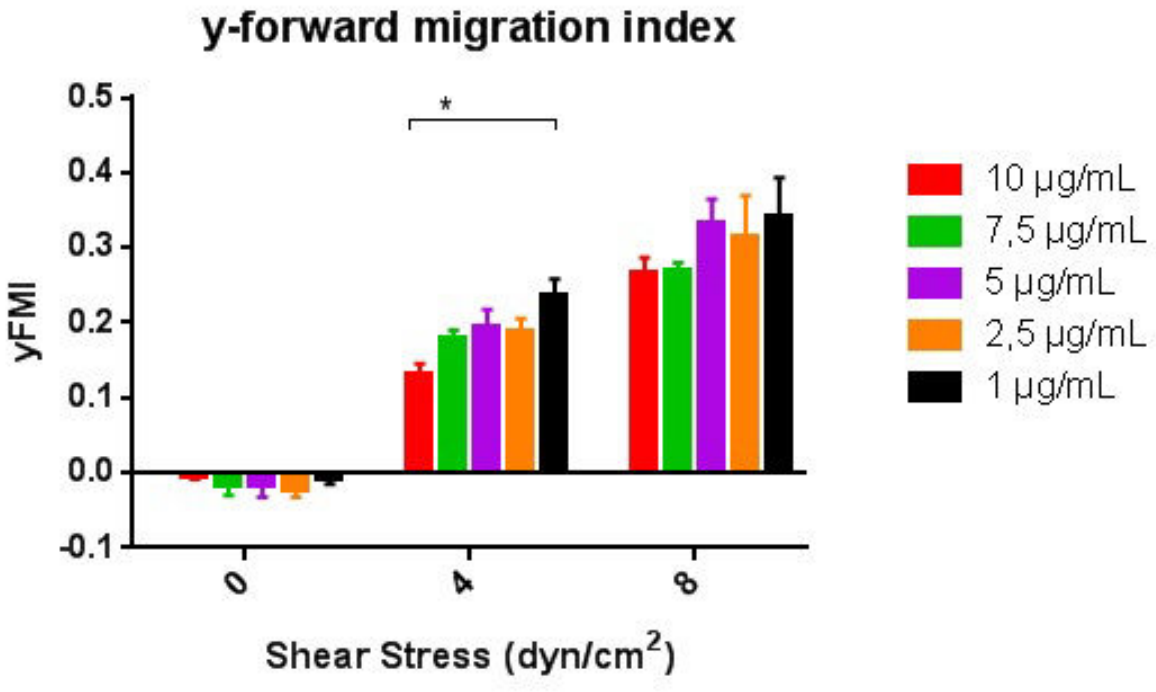

Figure 3.5: y-forward migrational index (n=3) dependent on shear stress and adhesion molecule surface density. All concentrations given are for ICAM-1

Looking at the yFMI it is evident that there is a more directed migration for decreasing densities of ICAM-1.

Diffusion coefficient and persistence time

To this point, all data acquired without shear stress attracted little interest, since all the characteristic features of cell motility emerge or are emphasized only in presence of flow. Using the theoretical background provided in 2.8.1, we introduce another way of analyzing the interaction between the cell and its substrate. Treating the cell as an object undergoing stochastic movement (with the sole additional introduction of a persistence time/length as confinement) one obtains a tool to mathematically describe the differences of the trajectories dependent on integrin ligation (or even without). Using the diffusion coefficient D, which describes the area covered by a cell within a certain time, instead of the previously used parameter of speed, we expand our description of cell motility. Before introducing the results, we summarize and apply the mathematical description given in 2.8.1 using the same methodology as in (*32*): The Fürth-equation as explained in 2.8.1

$$MSD = 2n_{\text{dim}}D(t - P(1 - e^{-t/P}) \tag{3.1}$$

can be used to describe the random walking behaviour of lymphocytes in the absence of flow. By simply setting n_{dim} =2 for planar movement and dividing 3.1 by t, we slightly transform the equation

$$\frac{MSD}{t} = 4D(1 - \frac{P}{t}(1 - e^{-t/P}) \tag{3.2}$$

When plotting the MSD/t data for a given data set (the experimental values for MSD can be evaluated by analyzing numerous cell trajectories), this modified version of the formula becomes more feasable:

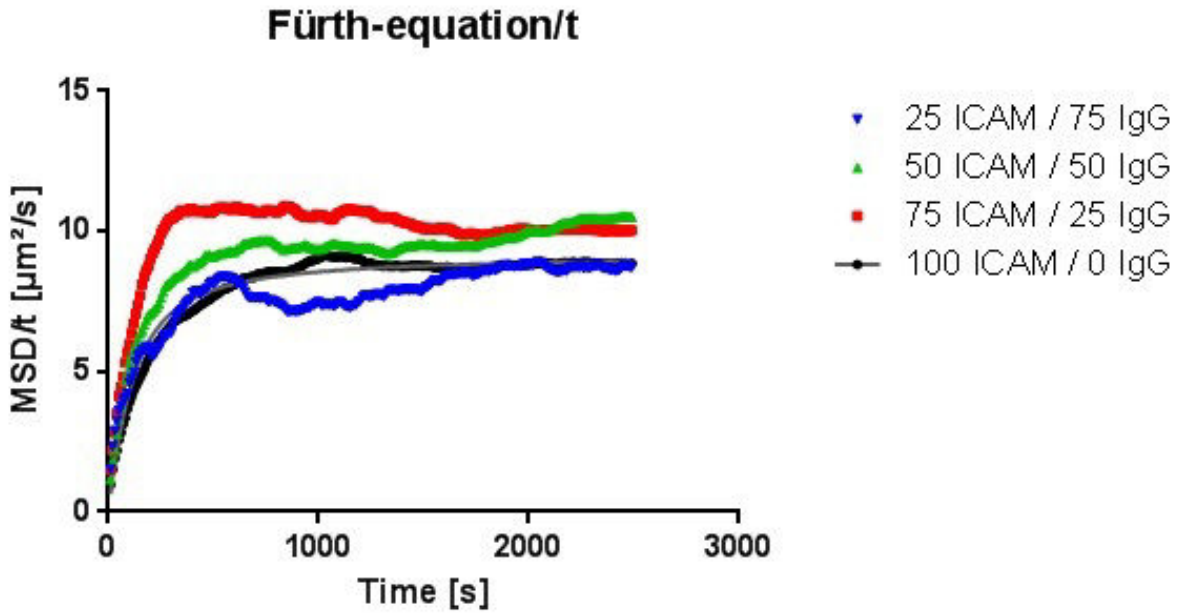

Figure 3.6: Diffusion data for 4 different substrates. The values for 100 ICAM / 0 IgG were fitted (grey). For these curves 700-1200 cell trajectories were averaged.Data from 141210.

Looking at figure 3.6, one can see that due to dividing each data set by t, the curves have two distinct regimes: A high slope in the beginning followed by convergence at the end. Each of these regimes is shaped by either P (valid for the beginning), where the Taylor approximation for the initial slope is calculated in 2.8.1:

$$MSD^* = \frac{2D}{P}t^2 \tag{3.3}$$

to transform to the $\frac{MSD}{t}$-form, we simply have to divide by t,

$$\frac{MSD^*}{t} = \frac{2D}{P}t \tag{3.4}$$

and we can identify $\frac{2D}{P}$ as our initial gradient. For t»0, the function converges to 4D. Using this knowledge, we can determine D and P by fitting the experimental values, although a characteristic quality of the cells helps to reduce this number to one: As already shown earlier in this chapter, cell speed remains constant under all circumstances given in the experiment, even under shear stress. Using the intrinsic speed definition from (*32*) mentioned in materials and methods

$$v_{\text{cell}} = v_{\text{intrinsic}} = \sqrt{\frac{2D}{P}} \tag{3.5}$$

we can use our experimental cell speed as intrinsic speed, and describe D only dependent on P with

$$D = \frac{Pv^2}{2} \tag{3.6}$$

leaving only P as variable to fit as shown in figure 3.6 in grey. Therefore the fact that cell speed stays constant during the whole experiment, the degrees of freedom can be reduced by one, improving the accuracy of the model.
Now, the influence of the substrate composition on the random migrational behaviour of the cells can be examined, and using the methods described above, multiple data sets of cell trajectories can be evaluated regarding the possible change of diffusion coefficient and persistence time depending on substrate interaction. Already in the shown example in 3.6 it is evident that the diffusion data for each substrate does not show striking differences.

ICAM/IgG	D [µm²/min]	P[s]
100/0	2.3	70.05
75/25	2.76	63.57
50/50	2.57	65.77
25/75	2.1	46.71

Figure 3.7: Values for D and P determined from the fit of 3.6

Looking at the values for D and P in table 3.7, we see that the difference in diffusion coefficient is neither big, nor follows it the same monotonous relationship as the substrate density. This, and the data shown in 3.8 show that the substrate density does not change diffusive behaviour on pure ICAM-1 substrates. What can be clearly seen in fig 3.8 is, that reducing potential binding partners on the surface does not lead to a significant change in mobility on the surface, neither D nor P change significantly. However, one effect is striking: the spreading around the mean value is quite pronounced, although experiments done within a short timeframe of days (represented by similar

colors) show more similar results than experiments done at a different time. This can finally be attributed to the different profile of integrins within each subset of cells, leading to the conclusion that in this case, individual integrin expression is the causing factor of different diffusion coefficients and persistence times on comparable substrates.

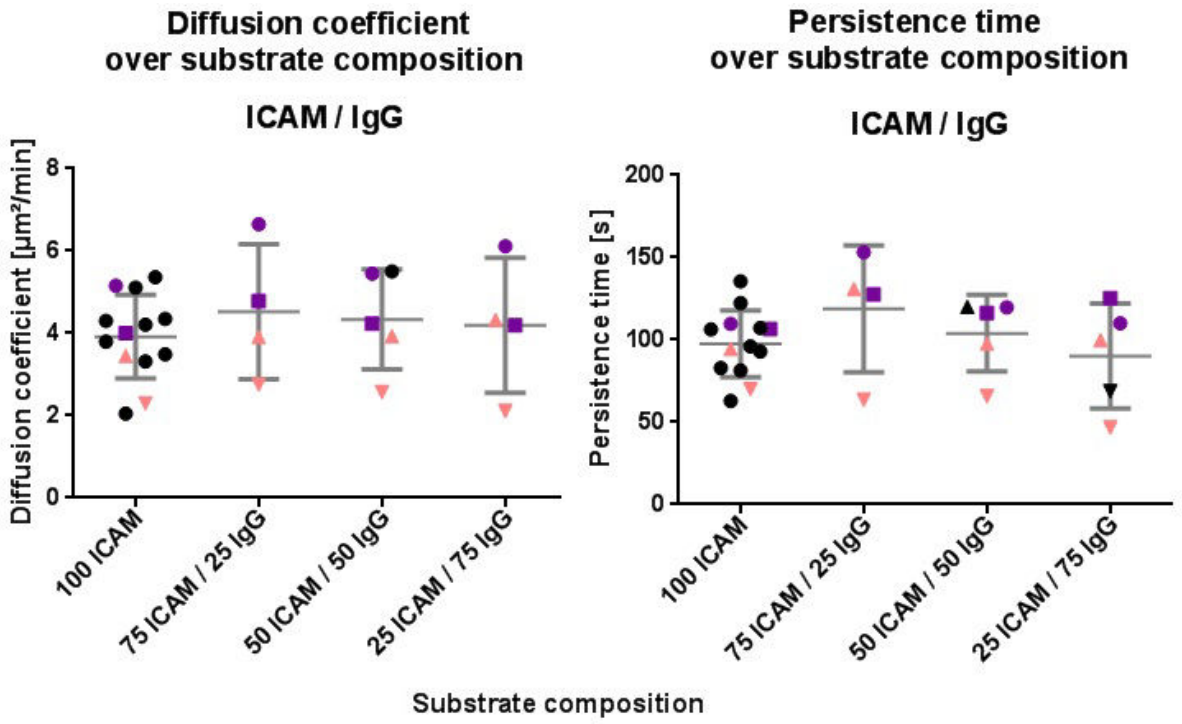

Figure 3.8: D and P dependent on substrate composition. Each dot represents the mean of all cells of one experiment. Data points with the same shape were done on the same day, data points in same color were acquired in the same week. Numbers next to ICAM and IgG refer to relative percentage of the mixture.There is additional data on 100 and 50 ICAM (black), because data fitting from previous experiments was also used.

Discussion

Briefly stated, the findings within this work prove that a decrease in ICAM-1 surface density

1. does not influence cell speed
2. does not change Diffusion coefficient or persistence time
3. decreases the quantity of adhering cells
4. increases the orientation of the cells against the flow (yFMI)

Knowing that the variations of the diverse distributions and conformational states of the cellular integrins cancel each other out on for a large amount of cells, especially when no drugs are used, all measured phenomena can be seen as a consequence of the substrate density with the applied shear stress acting as a lever to amplify or reduce the effects of the integrin-surface molecule driven migrational behaviour. Repeated quantifications of the surface concentration of ICAM-1 prove that the density of adhesion molecules is consistent. Therefore the mean squared displacement experiments can be regarded as a minimum experiment, the only influencing factors on cellular migration are the integrin-surface interactions, which again can be reduced to LFA-1 ligation with ICAM-1 (no other binding partner for LFA-1 is present on the surface and cells do not adhere in absence of ICAM-1). These interactions although are only determined by the overall integrin state of the used cells, due to the consistent surface preparation. As a consequence it can be said, that the random walking properties of the cell, namely the diffusion coefficient and persistence time, solely depend on the distribution, expression- and affinity level of LFA-1. Since these measured parameters do not vary over the measured concentrations, the motility apparatus of the cell, namely the actin-polymerization and force coupling with extracellular surroundings, is independent of the amount or strength of integrin ligation. Adding the information that the speed does not change over various substrate compositions and is also consistent over a wide range of experiments and time frames (see error bars in fig 3.2) the phenomenon can be explained by further reducing the possible causes to variances in internal cellular signalling for each individual blood bag. Summarizing, the observation that cell speed on ICAM-1 substrates does not change for various shear stresses (*23*) is also true for an additional change of density / affinity as shown in this work, but opposed to (*68*), where shear stress and cell speed behave reciprocal. The relation between adhesion and surface density under shear stress can be easily explained only using a mechanistic perspective: The reason why the cells are not getting washed away by the shear stress exercised by the fluid is the adhesive force provided by the integrins ligating the adhesion molecules. Considering that the cellular integrin state doesn't change for different surface densities (the fact that LFA-1 affinity increases under flow is known (*69*), but only has a binary switching effect and does not increase with increasing shear force) leads to the conclusion that by simply providing a lesser amount of adhesion sites, the added up binding strength for all ligation sites per cell decreases, which makes it easier for the current to detach the cells, an effect even more pronounced when increasing shear stress from 4 to 8 dyn/cm^2. Interestingly, the cellular response in terms of yFMI is very pronounced. Confirming the model described in (*22*) the uropod acts as wind vane guiding the cells against the flow. Increase in shear stress results therefore in a

more pronounced response from the uropod and stronger guidance. Additionally, reducing the potential binding sites for the integrins acts also as minor migrational cue against the flow, a phenomenon which can be explained by the fact that less adhesion points on the surface are available and therefore the cytoskeleton is anchored and fixed on less points which corresponds to a higher mobility to align against the flow. Results show that cells without cue provided by the flow do not show a change in persistence, therefore the signaling provided by the uropod might work using a different pathway. A possible explanation on the other hand, is that at a given persistence length, the cells are better adapted to orient themselves against the flow when they have to break up less surface ligations. Even with the flow, cells do not align themselves completely, as shown in the data provided, but they are perturbed by a constant stochastic movement orthogonal to the flow direction, induced by strong actin polymerization at the lamellipod. Lesser attachment in this case, might reduce the energetic costs for a directional change within the given time for the alignment of the cytoskeleton. Additionally, since the integrin distribution along the plasma membrane is not isotrope (compare fig 3.9), the cell might passively use the force exerted upon it by the current to realign the parts of the cell which are not too tightly attached.

3.2.2 Integrin affinity

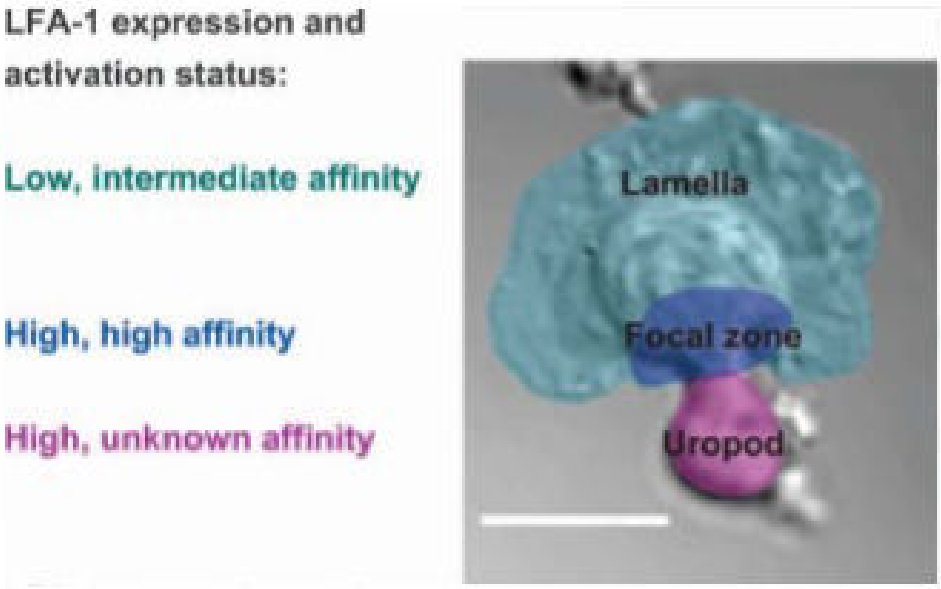

Figure 3.9: Amount and affinity state of LFA-1 is not uniformly distributed over the plasma membrane. Low expression levels with intermediate affinity are found in the lamellipod, whereas the focal zone has high, and the uropod even highest density (*70*).

As can be seen in figure 3.9, neither LFA-1 expression levels nor affinity are uniformly distributed along the plasma membrane but show different areas within the cell, implicating different purposes for each section regarding cell migration. The lamellipodium which quickly probes the environment and shows high fluctuation in form and alignment has therefore a lower overall LFA-1 affinity and amount than the focal zone providing tight attachment, followed by the uropod with high concentration but unknown affinity. As described in 1.2.3 the state of the integrin LFA-1 can be locked in a high affinity conformation by supplying manganese in sufficient quantities (3mM) to induce a stabilization of a hydrophobic ridge in the MIDAS of the β-chain. In doing this, the hitherto unknown condition for the integrin can be altered all over the plasma membrane and the measurements can be compared to the same conditions in a manganese-free environment.
When preparing these experiments, 3mM manganese (Mn2+) was added to the regular RPMI buffer while performing all measurement and incubation steps.
As a first proof that the observed phenomena can be directly linked to an increase in integrin affinity, fluorescence activated cell sorting (FACS) was performed

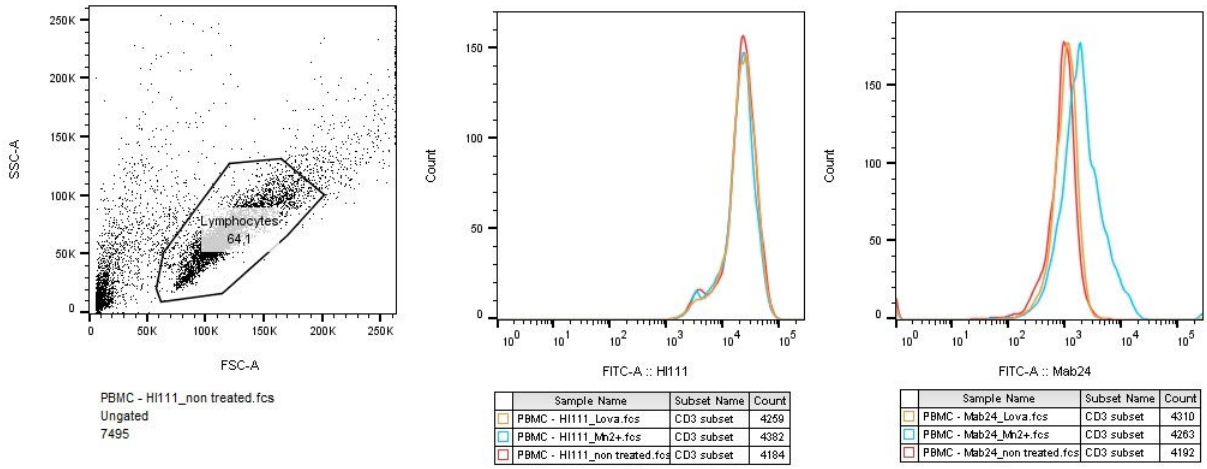

Figure 3.10: Cytogram (left) and histograms for detection of closed-conformation LFA-1 (middle) and open-conformation LFA-1 (right).

Figure 3.10 on the left shows a cytogram of the analysed cells. the x-axis, the forward scatter parameter (FSC-A), is an indication for cell size, whereas the y-axis, the side scatter parameter (SSC-A) indicates the granularity of the cells (apoptotic cells show an increased tendency to produce granules). Using these two criteria it is possible to select the correct subset of cells (framed and labelled 'Lymphocytes') for further analysis. The next two graphs show histograms with the x-axis representing fluorescence and the y-axis cell count for control cells (non treated), manganese-treated(Mn2+, ex-

posure to manganese analogous to previously described cells) and Lovastatin (a drug responsible for decreasing LFA-1 induced adhesion, results not used). The histogram in the middle shows fluorescence count for cells labelled with Hi-111 antibody, which tags LFA-1, but whose binding is significantly reduced for the high affinity conformation which would only be overrepresented in abundance of manganese (*71*). Evidently, there is no difference between control and manganese treated cells, showing that the treatment with divalent cations does not increase the amount of active LFA-1 contributing to adhesion. This is a proof that within the presented results in this chapter only a modification of already existing integrins has happened, the total amount of integrin has not been changed. The fraph on the right shows cells labelled with Mab24, an antibody marking the open, high-affinity conformation of LFA-1. Here, an increase in numbers of high-affinity LFA-1 can be measured.
These experiments are the first steps towards modifying both the substrate, as well as the integrin condition. Since only one component on the cellular side (LFA-1 affinity) as on the substrate site (ICAM-1 density) is involved, it is still rather easy to attribute changes in cellular behaviour to either one of these conditions. Possible interesting observations would include if a decrease in density on substrate side would compensate an increase of affinity on the integrin side and vice versa or if there is a hierarchy in influencing cell motility properties between those two.

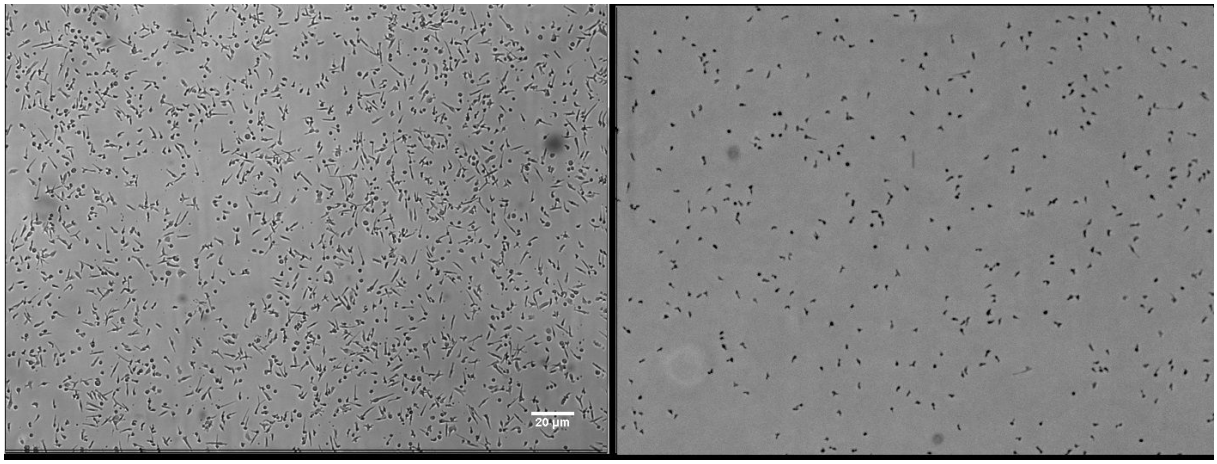

Figure 3.11: Cells under 3mM manganese (left) vs control (right). Images immediately after exposing to 8 dyn/cm^2 shear stress.

First distinguishing features are the amount of cells and their morphology: Whereas the Mn_{2+} cells have a much more pronounced and elongated uropod attached to the surface, the phenotype of the control cells corresponds with literature having an upright uropod exposed to the shear stress.

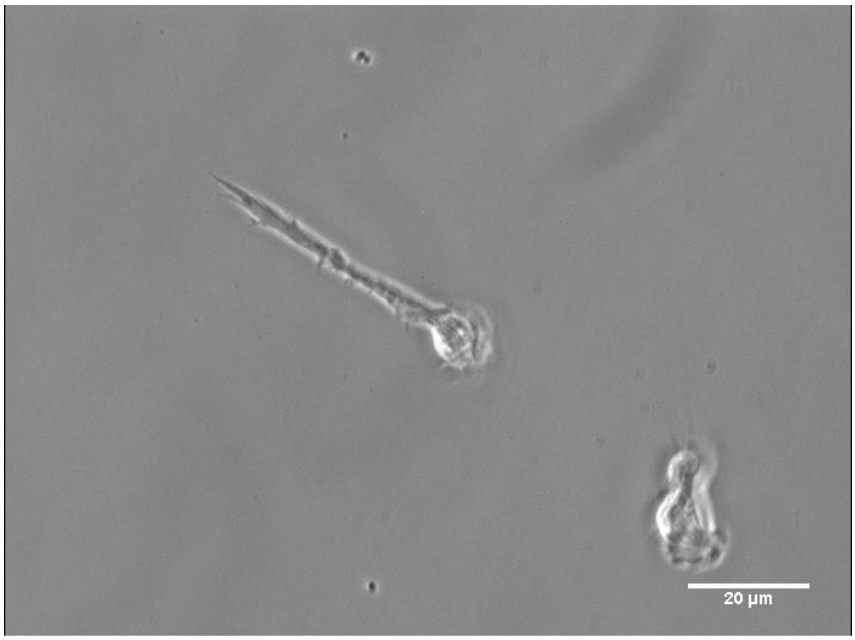

Figure 3.12: Cells under 3mM manganese: 'leashed' cell with elongated and adhering uropod next to regular cell. Substrate:10μg/ml ICAM-1, 4 dyn/cm^2 shear stress applied.

Figure 3.12 shows again in detail the differences in phenotype on one image, as both populations coexist in the same environment. The cell in the middle has a clearly elongated uropod and exceeds the usual cell length compared to the regular specimen on the bottom right which shows normal proportions.

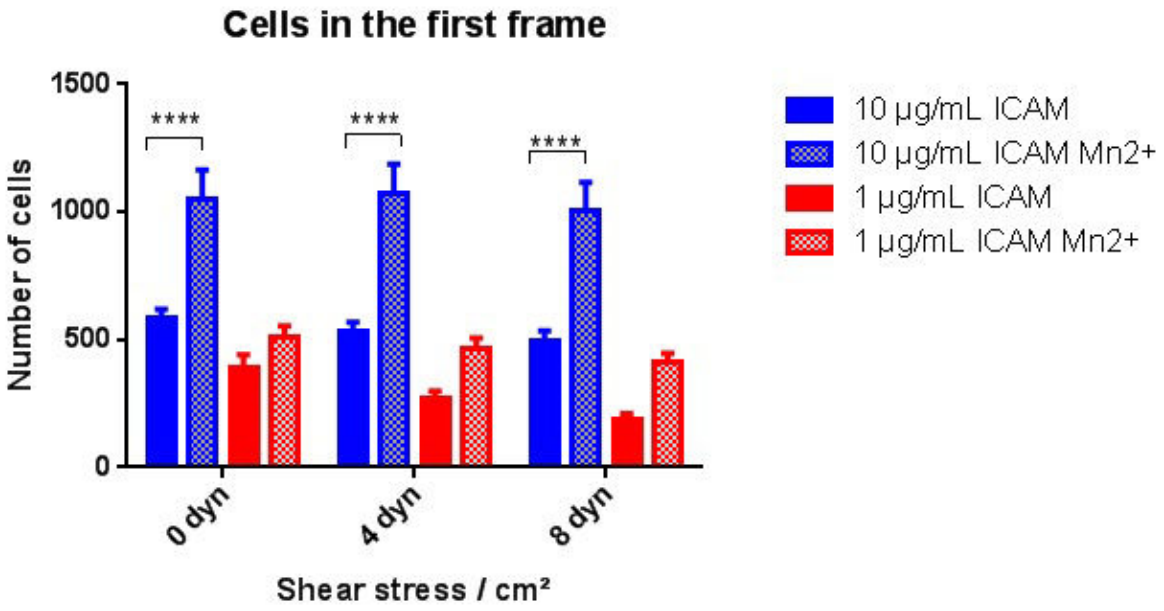

Figure 3.13: Cells counted on the first frame(n=4) dependent on shear stress and adhesion molecule surface density with and without the influence of 3mM Mn2+.

The increase of the amount of cells is evident and since the concentration of the cells in suspension used to incubate the channels is the same. These cells represent the first cell count after rinsing the sample with 1 dyn/cm^2 for approximately 30 seconds, which means only the adhering cells are counted, whether they move or not. Therefore, the increase in numbers between control and manganese treated cells can be attributed to the altered integrin state. Although analyzing the videos, there is a clearly observable decrease in motility when tracking the lymphocytes. This makes it interesting to look at the fraction of stuck cells determined by the following relation: $\frac{cells\,in\,the\,first\,frame - cells\,tracked}{cells\,in\,the\,first\,frame}$. Using this fraction, all cells which are not moving at least 30 μm during the time they are tracked are considered immobile.

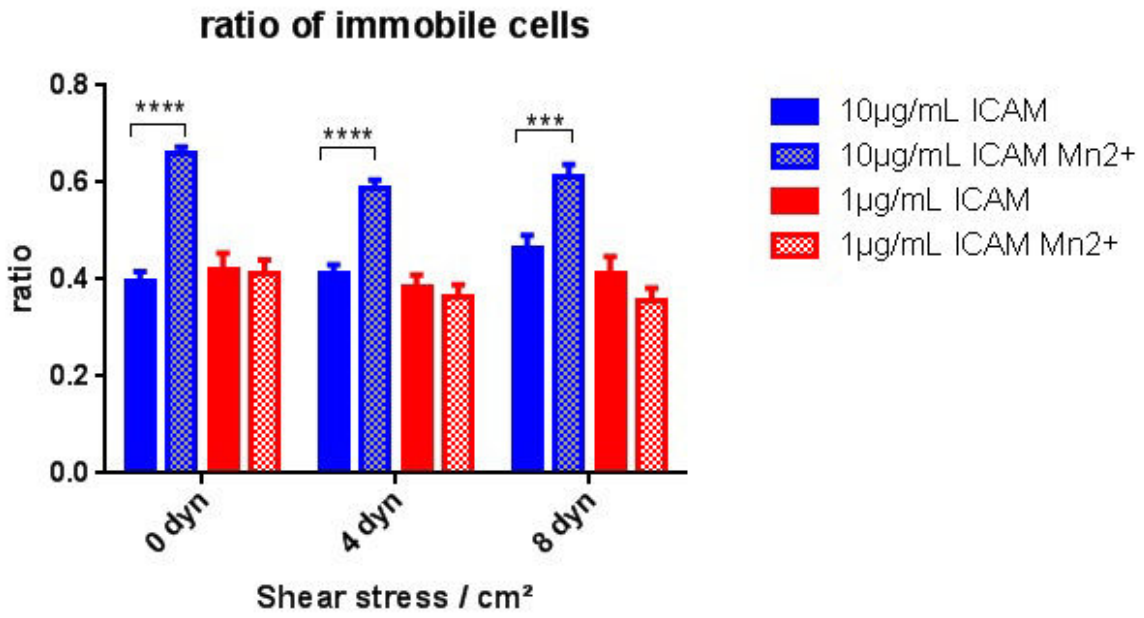

Figure 3.14: Ratio of immobile cells/cells in first frame (n=4) dependent on shear stress and adhesion molecule surface density with and without the influence of 3mM Mn2+.

In combination with fig. 3.13 it is evident, that not only the amount of cells overall is increasing, but also the amount of cells who are not migrating due to the influence of manganese. As a next step it makes sense to look at adhesion using the same criterium as for the absence of manganese in figure 3.4 since here only moving cells are tracked and counted.

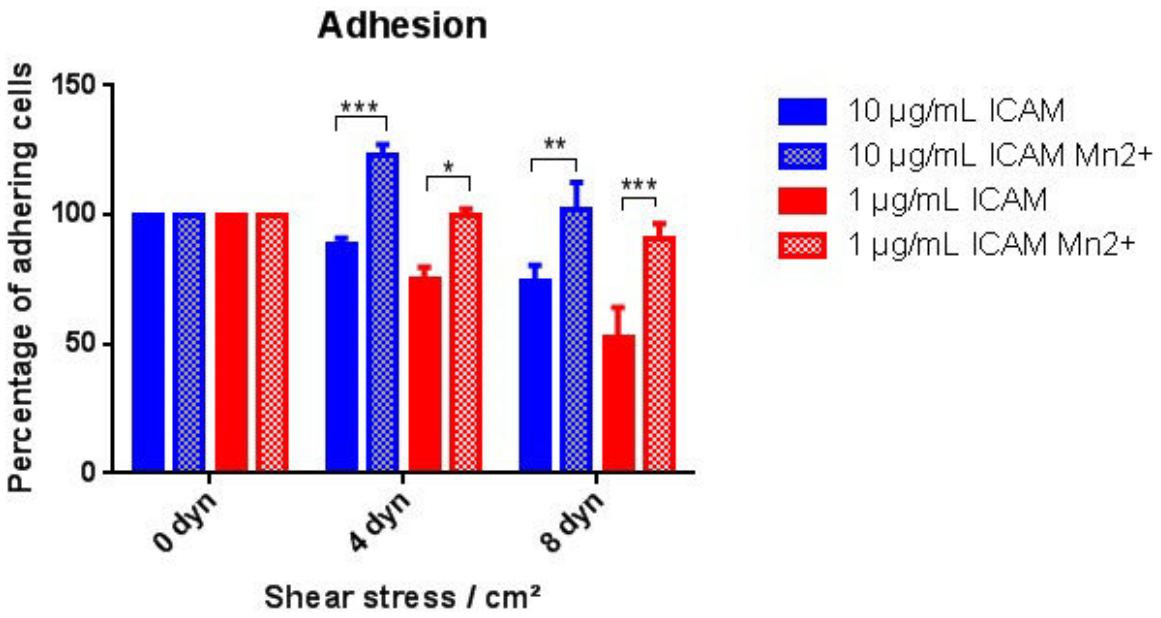

Figure 3.15: Adhesion (n=4) dependent on shear stress and adhesion molecule surface density with and without the influence of 3mM Mn2+.

As a matter of fact, the amount of tracked cells under flow is higher than without flow as can be seen in the ratios in 3.15. Whereas there is only statistical significance for higher concentrations of adhesion molecule in the previous figures, manganese seems to induce migration on both high and on low densities of ICAM-1. Nevertheless it has to be said that this is at least partially an artefact: Counting the cells confirms the increase in affinity, although the adhesion ratios shown in figure 3.15 are ratios of moving cells. Considering the high number of immobile cells due to their stuck uropod (explained below), a cell whose uropod is attached to the substrate might not appear to be migrating in the absence of flow, but starts movement under flow, although in its very confined space allowed. This would be enough to accumulate the 30μm minimum length to be counted as moving, but nevertheless this is not 'real' cell migration due to the very confined space limited by uropod length.

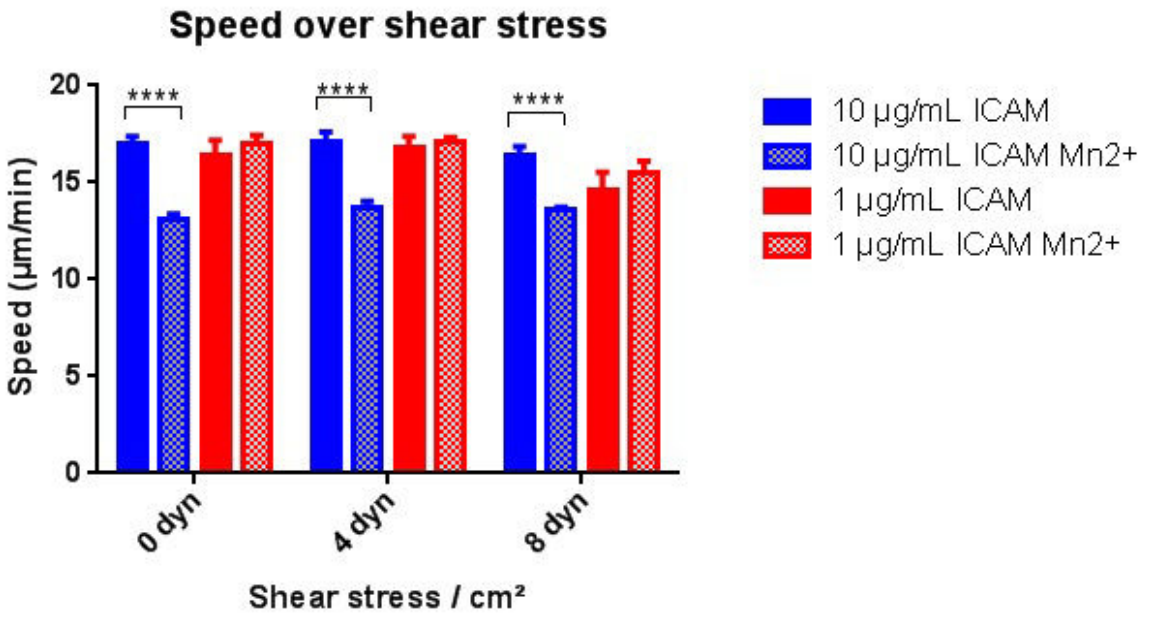

Figure 3.16: Cell speed (n=4) dependent on shear stress and adhesion molecule surface density with and without the influence of 3mM Mn2+.

With a high statistical significance it can be seen in figure 3.16 that manganese seems to lower cell speed, interestingly only on substrates of higher density. This is a finding that would contradict our previous findings that cell speed is independent of adhesion. Although interesting, this graph is the result of an artefact: As one can see in the movies and trajectories of the cells for 10μg/mL ICAM-1 with added manganese, the affected cells are attached to the substrate on their uropod, which is therefore no longer erect but rather acts as a leash limiting the random cell movement to a confined small area. The reason for these cells still showing up as moving lies within the selection criteria of the MATLAB program evaluating the trajectories. As mentioned in 2.3, only moving cells are taken into account when analyzing data concerning cell motility. Moving cells in this case means cells who travel a minimum of 30 μm in total. If a cell is attached at the uropod circling around its fixed point, it still counts as migrating although heavily confined. Besides looking at the movies of the moving cells, there exist other quantifiable characteristics which allow us to identify the 'cells on a leash' (this term is used to avoid the confusing alternatives of "adherent", "attached" or "fixed" cells):

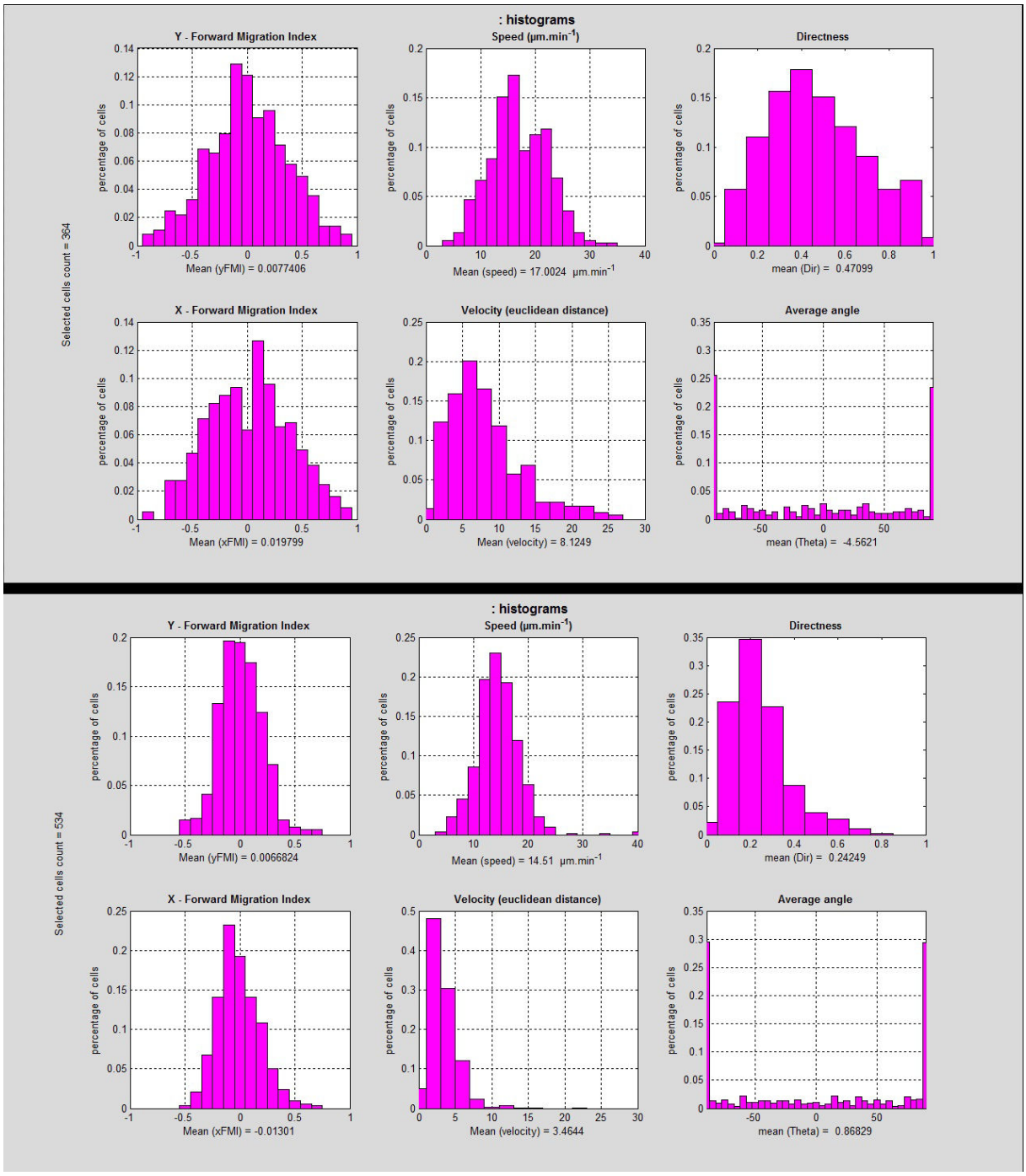

Figure 3.17: Histograms yFMI, speed, directness (linear distance/total distance), xFMI, euclidean velocity(directness/time) and Theta (average angle between xFMI and yFMI) for control cells (top) and cells under 3mM Mn2+ (bottom) with absence of flow. Data from 150630

Comparing control cells and cells under the influence of manganese in figure 3.17, it is evident that the spectrum of nearly all measured parameters are significantly smaller for the cells with Mn_{2+}. the the width of the xFMI and yFMI (and furthermore the

directionality) curves are smaller, meaning that less directed motion in one particular direction is in favor for the altered cells. One can argue that for random motion on an isotrope substrate these values should be equally distributed for both specimen of cells. This is only partially true: Where a non-leashed cell has the choice to go in any direction at any point in time, the leashed cells, once they reach their maximum perimeter, are reduced to advance in radial direction, only allowed to go back or move tangentially leading to less directionality in movement (as can be seen in the figure). Although both cells move in a stochastic manner, this reduction of possibilities delivers that measurable difference besides the reduction in speed to detect leashed cells. Interestingly this phenomenon only occurs when high affinity of the integrin and high density of the substrate appear simultaneously. The speeds and movement patterns for 1μg/mL ICAM-1 are not altered.

Still the most striking change manganese has on cell motility lies within the altered y-forward migrational index:

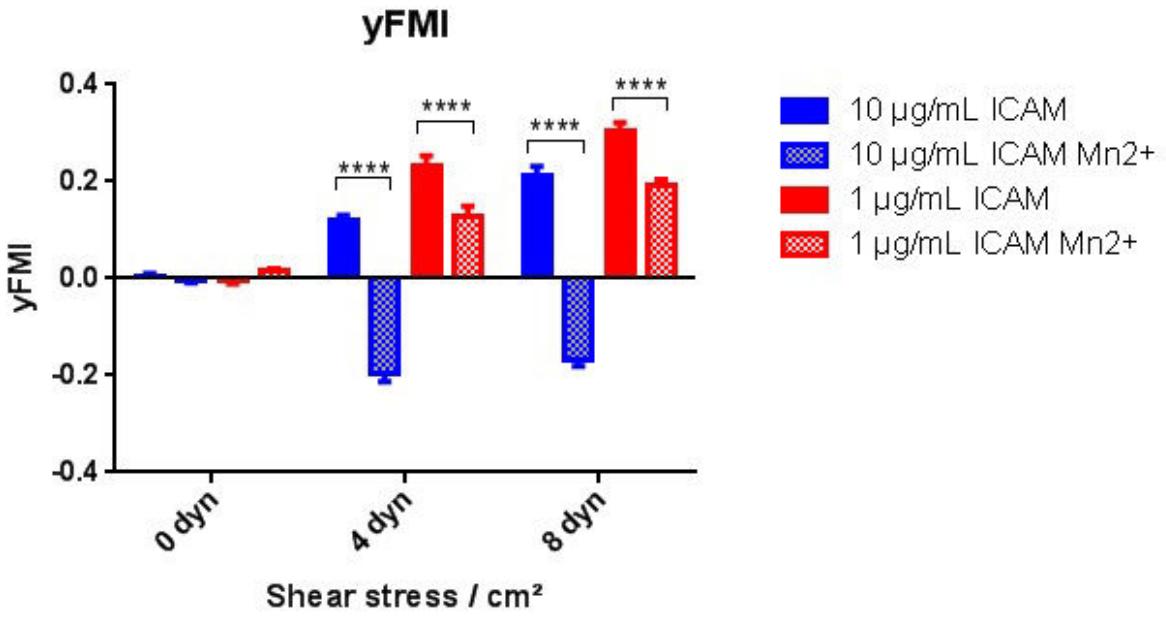

Figure 3.18: yFMI (n=4) dependent on shear stress and adhesion molecule surface density with and without the influence of 3mM Mn2+.

Again, as seen in figure 3.18 an even stronger effect on T-cells is visible, depending not only on the incubation of the divalent cation but also on the density of the substrate. Most strikingly, the cells switch their direction of migration in between 10 and 1 μg/mL of ICAM. Also this can be explained as an artefact analogous to the phenomena explaineing the reduced cell speed. The affected cells again are cells on a leash, their uropod is

attached to the substrate. Although the cells do not migrate against the flow anymore, this finding does not contradict the models presented in (*22*, *23*). The cell still moves in the opposite direction in which the uropod is pulled, with the difference that it is not hydrodynamic shear stress which moves the uropod but the tension applied to it by the moving cell. In an anisotropic environment created by flow, this might although result in alignment with the flow as further explained in 3.3. As demonstrated, the switch in high affinity to LFA-1 in combination with dense substrates (10 μg/mL incubation volume) leads to different phenotypes and movement characteristics. Therefore it might be interesting to determine the reversal point and directional behaviour dependent on substrate density.

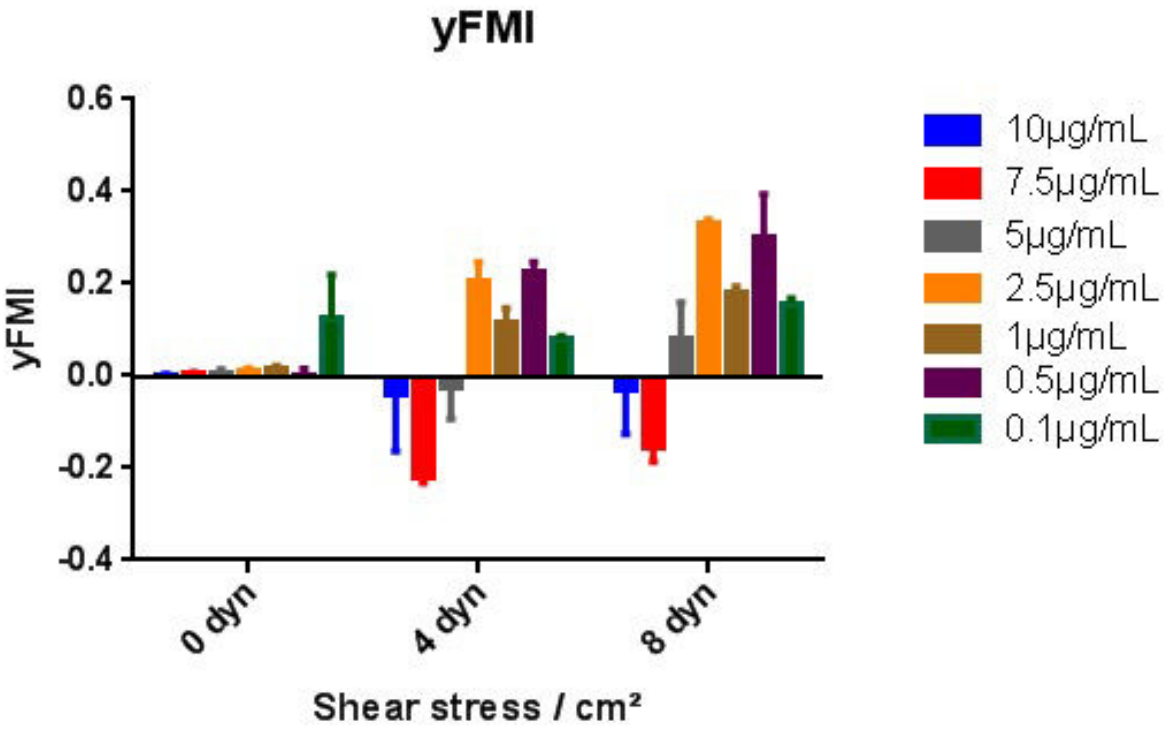

Figure 3.19: yFMI (n=3) dependent on shear stress and adhesion molecule surface density with 3mM Mn2+.

There is no linear correlation between substrate density and yFMI under the influence of manganese although interestingly the turnover point for the directional change seems to be dependent on the applied shear stress as can be seen in figure 3.19 where it changes from 5/2.5 μg/mL for 4 dyn/cm^2 to 7.5/5 μg/mL for 4 dyn/cm^2. Nevertheless it seems that an optimized concentration for each directional orientation exists. Finally, the phenotype of the T-cells also changes dependent on the substrate density

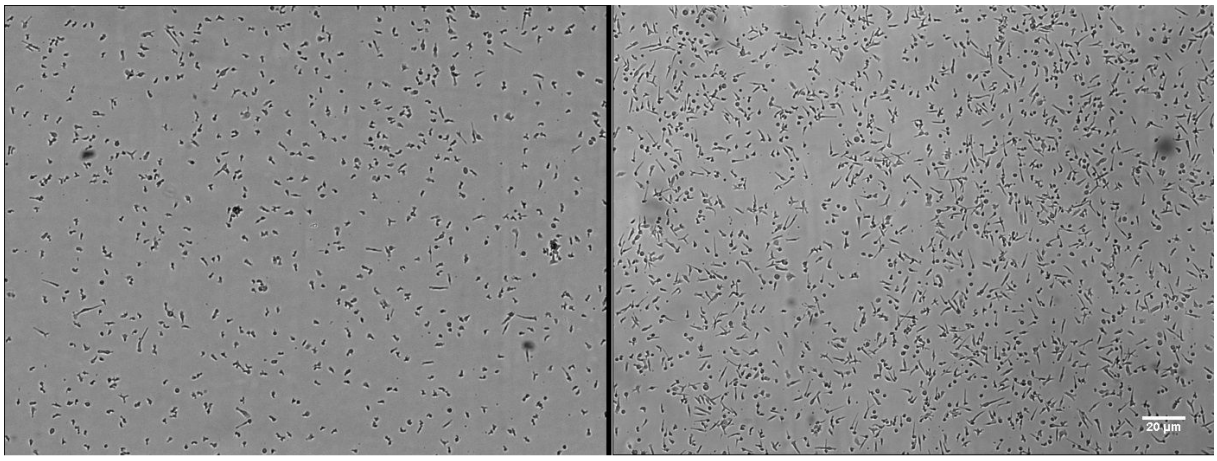

Figure 3.20: Cells under 3mM manganese: 1μg/mL ICAM-1 (left) vs 10μg/mL (right) Images immediately after exposing to 8 dyn/cm^2 shear stress.

The differences in phenotype are clearly visible, whereas the cells show their well polarized shape on 1μg/mL substrates, their uropod is particularly elongated and stuck to the surface on 10μg/mL.

As a last demonstration to prove that the movement of the leashed cells cannot be mistaken with regular random two-dimensional migration we can compare the MSD/t data for control cells, and cells exposed to manganese:

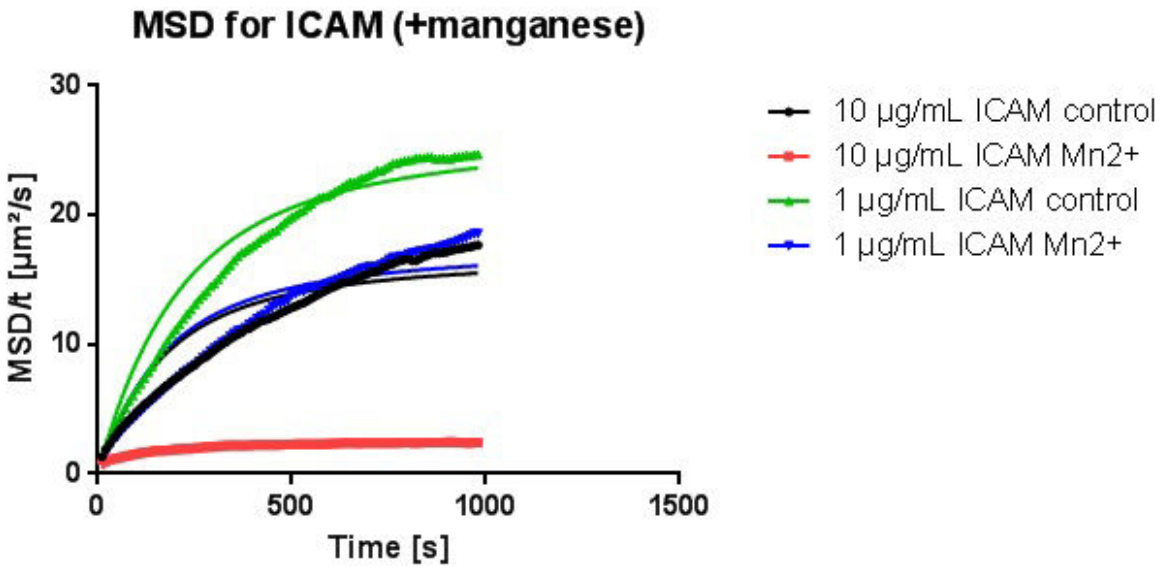

Figure 3.21: Diffusion data for ICAM-1 substrates with control cells and cells exposed to manganese. Data from 150617.

Figure 3.21 shows the consequences of confinement for cells: The manganese treated cells on high density substrates do not follow the diffusive behaviour described by the Fürth-equation so their MSD/t value is significantly lower. The rest of the cells behave according to the laws of unconfined diffusion. Noticeably, when comparing the cells treated with Mn_{2+}, only the high density substrate makes teh cells immobile, while the low density substrate show similar results as the high density substrate of the control cells confirming the existence of a threshold value for uropod detachment and regular behaviour.

3.2.3 Integrin expression

The data in 3.2.2 shows, that integrin affinity has significant influence on cellular migrational properties up to the point where abundant manganese in the medium renders the cells immobile due to the switch to high affinity of LFA-1 to ICAM-1. Whereas this described experiment works with the regular amount of expressed LFA-1 and increases their affinity, also attempts have been made to increase the total amount of expressed LFA-1 expressed by the lymphocytes with and without additional affinity increase. For this, the amount of the mitosis inducing stimulant phytohaemagglutinin-L, was quadrupled while culturing the T-cells to increase general integrin expression (see 2.1). Although cytometry data only delivers a relative amount of increase of integrin compared to the control cells who were stimulated with the regular amount, the increase in used PHA-L results in a significant difference in LFA-1 expression. This allows to examine if this change in integrin expression has similar effects as induced affinity increase. Furthermore PHAx4 (the term "PHAx4" refers to the quadrupled amount of PHA-L used) stimulated cells were additionally treated with manganese to alter both cellular and substrate environment, resulting in the theoretically highest induced adhesion conditions on pure ICAM-1 substrates.

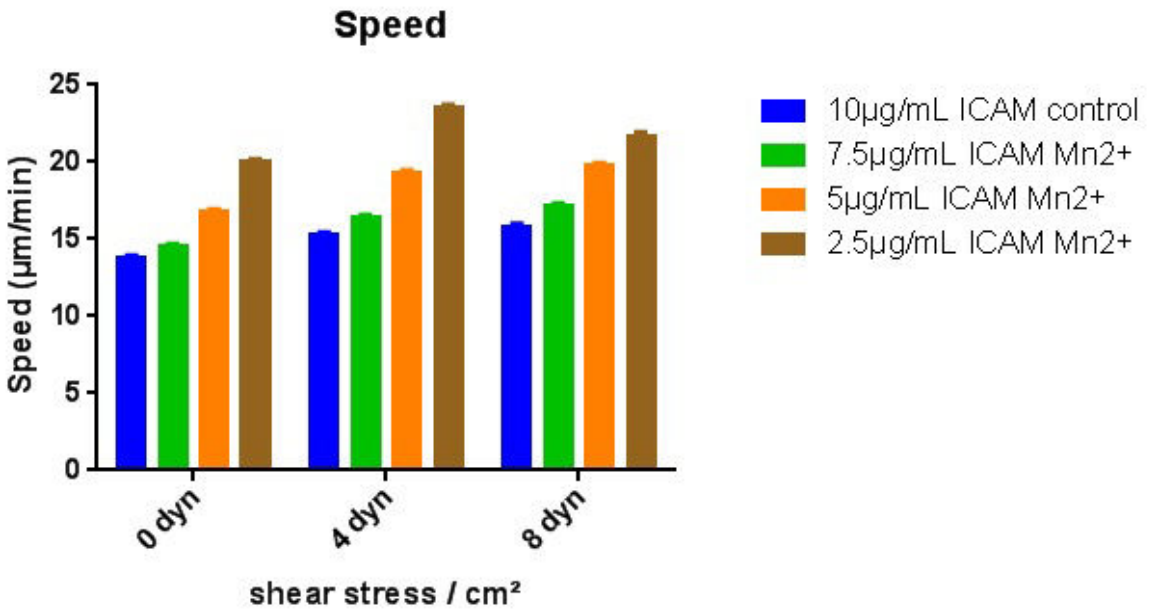

Figure 3.22: Cell speed dependent on shear stress, manganese exposure and surface density

At the first look, figure 3.22 does contradict the finding presented in this thesis that cell speed on pure ICAM-1 substrates are independent of the adhesion molecule density. The visible increase of cell speed shown although, cannot be explained without the interplay of cell state, shear stress and substrate composition. Compared to PHAx1 control cells from previous experiments, the PHAx4 control cells show very low cell speeds. As a matter of fact, experience shows that T-cell speeds below 15 $\mu m/min$ are an indication for abnormal cell motility, namely restricted motility properties. In this case, the first three data sets show indications for this due to their leashed cells. Again, only the data set on the lowest substrate density shows differences by exhibiting the highest cell speed. A look at the videos confirms, that only this data set consists of non-restricted cells possible to migrate without integrin-induced confinement.

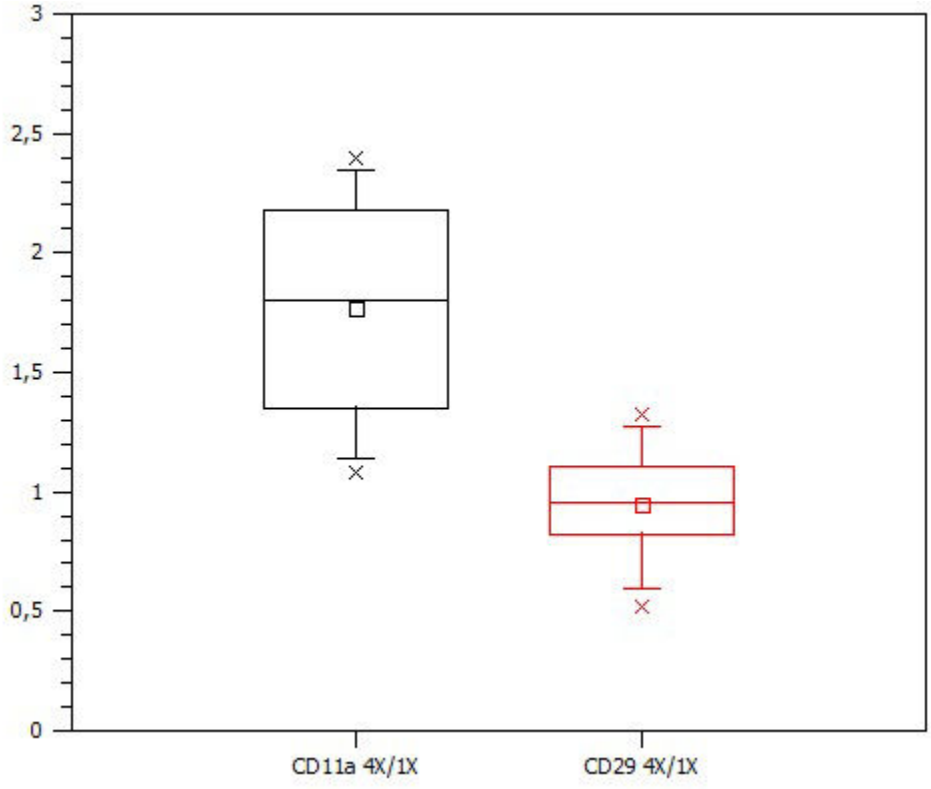

Figure 3.23: Relative expression of LFA-1 (left) and VLA-4 (right).

Figure 3.23 depicts the relative expression Relative expression of LFA-1 (left) and VLA-4 (right) by immunostaining. For this, CD11a, the characteristic αL-chain of LFA-1 was fluorescently labelled and the fluorescence output provided by PHAx4 stimulated cells was divided by the output by the PHAx1 cells. The same procedure was performed for CD29, the characteristic β1-chain of VLA-4. Whereas there is no increase in expression for VLA-4 upon hyperstimulation with PHA-L, a clear increase for expressed LFA-1 can be seen for the same conditions proving the succesful effects of increasing LFA-1 numbers and showing the differences responsible for altered motility properties.

As for the previous measurements, all channels were incubated with the same solution, containing cells in suspension with the same concentration throughout the experiment. Therefore, after seeding cells for 10 minutes and subsequent washing with $1 dyn/cm^2$ for approximately 30 seconds, the amount of adhering cells on the substrate is dependent on the varied conditions like presence of manganese and substrate density.

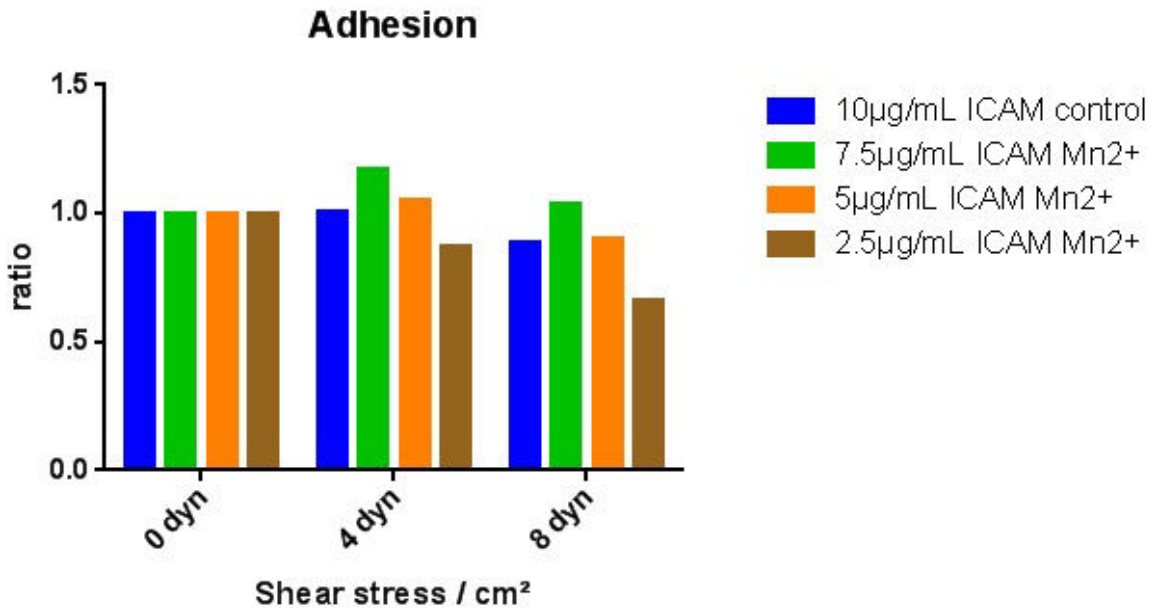

Figure 3.24: Adhesion dependent on shear stress, manganese exposure and surface density.

In figure 3.24 the adhesion is measured as usual by calculating the ratio of tracked cells for each shear stress divided by the tracked cells for 0 dyn/cm^2. A light decrease in surface density to 7.5$\mu g/ml$ cannot compensate the drastic increase in numbers induced by exposure to manganese, showing that increase in integrin affinity and expression are cumulative. Although now that we are measuring properties of motility an additional look at the videos has to be taken. Again, tracked cells are cells who move for a minimum of 30 μm during the time they are tracked. Similar to PHAx1 cells (cells only stimulated with the regular amount of PHA-L during cell culture) which were exposed to manganese, the hyperstimulated lymphocytes already show leashed cell behaviour (moving in a strongly confined space determined by uropod length) without manganese. Therefore this effect can be credited to the PHAx4 treatment. Again a proof that increase of affinity has the same consequences as increase of integrin expression regarding cell motility. The increase of adhesion under shear stress can be easily explained under leashed cell conditions: The same cell can be counted as immobile under the absence of shear stress and then be defined as mobile when exposed to flow as soon as the current induces the strongly confined cell movement limited by the cell's uropod. Again, only the data set for 2.5$\mu g/ml$ does not follow the patterns for leashed cells but rather those for regular migrating cells with upright uropod.

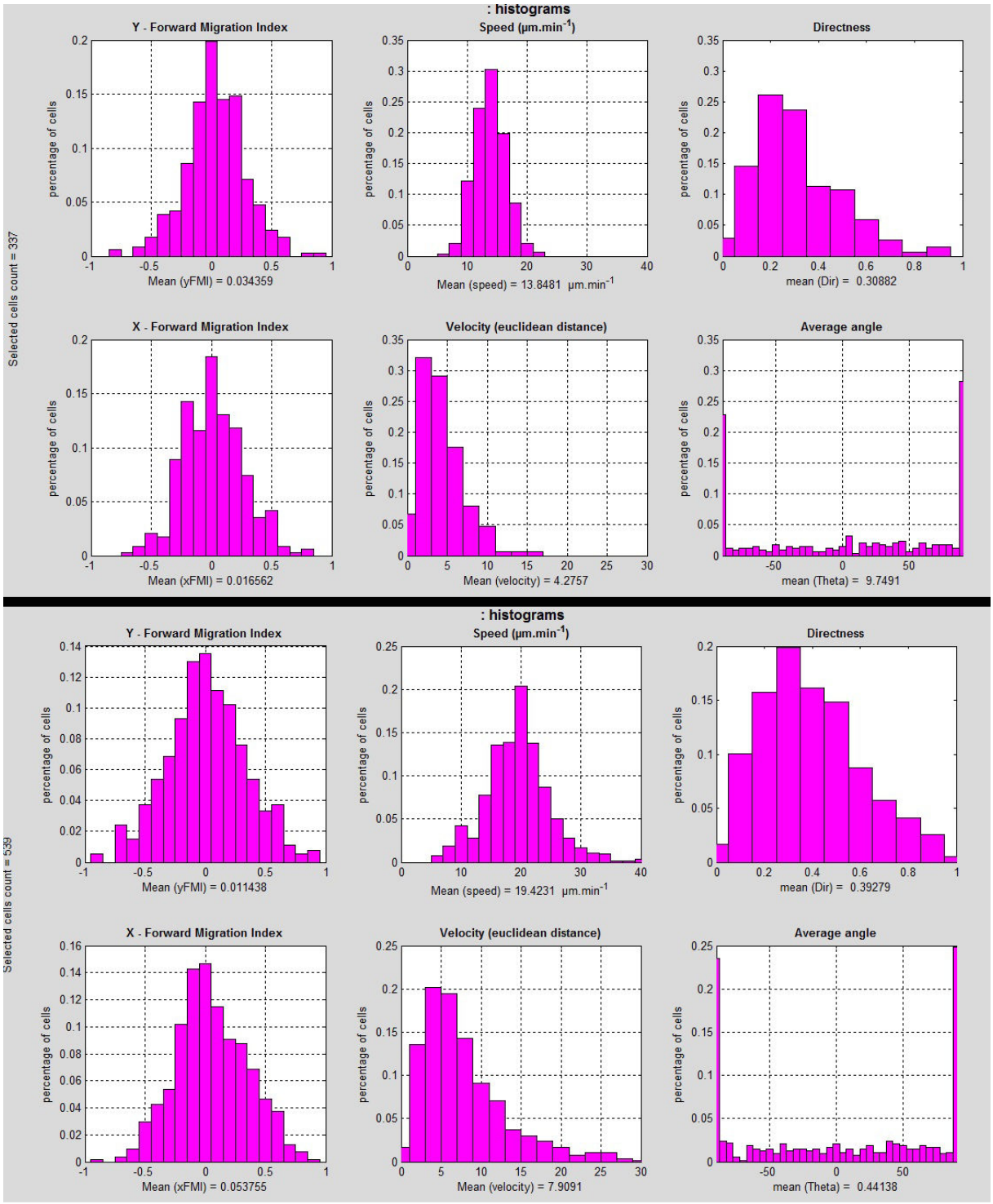

Figure 3.25: Histograms for yFMI, speed, directness (linear distance/total distance), xFMI, euclidean velocity(directness/time) and Theta (average angle between xFMI and yFMI) for control PHAx4 cells on $10\mu g/ml$ (top) and PHAx4 cells exposed to manganese on $2.5\mu g/ml$ (bottom) under absence of flow.

As a proof to the statement made regarding the $2.5\mu g/ml$ data set, we look at the

histograms of these cells in comparison to the stuck control cells (figure 3.25). Applying the same criteria as used in analysing the cells in figure 3.17, we see that again the difference in the distributions of directness and resulting euclidean velocity. Again freely diffusing cells are characterized by broader distributions of their values due to their lack of confinement, although the difference is not as striking as it is in 3.17. This can be explained by the ongoing presence of manganese which still lowers average cell motility. Although a final look at the yMI makes the difference evident:

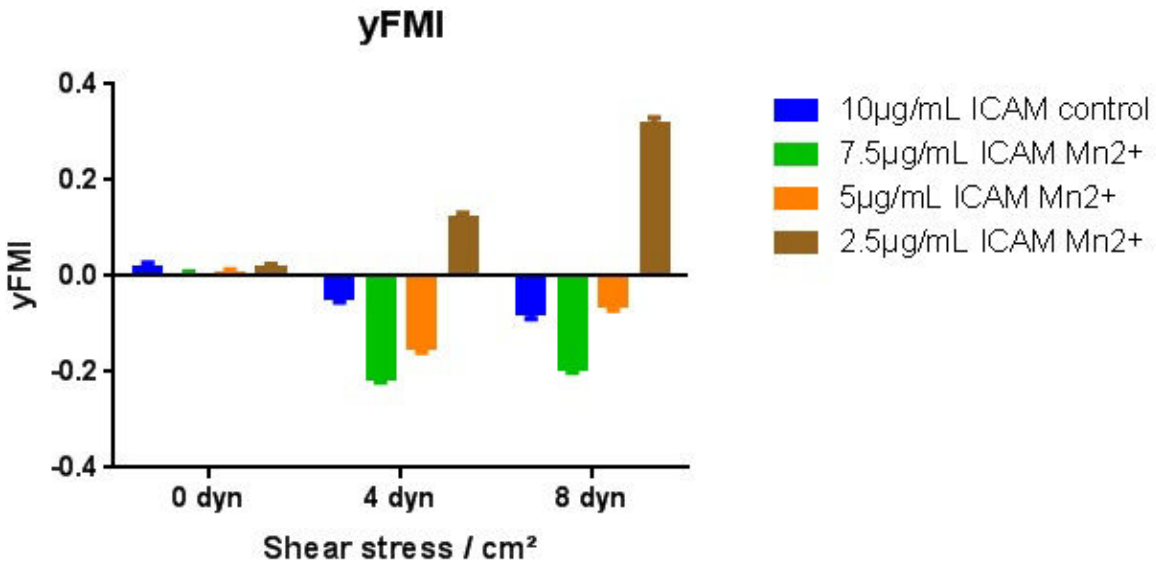

Figure 3.26: yFMI dependent on shear stress, manganese and substrate density

Whereas the yFMI on this substrate should increase with increasing shear stress and decreasing adhesion molecule density for unaltered cells, we see very low and negative values even under flow. This i s a direct consequence of leashed cells and their feedback between flow alignment and stuck uropod already described. The 2.5$\mu g/ml$ makes a striking difference in showing expected migrational behaviour and migration against the flow. At this point it can be clearly pointed out that the increase in integrin expression has the same effect as an increase in integrin affinity, and that the behaviour resulting in the different data is a result of the stuck uropod. Furthermore we see, that the increasing forces provided by increasing shear stresses are used to break up the strong bonds between uropod and substrate upon which the cell resumes its regular upstream migration.

The remarkable similarities between the data shown for PHAx4 cells (even in absence of divalent cations) and the data for manganese exposure prove that both the increase of LFA-1 affinity and the increase of LFA-1 amount induced by hyperstimulation have

the same effects on migrational behaviour of T-cells.

Generalized speed over adhesion

As shown in previous chapters, cell speed on ICAM-1 surfaces is independent of substrate density. The only reason cell speeds might diverge from this finding, is if the regular cellular motility machinery is perturbed by integrin manipulation. To make data more comparable, it is possible to look at all acquired data, with and without drugs, under the more generalized viewpoint of adhesion, which combines influences from cellular, as well as substrate side.

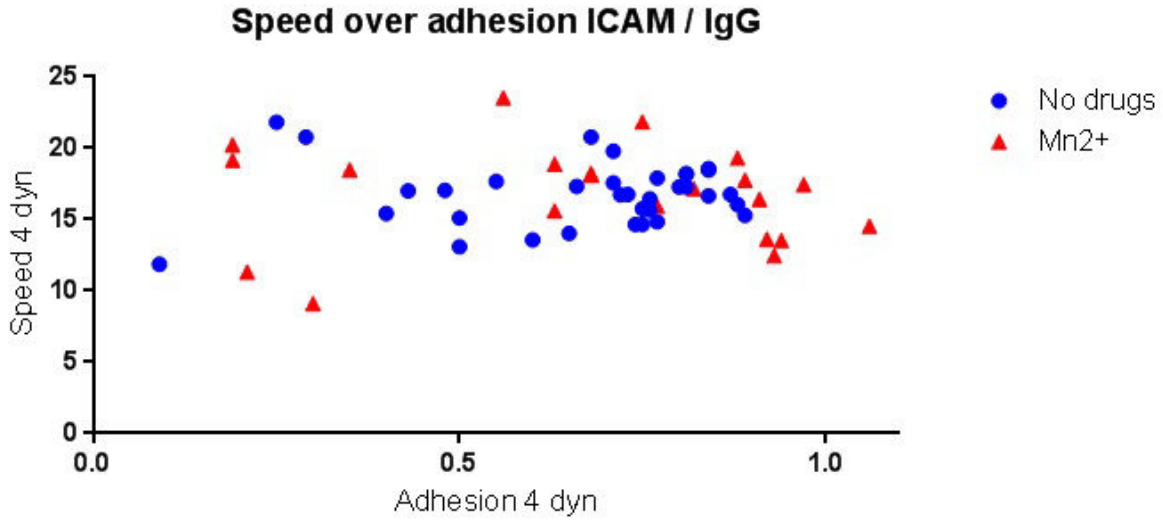

Figure 3.27: Speed over adhesion (l4/l0) under a shear stress of 4dyn/cm^2. Each point represents the average cell speed of one measurement

Figure 3.27 shows this generalized property for control cells as well as cells with increased (Mn_{2+}) integrin affinity. Initially it was thought that this graph would have a more gaussian shape as in (*72*): Low speed on low adhesion due to minimal contact points where integrins can transmit the forces of the cytoskeleton, not unlike slipping car tires on ice, followed by an optimized spot of high speed and medium adhesion where the cellular motility apparatus is able to propel the cell with maximum efficiency, ending again with lower speed on high adhesion, where a high amount of ligation slows the cell down due to the effort necessary for rupturing the bonds between cell and substrate like a car tire in mud. Plotting the data although, using the l4/l0 definition of adhesion (see 2.3) yields a different insight: Whereas all the other relevant parameters are influenced by it, cell speed is independent of adhesion as explained in 3.3.

3.3 Discussion

The experiments exposing the cells to manganese in sufficient concentrations (3mM) yield a lot of new information. Same effects have been achieved by hyperstimulation of the cells with the quadruple amount of PHA-L although further experiments in this regard have to be performed. Summarized, the changes compared to the control experiment without altering the integrins are the following:

1. Change in cell morphology
2. Significantly higher amount of cells adhering in the first frame after washing as well as stuck cells during the experiment
3. An increased ratio for tracked cells although stuck cell count also increases
4. The tendency to go more with the flow, also dependent on substrate density, to the point when cells change migrational direction

In introducing manganese into the system we do not only influence the static component of the integrin-adhesion molecule setup, namely the substrate, but we alter the affinity state of the integrins. Whereas the surface density of ICAM-1 can be easily and quantified and reproduced we have no exact information about the amount and distribution of LFA-1 on the cellular surface let alone the changes induced by the divalent cation, only holistic effects can therefore be observed and from now on changes in cellular behaviour cannot be only attributed to a reaction to the exposed surface, but one has to consider as well changes in the cellular state and interdependences among those two with consequences on movement patterns. Nevertheless at least relative increases in LFA-1 expression after PHAx4 treatment can be shown resulting in the same migrational behaviour as integrin affinity increase. The most obvious and striking two changes are the emergence of a different phenotype and the increased amount of cells adhering to the surface. For the majority of cells, an elongated uropod can be observed, elongated because it appears to be stuck on the surface as opposed to the erect uropod in the control measurements. A possible explanation to this would be that integrins in the trailing edge are usually switched to low-affinity states to keep the uropod upright and non-adherent. An adequate dosage of manganese although might induce a conformational switch also in this part of the cell to alter regular adhesion patterns described in (*6*) in a way that the high-affinity zone also incorporates the trailing edge. Interestingly we saw in 3.2 that a decrease in adhesion molecule density leads to a decrease in adhesion. Whereas this holds still true for these experiments, we see a direct, complimentary effect if we influence the system from the cellular side: By increasing

overall integrin affinity we increase cellular adhesion. The underlying mechanisms lie at hand, a tighter bond to the substrate induced by higher affinity of LFA-1 leads to more firm adherence. Same can be achieved by an increase of integrin expression. To put this in a greater context it is interesting to see that both adhesion molecule density and overall integrin conformation and amount change adhesion levels but speed remains still constant if the cells are not stuck. Therefore it is safe to say that the simplest straight forward assumption that adhesion and speed are related due to the fact that the energetical costs of rupturing bonds increase with increased adhesion is wrong, a fact which is confirmed by the difference between possible actin polymerization speeds and provided energies and net cellular speed. Especially the findings illustrated in figure 3.27, seeing that adhesion and speed are independent properties for effector T-cells, contradicts the distribution published in (*72*) which shows a more bell shaped relation between speed and adhesion saying that integrin expression levels, adhesion molecule density and their binding affinities influence adhesion and therefor cell speed. It has although to be said that in this mentioned study CHO-cells were migrating on fibrinogen- or fibronectin-coated surfaces. Both proteins are not ligating LFA-1 which is the only involved integrin in our studies and therefore different dynamics apply. Additionally it can be remarked that also during this thesis bell curve studies with ICAM/VCAM mixes were performed. These studies could be compared with the ones in (*72*), because VLA-4 is both ligating fibronectin and VCAM-1.

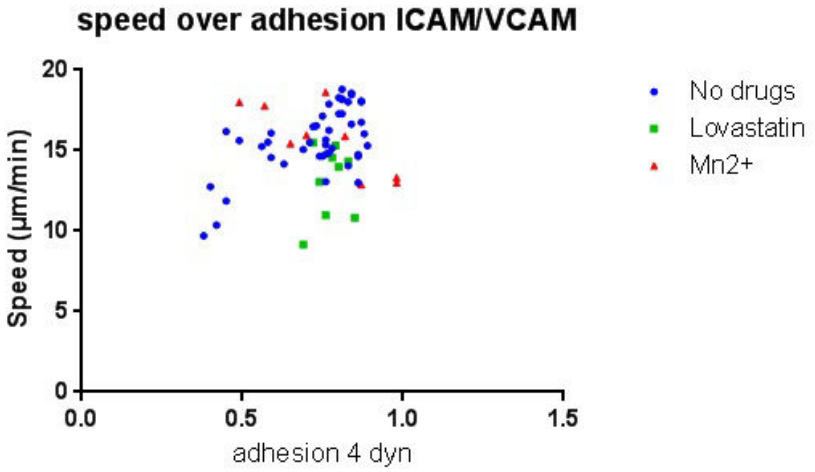

Figure 3.28: Speed over adhesion (l4/l0) under a shear stress of 4dyn/cm^2. Each point represents the average cell speed of one measurement

Figure 3.28 is only shown to demonstrate, that as soon as other integrins than LFA-1 are additionally engaged, cell speed is no longer uniform over adhesion. Nevertheless

this figure is just presented in context to (*72*) and the corresponding figure (3.27) for ICAM-1/IgG and any deeper research on the connections of involved components has not been done in this work. Under the influence of manganese or after hyperstimulation with PHA-L, the cells switch their direction of migration from going against the flow to an alignment with the flow, although only if a sufficient amount of adhesion molecule is provided. Although they really might align with the flow opposed to the control cells, this effect is like the decrease in speed an artifact of their attached uropod as explained below.
It is important to say although, that out of this frame cellular behaviour cannot be extrapolated anymore and different rules apply. These differences can be explained when looking at the phenotype of the cells as can be seen in figure 3.11: Whereas the cell shape ressembles the ones without additional manganese for lower concentrations, the uropod is adherent and severly elongated for high densities with the consequences described above. In context of this findings, the flipping points seen in fig 3.19 or in fig 3.26, together with their corresponding shear stresses, appear to be the threshold conditions for which the following happens: first the uropod is stuck to the substrate due to strong adhesion in combination with a sufficient amount of adhesion molecule to keep it attached to the surface, if either shear stress increases, whose force would help break up the ligation, or ICAM-1 density decreases, which would mean that the amount and therefore the force of adhesion and ligation decreases, the uropod switches from attached state to the common erect phenotype and regular migratory behaviour. This can be phrased out by a simple model based on receptor - ligand kinetics:
If $[I]$ the concentration of the integrin in it's unaltered form found on a control cell and $[L]$ the surface concentration of ligand (ICAM-1) on the substrate, $[IL]$ describes the concentration of formed integrin-ligand complexes and the binding kinetics expression

$$[IL] \rightleftharpoons [I][L] \tag{3.7}$$

If the reaction is at an equilibrium, meaning that the concentrations on both sides do not change anymore under conditions of cell migration, we can define k as their equilibrium constant. Under the influence of manganese, we increase the general level of integrin affinity, described as $[I]^+$ or we decrease the density of adhesion molecule, $[L]^-$. The case of manganese treated cells on 10μg/ml ICAM-1 substrate can therefore be described as

$$[IL]^+ = k[I]^+[L] \tag{3.8}$$

and is non-migrating under all observed circumstances and applied shear stresses until 8 dyn/cm^2. Although there is a condition

$$[IL]^{+-} = k[I]^{+}[L]^{-} \tag{3.9}$$

which is functional (migrating) at a given shear stress if we reduce $[L]^{-}$ below a certain threshold. The same holds true if we set $[I]^{+}$ as integrins with unmodified affinity but higher concentration. To summarize: we can increase $[I]$ by either increasing affinity (manganese) or expression level (PHA-L stimulation) and decrease $[L]$ by reducing adhesion molecule density in a way that there is a shear stress dependent threshold condition $[IL]_t$ for which

$$if\,[IL] > [IL]_t \tag{3.10}$$

the cells do not move.

Regarding guidance, the proposed model in (*22*) where the alignment of the uropod determines the movement direction of the cell is still true for stuck cells. Even an adherent uropod still continues its signalling process to the cell body, although it is no more the shear stress of the medium which determines the spatial orientation of the trailing edge, but the uropod. In other words: The cell will move antiparallel to the elongated, adherent uropod. Similar effects have been already shown in the paper cited above, where dielectric beads where attached to the uropod which were magnetically excited and so a pulling force non-aligned to the flow was exerted on the cells, showing that it is indeed the alignment of the uropod and not the direction of flow which determines the cell trajectory. Considering this explanation although, the stuck cells should show random behaviour, even under flow. Nevertheless the shear stress could either help align parts of the cells not so strongly adherent to the flow or would influence the random polymerization in the lamellipod by energetically favouring filament growth along flow axis. In both cases mechanical stress would be exerted via the cytoskeleton on the trailing edge to re-align with the rest of the cell. This would result in a self-amplifying feedback between the aligned cell body and the attached uropod, where the leading edge pulls the trailing edge along the flow axis.
Cells might respond to the integrin amount or affinity increase also by staying inert. In this case the adhesion in the trailing edge of the cell is that high, that although the lamellipod might be able to move, it can only circle around the firmly adhesive part of the cell. In this case the uropod acts as a leash on a pole not allowing any translation longer than cell length. This phenomenon can also only be observed on high concentrations of ICAM-1 and since the lymphocytes are only fixed at the uropod but not at the leading edge, it can be said that Mn$-2+$ induced adhesion increase is spatially anisotrope, most probably due to different integrin densities. This would lead to

the following conclusion: LFA-1 might be present in the uropod at any time, although in a low-affinity state which allows the erect phenotype. This would be irrelevant in a non modified state where affinity is low, but crucial if these reservoirs suddenly get tapped by the increase of manganese. Probably the density of LFA-1 in the trailing edge is higher, accumulation of integrins at the back due to cytoskeleton mechanics seems plausible. If integrin affinity is artificially increased by divalent cations, LFA-1 in the uropod becomes the dominant driving force for integrin driven motility and overrides the effects of normal signaling leading to the consequences presented above.

Chapter 4

Quantification of lymphocyte migration on ICAM/VCAM substrates

4.1 Quantification of lymphocyte migration on ICAM/VCAM substrates

As an expansion to the previously executed experiments, in this part another type of adhesion molecule, vascular cell adhesion molecule-1 (VCAM-1), was added. As explained in 1.2.2, the binding of VLA-4 and VCAM-1 is together with the pair ICAM-1 / LFA-1 responsible for the adhesive properties of the leukocyte, although it expands the motility properties of the cell in triggering rolling movement with the flow, as well as extravasation. Although several experiments have been performed where substrates coated with ICAM/VCAM mixtures were combined with Mn^{2+}, like for 3.2, none of these experiments and conclusions were further elaborated since it is too difficult to concatenate cause and effect of the involved interdependent parameters. For example manganese could affect LFA-1 on two potential binding sites, whereas VLA-4 can only be affected on one (*5*), which might change the sensitivity towards the cation or the extent to which affinity is modulated. This, in combination with the unknown factor of integrin expression and affinity state made these experiments too difficult to control. Nevertheless these experiments who solely focused on substrate composition already yield a vast amount of information due to the enhanced motility properties the cells obtain due to the involvement of VCAM-1. Again the experiments are prepared as described in 2.4.1, 2.7, 2.8 although this time ICAM-1 and VCAM-1 are mixed, which means that the density of active molecules is always kept constant (IgG in the previous mixtures did not engage the cells). Various ratios of the two adhesion molecules are mixed and the same cellular attributes as in 3.2 are examined to see if there is a drastic switch in cellular behaviour on VCAM-1 substrates as described in (*68*) and if the mixed

integrin composition changes cell speed. Observations made in this chapter delivered for the first time quantifyable data on the rolling phenotype of lymphocytes under the influence of VCAM-1 and stress out the importance of integrin variability among different cell donors.

Disclaimer: Whereas previously the concentration of surface molecules was written in μg/mL, it will be written in percentages for the following data. This is for readability's sake and for the following reasons: ICAM-1 and VCAM-1 have different molecular weights, but the mixtures were prepared in a way that the relative ratios represent the ratio of the numerical amount of molecules and not weight ratios. Therefore, for example, 50 ICAM / 50 VCAM is a mix of the same volume of 10 μg/mL ICAM-1 solution with 13.5 μg/mL of VCAM-1 solution resulting in a ratio of molecules of 1:1.

4.1.1 Phenotypes and movement types

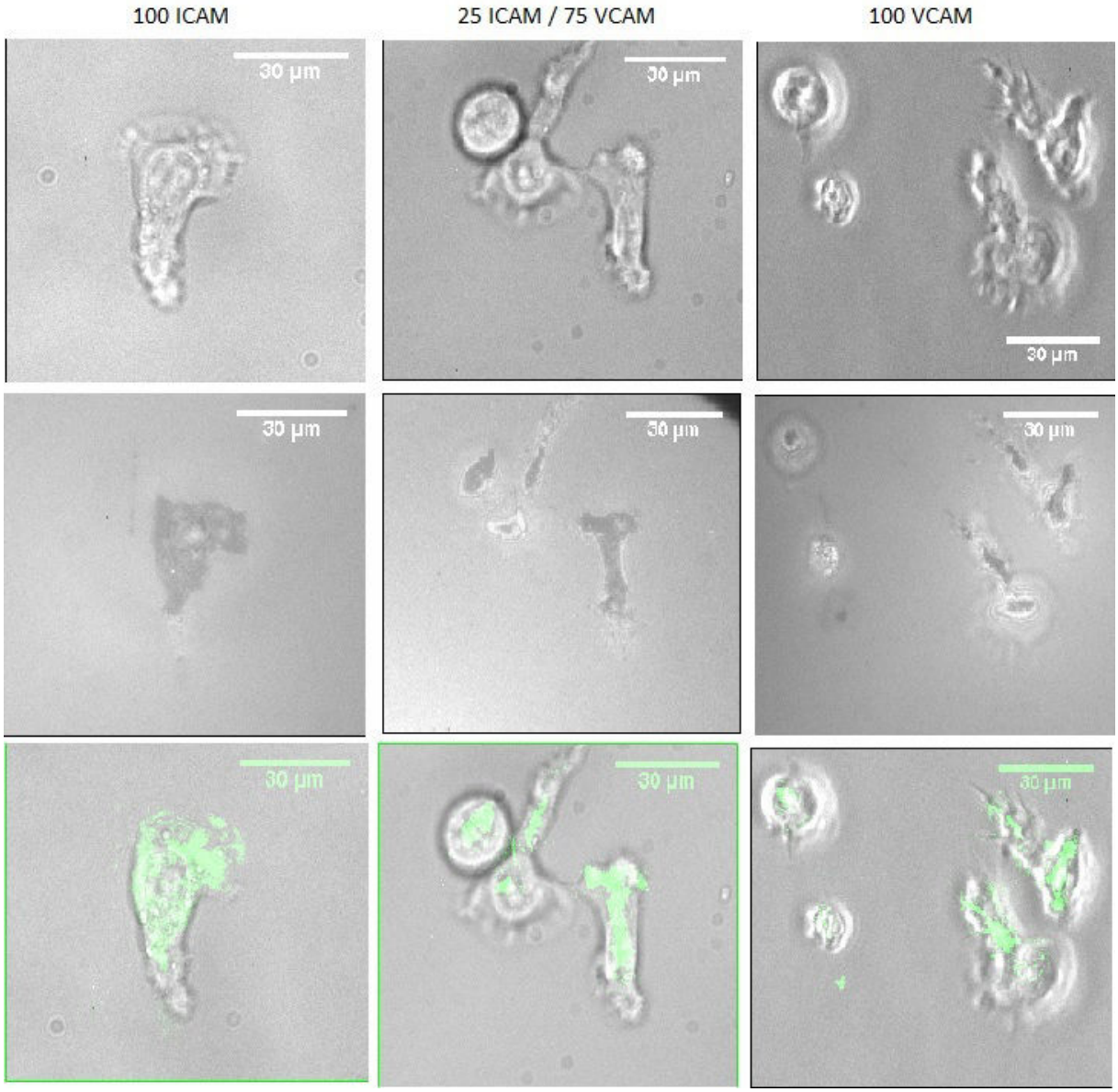

Figure 4.1: Bright field (top row), RICM (middle row) and merged images (bottom row) of cells under 100 ICAM (left), 25/75 ICAM/VCAM (middle) and 100 VCAM (right) substrates. All images taken under shear stress of 4 dyn/cm^2, green areas on the cells show contact area with the substrate. scale bar is 30μm

Analysing the state of the cells using transmission microscopy, there is already an evident difference between substrates containing ICAM or VCAM. The former follow the classical phenotype which is already known, well polarized with erect uropod in the back and lamellipod in the front, a shape sustained by all of the migrating cells. When introducing VCAM though, there exists another phenotype: Round, unpolarized cells

with no pronounced cell front or back (middle in fig 4.1. The cell shown for 100 ICAM is the classical polarized cell, migrating against the flow, with detached uropod. in the middle row we see a stuck, unpolarized cell to the left, in the middle a polarized cell migrating with the flow and on the right again a polarized cell migrating with the flow. in the 100 VCAM column, the uppe runpolarized cell is shortly before starting to roll with the flow, while the second unpolarized cell below it is stuck. the lower polarized cell goes with the flow while the upper polarized cell is stuck as well.
In the absence of shear stress, the polarized specimen migrate in a random manner always with constant speed while sustaining their shape and polarity. As a matter of fact, from observing this phenotype no conclusion can be made about the substrate composition unless quantified data about the cell trajectories is available. Unpolarized cells although mostly remain strongly attached, not showing any signs of migration except little fluctuations around a fixed point or a very little radius of movement.
To summarize, two phenotypes of cells appear upon the introduction of VCAM-1:

1. polarized cells moving with constant speed in a random manner like on pure ICAM-1 substrates

2. unpolarized, inert cells probing their immediate environment, although attached to a fixed point

Under exposure to shear stress although, migrational behaviour happens to be more complex with the introduction of VCAM. Several subpopulations of cells emerge, their ratio dependent on the amount of VCAM available on the surface. Among the polarized cells, the expected 'ICAM-like' behaviour is still present: erect uropod and migrating against the flow. Additionally there are cells who are also polarized, but migrate either with the flow or remain stuck (figure 4.1 on the right). This seems to be again a consequence of an attached uropod, following the same explanations as given in 3.3. Among the unpolarized cells, there is also an emergence of different subpopulations. Again the ones remaining firmly adhesive, stuck at the surface and only slightly moving around a fixed point, but also rolling lymphocytes. To be precise: Also rolling lymphocytes do not roll all the time, but might switch to short adhesive resting phases on the substrate for brief periods of time ($<$1min). Although the link between VCAM-1 and rolling cells is already known (*13*), quantified data on T-cells undergoing this special form of migration is not available. Rolling describes an act of movement with the flow with a velocity much higher than observed on firmly adhesive cells. In this case, attachment and detachment to the substrate are much more dynamic and fast, a fact that also corresponds to the difference in on- and off-rate of ICAM-1 and VCAM-1 with their corresponding integrins (*73*). Even though rolling cells align exactly with the flow, they can be clearly

distinguished from simply detached and passively swimming cells in the current just by comparing rolling speeds with the speed of detached cells and the fact that afer a certain period of time they again firmly attach to the surface and switch to the previously described movement type.
Summarizingly what can be observed are the four different types of movement under flow:

1. polarized cells:
   (a) migration against the flow as on pure ICAM-1 coated substrates
   (b) migration with the flow with attached uropods
2. unpolarized cells
   (a) inert cells probing their immediate environment, although attached to a fixed point
   (b) cells switching between diffusive and rolling movement

These different movement types are, as the phenotypes, dependent on the mixture of the substrate as will be shown. Considering the various forms of migration observed, the MATLAB program used for tracking was updated to not only track cellular trajectories, but also to distinguish between the types of movement described above.

Bimodal movement detection with MATLAB

To distinguish the crawling, adhesive cells regarding their upstream or downstream behaviour, they were sorted by their either positive or negative yFMI, inert cells can easily be detected by chosing the cells who were counted at the beginning of the experiment but not tracked (since only cells moving a minimum distance of 30 μm are tracked, this means only moving cells contribute to the quantified data like speed, yFMI, etc., not moving cells are counted separately). Since the original custom cell tracking software is only calculating the average speed per cell, it was not suited for the analysis of the data of the rolling cells (whose movement is characterized by various abrupt speed changes). To better distinguish the two types of movement another system was chosen. First the displacement of the cell is plotted in a distance over time diagram see figure 4.2.

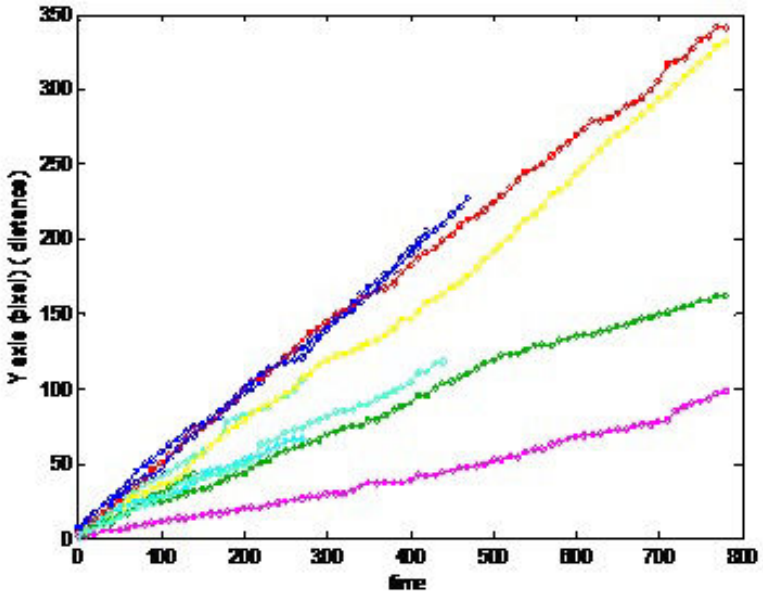

Figure 4.2: Showing the dependancy of distance over time for ICAM-only substrates

If the trajecory shows linear behaviour in this diagram, that would mean that the cell has a more or less constant speed, if however there are jumps in the linearity, this would induce a break in the constant speed, suggesting a faster movement, see figure 4.3.

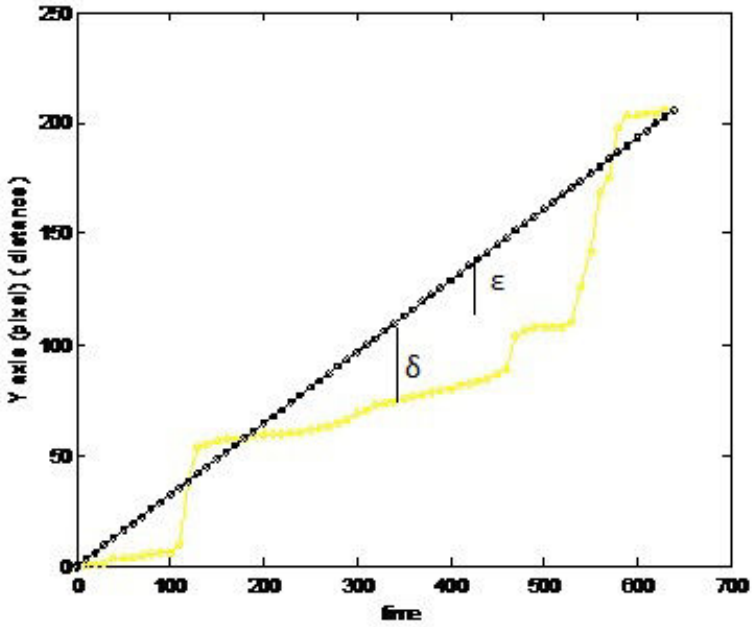

Figure 4.3: Triggering the rolling pattern recognition by ϵ-threshold

The criterium for determining if a movement pattern is more ICAM (constant and diffusing) or VCAM (rolling with the flow)-like is by linearly connecting the start and endpoint of the slope (yellow), which gives us a the theoretical linear movement of this cell (black). Now one has to define a threshold value epsilon, which describes the tolerance of the program to regard a trajectory as linear or not, the lower epsilon, the stricter and therefore less numerous are the constant movements. Now the program analyses the slope by measuring the difference between linear slope (theoretical constant speed) and real trajectory (delta) comparing it to epsilon. If delta is bigger than epsilon, this movement step is regarded as rolling. This can be done for every movement step of every cell for statistical data and was applied for the most quantified data in this work. Another method used is just by measuring the angle between y-axis and trajectory: If the included angle θ is smaller than 15° and its standard deviation is smaller than 20, the cell is considered rolling. To distinguish both methods they are called epsilon- and theta-method. The reason why two different methods are used, is because dependent on the behaviour of the cells, the recognition of the trajectories by the program and other external circumstances, cells are considered rolling or not. Therefore, an initial survey of the efficiency of movement pattern recognition has to be done by the experimentator before chosing the right method. For this, one simply plots the trajectories the program considers as rolling and compares them with all cell trajectories. Also it has to be said that the number of rolling cells is underestimated by both methods out of the following reason: When assembling the trajectories out of the image sequence, the MATLAb algorithm determines the position of the cell in then-th image, and looks for the same cell in the n+1-th image in the immediate corresponding surroundings. Due to the fast displacement characteristical for rolling cells, this algorithm might not identify the same cell correctly lose potential rolling cells.

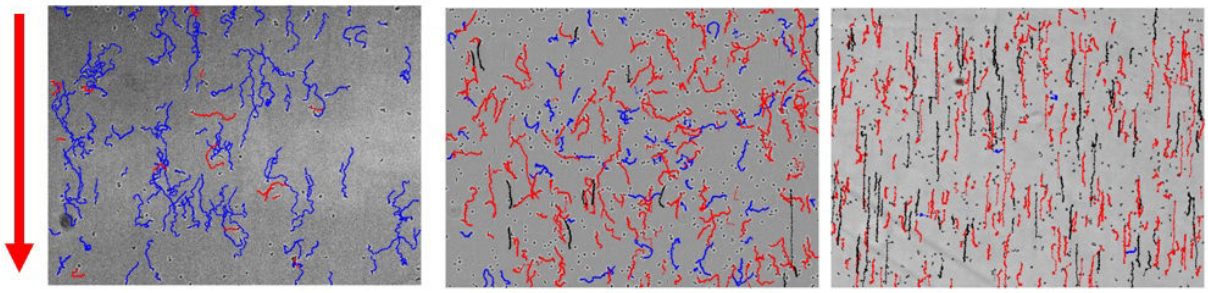

Figure 4.4: MATLAB output of trajectories of cells exposed to 4 dyn/cm^2, blue trajectories represent cells migrating against the flow, red trajectories represent going with the flow while black trajectories represent rolling cells (epsilon-criterium used). Substrate compositions are 100% ICAM (left), 25%ICAM/75%VCAM (middle) and 100%VCAM (right).

These criteria implemented in the software now can be used to sort cells by their movement type, analyze them according to their movement type and quantify the data.

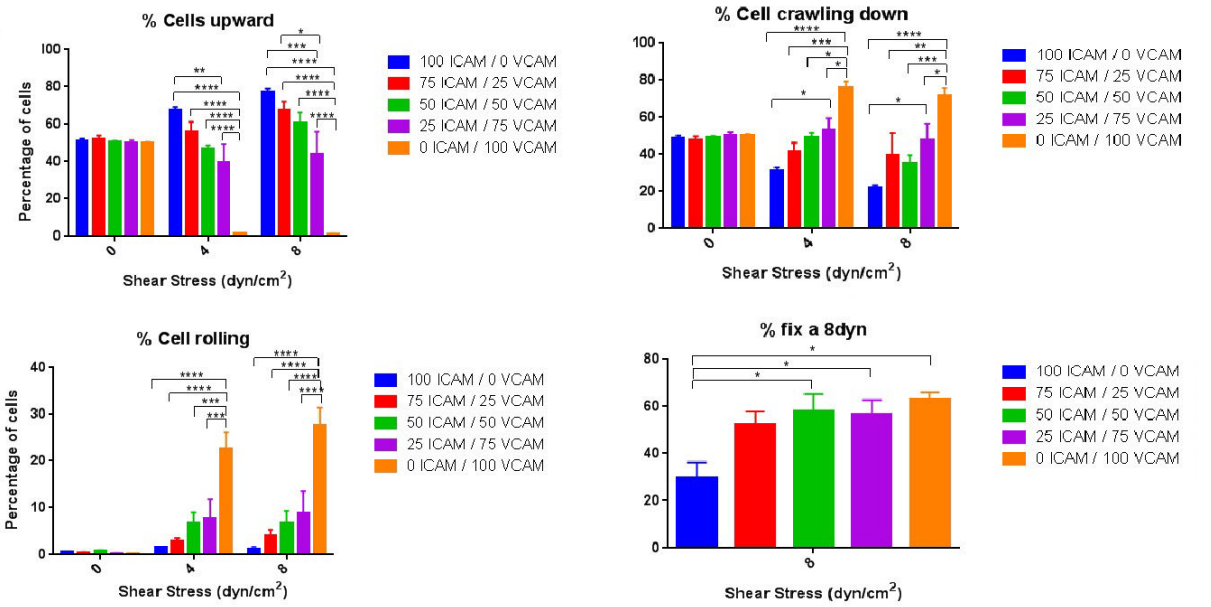

Figure 4.5: Quantitative and averaged output of selected cellular movement attributes depending on substrate composition and shear stress. From top left to bottom right percentages of cells migrating against the flow (upward), with the flow (downward), percentage cells rolling and immobile at 8 dyn. Theta-criterium used to determine rolling cells.

Figure 4.5 gives insight about the relative distribution of cells rolling. The amount is only substrate-dependent, not shear stress dependent. Note the linear rise with the linear shift in substrate composition until the point of VCAM-1 only substrate, where the percentage of rolling cells drastically increases. The remaining moving cells, the firmly attached ones who never show any rolling behaviour, also react to the increased amount of VCAM-1 with a decreasing percentage of cells migrating against the flow, until an abrupt change for VCAM-1 only, where nearly all cells migrate with the flow (downward).

4.1.2 Ligand mixture

speed

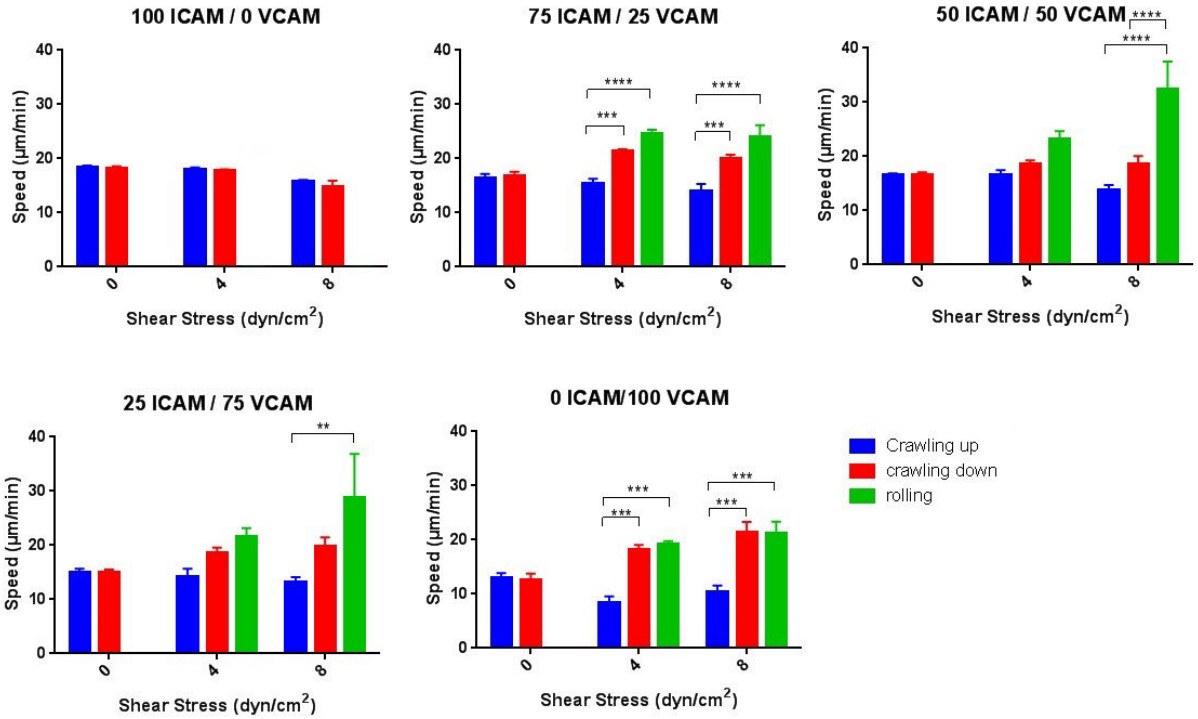

Figure 4.6: Speeds for mobile cell phenotypes dependent on substrate composition. To determine the amount of rolling cells, the theta-method was used in this data set.

Looking at figure 4.6, we see a clear dependence of migrational behaviour depending on substrate. Upon the increase of VCAM-1, the initially equal distribution of the speeds for the movement patterns shifts towards faster movement with the flow and rolling while migration speed against the flow remains steady. It stands out that the tendency to roll faster with the flow is not kept up for VCAM-1-only substrates, but decreases again, although statistical significance in the differences is higher than on most mixed substrates.

Adhesion

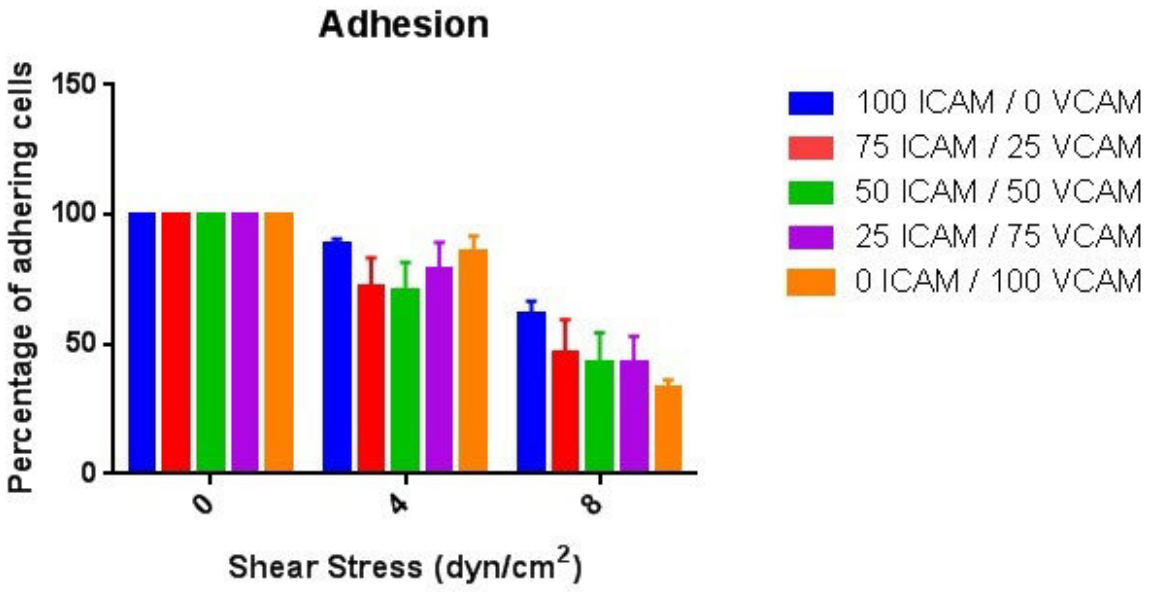

Figure 4.7: Adhesion for all moving cell phenotypes dependent on substrate composition. The adhesion vs. track definition of adhesion from 2.3 was used.

Although the percentages of adhering cells for the various substrates seem to be varying, there is no statistically significant difference among them. This seems plausible, since opposed to 3.2, where ICAM-1 was stepwisely substituted with non-reactive IgG, the total amount of possible binding sites was kept constant. What can be seen again, is the decrease in adhesion with increasing shear stress which is a direct result of washing away cells who cannot adhere as strong.

yFMI

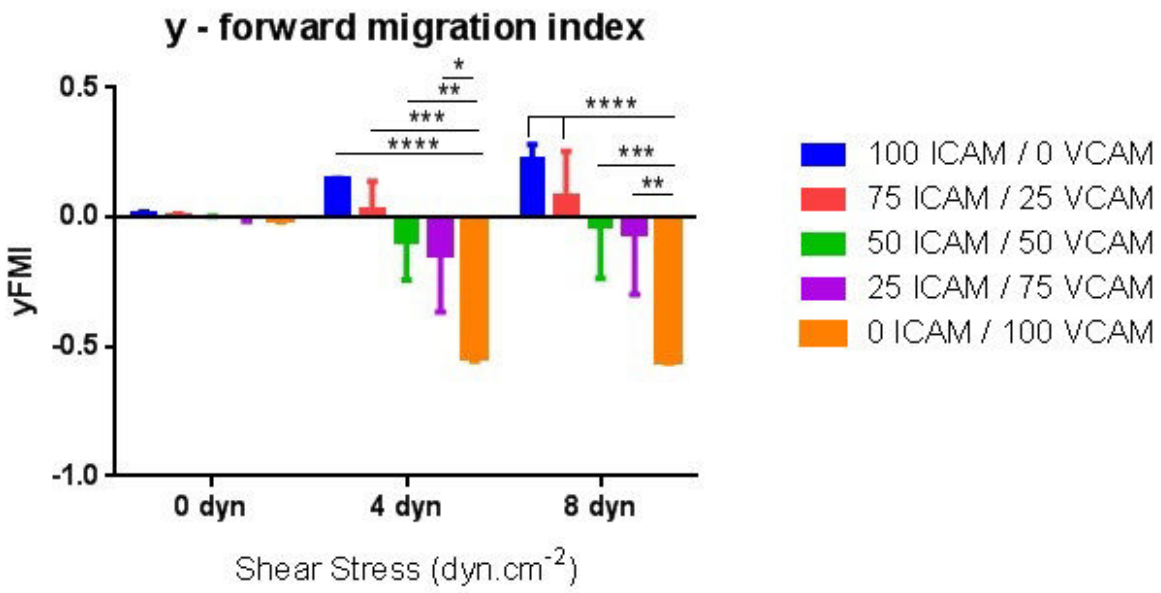

Figure 4.8: y-forward migrational index for all moving cell phenotypes dependent on substrate composition.

Evidently, the change in y-forward migrational index is gradually increasing with the amount of VCAM-1 as opposed to other possibilities where the pure presence of VCAM-1 over a certain threshold value would induce an "all or nothing" switch from against, to with the flow. Also the reaction of the cells to both types of adhesion molecules is not equally high: the migration with the flow on pure VCAM-1 has a higher absolute numerical value, is therefore more direct, than the movement against the flow on pure ICAM-1. Although the statistical significance is high, the big error bars cannot be neglected. They result from averaging over several experiments, where the general tendency is still followed, although the turnover point from upward to downward migration is reached at different substrate densities, a phenomenon which will be explained in the results section. To further elaborate this fact, it is interesting to look at the individual measurement regarding turnover point and subpopulations of cells:

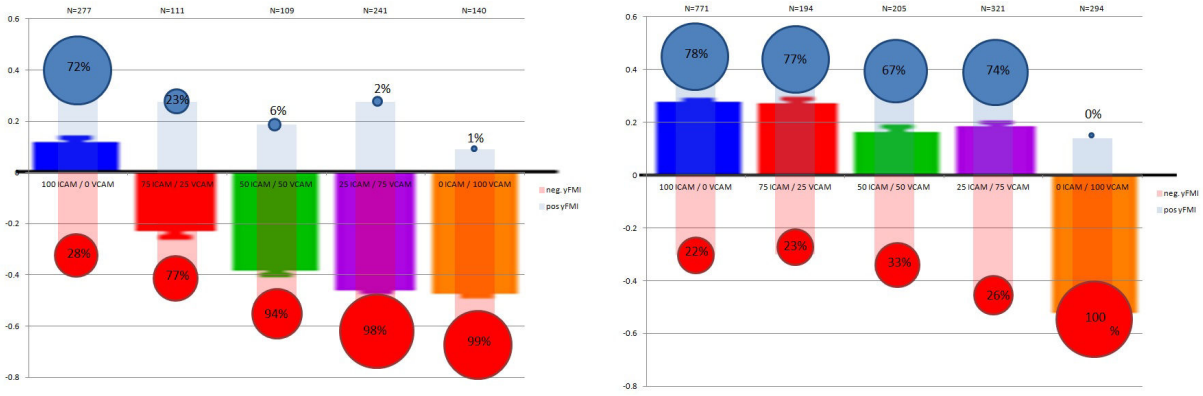

Figure 4.9: y-forward migrational index for all moving cell phenotypes dependent on substrate composition for two single measurements (left: 16.4.2016, right: 4.6.2015). Non-rolling cells were split up in two populations, either going with or against the flow, and analyzed separately. Incubation concentrations for ICAM / VCAM in percentage of total incubation volume. N = number of cells, percentage in bubbles equals percentage of cells going up/downward compared to the whole cell population.

Figure 4.9 shows individual yFMI values for the usual substrates for two individual experiments. Notably, the tendency to go more and more with the current is conserved here, although the turnover points are situated differently. Whereas on the left experiment the presence of VCAM is enough to switch movement direction, the right experiment shows exactly the opposite. As a matter of fact, this is the reason for the high standard errors of measurement in the averaged graph in 4.8. Another striking fact is that for each subgroup of cells the yFMI does not increase or decrease dramatically upon changing the adhesion molecule composition, as long as both molecules are present. It rather stays the same although the relative populations going from one direction to the other are changing. Pure ICAM-1 or VCAM-1 substrates although induce a change in the absolute yFMI value.
Complementary to this, it can also be shown that the emergence of these two subpopulations is dependent on shear stress:

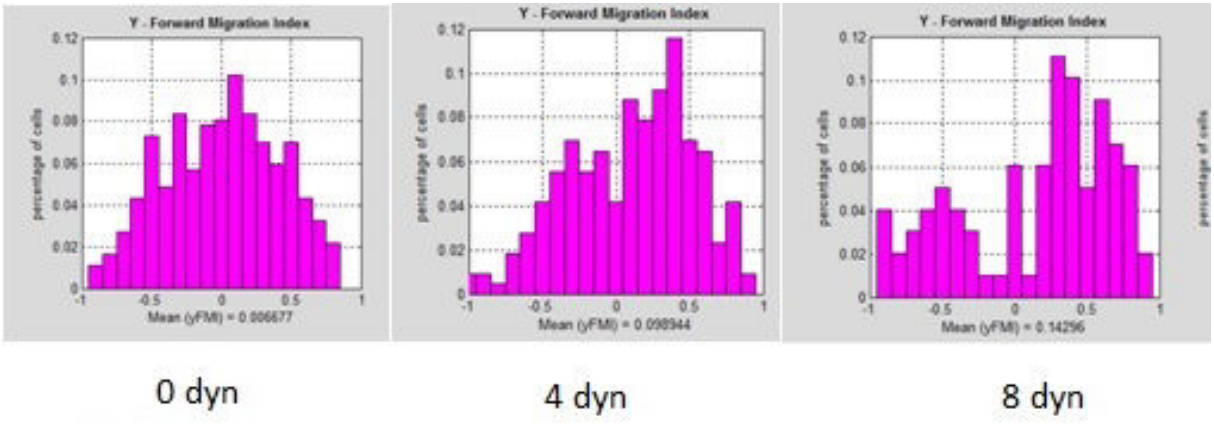

Figure 4.10: Increase in shear stress/cm^2 results in an increased separation of the two subpopulations

In 4.10 a histogram is shown linking the yFMIs of the cells with their relative occurence. Whereas the bell curve at the absence of shear stress is expected, an increase in shear stress separates the two emerging populations more and more clearly in the two regimes above and below 0 dyn/cm^2.

Fürth equation on ICAM / VCAM substrates

Again, the findings in this chapter are mostly based upon data obtained under flow, since this is the condition needed to uncover all of the present phenotypes. Another question that arises from these circumstances is if these phenotypes are an intrinsic property of the cell or if their emergence gets triggered under flow. One could ask the question from a different angle: Does the cell know in advance how to behave under the exposure to shear stress? Again the methods described in 2.8.1 are used to examine the influence of surface interaction with diffusion coefficient and persistence time. Whereas the total density of possible binding partners was decreasing with decreasing ICAM-1 (see 3.2), we substitute here with VCAM-1,not with an inert molecule like IgG. This means that the quantity in available bindings is potentially the same, although the the specific on- and off-rates are obviously different. Therefore it would be interesting to see a potential connection between either the pure binding properties of involved adhesion molecules (as the mentioned on- and off rates) on diffusion or if a possible intracellular signaling difference is responsible for altered motility.

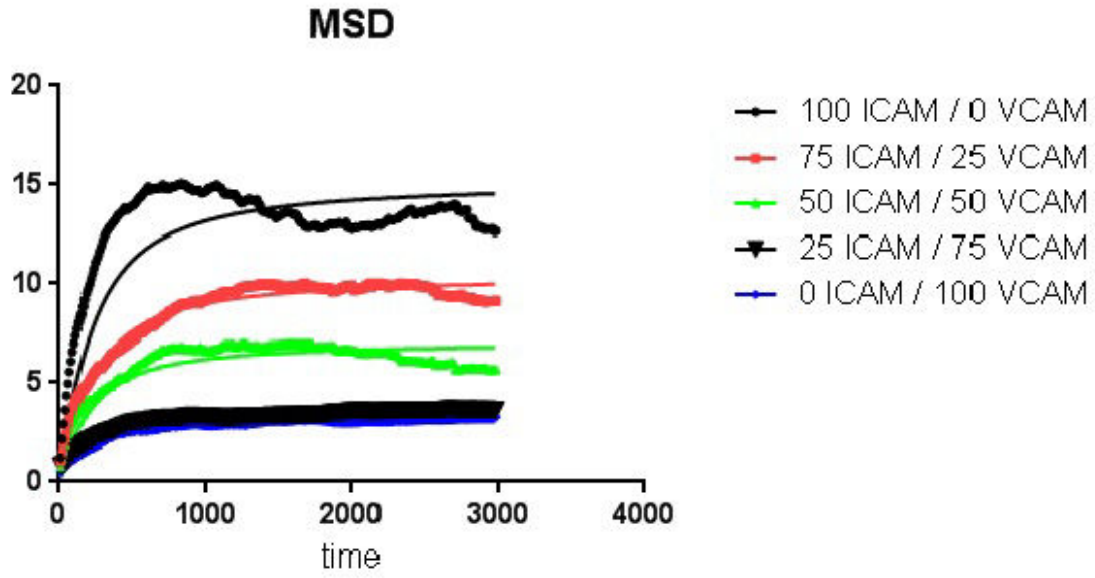

Figure 4.11: Diffusion data for 4 different ICAM / VCAM compositions including their fits. Data from 150416.

150416	D	P	v
100/0	3.8	135.5	14.23
75/25	2.6	139.5	11.62
50/50	1.78	127.1	10.03
25/75	0.87	52.53	10.95
0/100	0.77	66.29	9.139

Figure 4.12: Fitted values for D and P from the experiments shown in figure 4.11

Opposed to the diffusion data on pure ICAM-1 substrates, there is a clear, even nearly linear visible relation between relative amount of ICAM-1 in the mix and diffusion coefficient D. Looking at the exact values for D 4.12 confirms this first impression.

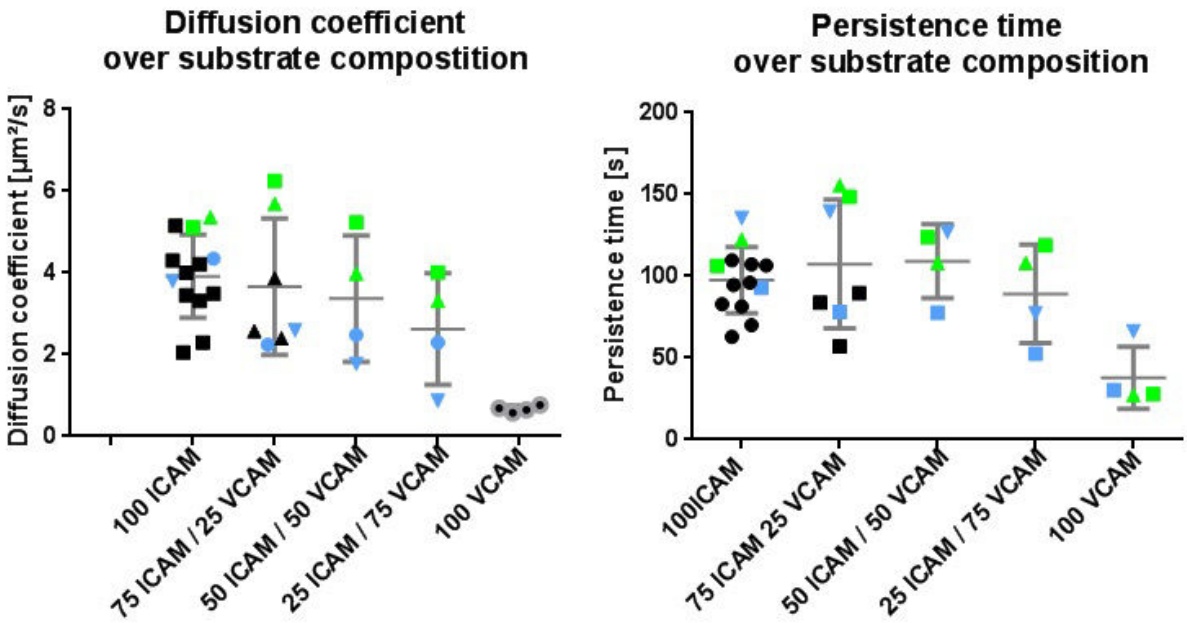

Figure 4.13: Diffusion coefficient and persistence time for cells on different substrate compositions. Each dot represents the mean of all cells of one experiment. Data points in same shape are done on the same day, same colors were acquired in the same week. There is additional data on 100 and 75 ICAM (black),because data fitting from previous experiments was also used. Numbers on x-axis represent mixing ratio of ICAM-1 and VCAM-1 in percent.

After looking at individual MSD plots comparing various data sets yield new insight: As opposed to 3.8, there is a decrease of the diffusion coefficient D with increasing amount of VCAM-1. Whereas this decrease appears to be nearly linear as long as ICAM-1 is in the mix, the drop is measurably higher for only VCAM-1. The spread among the individual data points is again high, with two clearly distinguishable subpopulations. Both behave independently as described above resulting in the same effect for the mean. The behaviour for the persistence time is slightly different: increasing slightly as soon as VCAM-1 is added to peak at the 50/50 mix. Decreasing afterwards it reaches its low also at pure VCAM-1.

Opposed to experiments on pure ICAM-1, the yFMI on mixed substrates also resulted in a much higher standard error of measurement. Knowing that the results of the individual experiments is highly dependent on the individual condition of the cells (i.e. blood bag) it might be interesting to look for a possible connection between yFMI and diffusion coefficient.

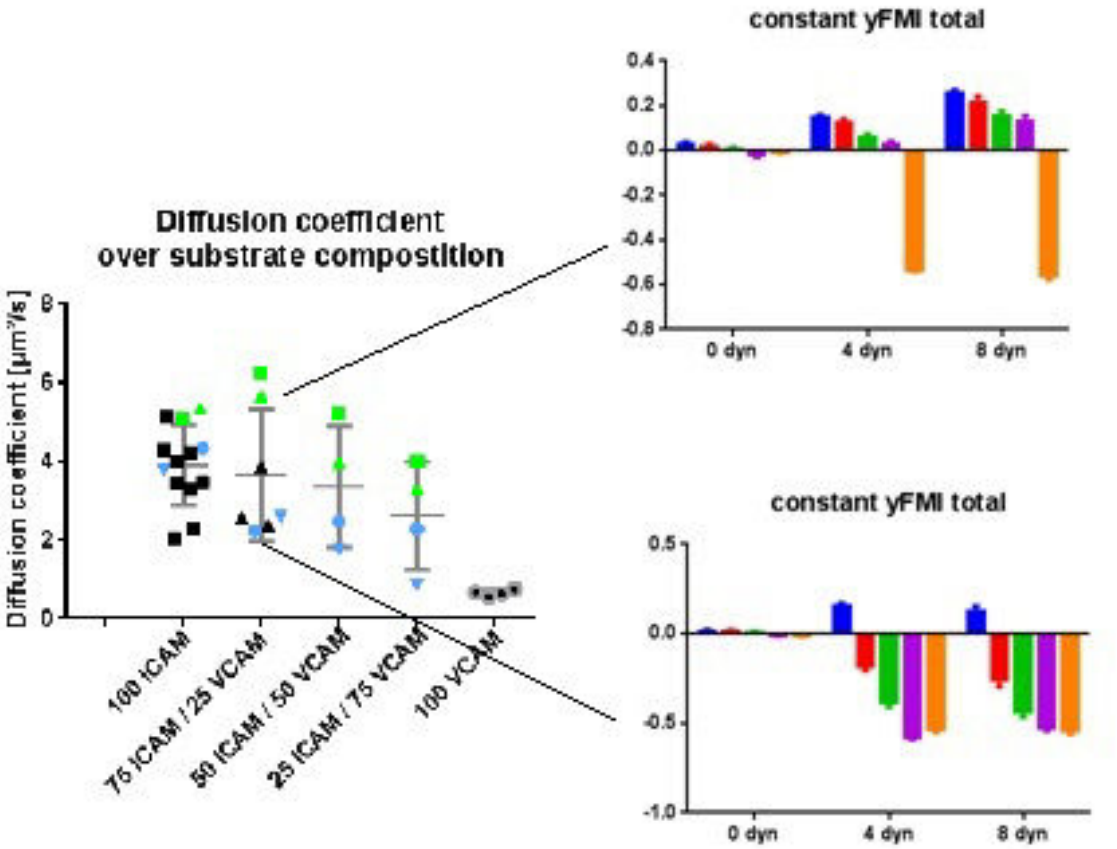

Figure 4.14: Correlation between the yFMI results of individual experiments and their diffusion coefficients. Cells which tend to go upwardsfor the majority of substrates have higher diffusion coefficients than cells who go with the flow easily.

Looking at 4.14, this connection is evident. Two representative individual results for the yFMI-measurements have been picked, although all data sets follow the same rules without any exception. The high SEM in 4.8 is the result of the two emerging types of cellular behaviour: One group always maintains overall migration against the flow unless ICAM-1 is completely removed from the substrate, following in strong migration with the flow. The second group only goes against the flow on pure ICAM-1 substrates but orients itself immediately with the flow upon the addition of VCAM-1.
As already mentioned before, the amount of adhesion molecules on the prepared substrate, relative and absolute, is always very consistent, therefore the only possible ex-

planation for the different behaviour of the cells lies within the integrin profile of the cells. To show this, one can use manganese to increase the affinity states of the integrins and look at the change of the diffusional parameters.

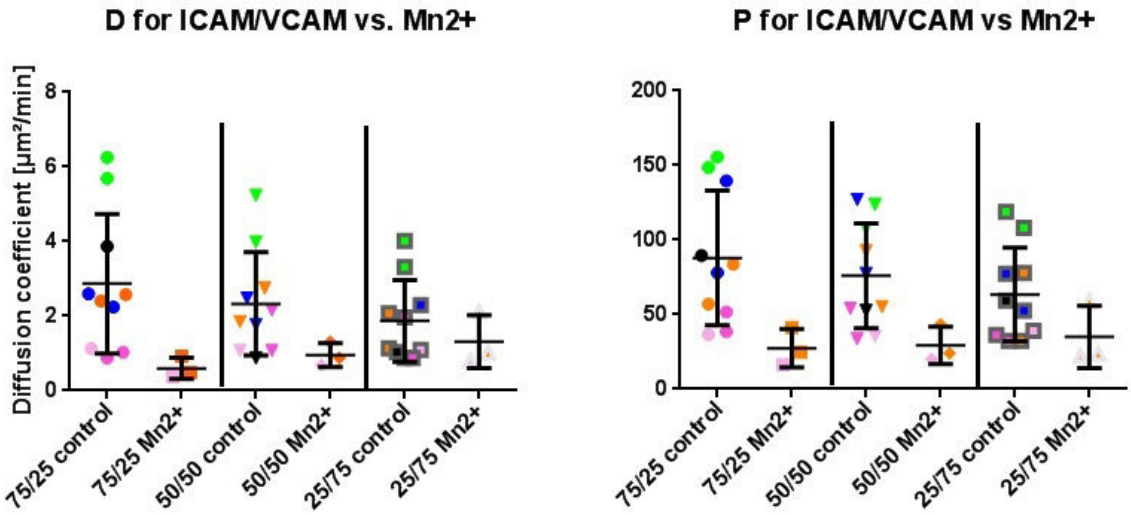

Figure 4.15: Influence of manganese on the parameters diffusion coefficient and persistence time. Each dot represents the mean of all cells of one experiment. Numbers on x-axis represent mixing ratio of ICAM-1 and VCAM-1 in percent.

In figure 4.15 we see that, upon adding Mn_{2+} the diffusion coefficient D decreases compared to control. The difference between manganese and control decreases as a function of the decrease of ICAM-1. Looking at the persistence times, the qualitative effects seem to be conserved through all substrates although the values appear to be constant for all concentraions for Mn_{2+}.

4.2 Discussion

A brief summary of the effects like for the previous chapters is difficult for the mixed ICAM-1/VCAM-1 substrates, due to the high interdependencies of shear stress, integrin state and adhesion molecules regarding the observed phenomena. Also working around these interdependencies on the cytosolic side is difficult, as talin, one of the main proteins connecting the cytoskeleton with the integrins, binds to both LFA-1 and VLA-4 and other associated proteins like vinculin, kindlin again bind and regulate talin activity (see fig 1.12.Only paxillin which binds the β4-chain of VLA-4 might have the potential for a selective modification without influencing LFA-1. Apart from the last example, any intervention on the side of aforementioned proteins would affect both LFA-1 and VLA-4.

The most striking difference is the emergence of diverse subpopulations within the cells, a phenomenon not observable on uniform substrates. Looking at the RICM images of the polarized and unpolarized specimen, one can see that the measured adhesion patches are different in size as well as in position on the plasma membrane. Knowing that integrin density and affinity state is not isotrope, and that the affinity state of LFA-1 is different along the plasma membrane (*6*), it appears plausible that different areas of adhesion can be linked to the involvement of different integrins. We observed phenotypes of cells whose uropods are attached and not erect leading to the assumption that VLA-4 in polarized cells is located rather in the rear end of the cells leading to this attachment, whereas in unpolarized cells the concentration seems to be dominant at the cell center. Even if postulating that the amount and state of VLA-4 in both phenotypes would be the same it is yet unknown what causes the emergence of the phenotypes. A dominance in either of the involved molecules could be examined with FACS leading to a possible answer to this question. Applying shear stress on the cells, the adhesion patches for the unpolarized cells are not changing between inert cells and rolling cells, which makes the choice of the movement type clearly dependent on the affinity state of VLA-4 and intracellular signalling, evidently in pure VCAM-1 substrates. Also for polarized cells under flow RICM yields another proof for an already mentioned concept. As also visible in 4.1 on the left, we see cells who are adherent at the cell front and middle, or at the cell back. The latter case proves that the uropod is attached, explaining their movement with the flow due to the alignment of the cell body around the fixed part and the resulting feedback mechanism as already described above. To confirm that the uropod is really attached on the substrate, if VCAM-1 binding is involved, confocal microscopy was used (fig 4.16).

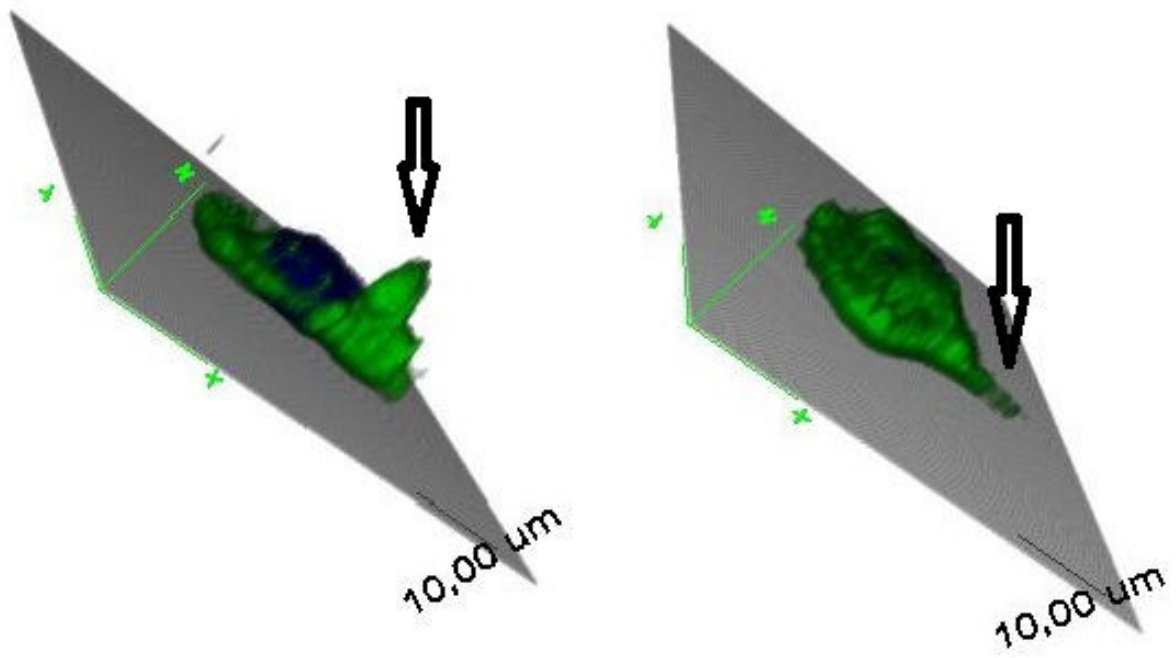

Figure 4.16: 3-D reconstituted confocal microscopy presentation of an effector T-cell with upright uropod on ICAM-1-only substrate (left, marked with arrow) and attached uropod on 25 ICAM/75 VCAM substrate (right, marked with arrow). staining: WGA-FITC, fixed under flow with 2% paraformaldehyde for 10 minutes, LSM 510 Meta UV microscope, x63 magnification, fixed stacks with 0.31 μm height. Courtesy of Thomas Sbarrato.

Looking at the yFMI data, a big dependence on the integrin state of the individual cell populations is visible, a phenomenon not addressed in other publications showing similar experiments (*68*), who always see upstream migration as soon as ICAM-1 is present on the substrate. This can be explained by the different donors whose lymphocytes appear to be variable in their composition of integrins. The data shows a gradual decrease in yFMI with a decrease of ICAM-1 and increase of VCAM-1 leading to an orientation of the cells more and more with the flow. Whereas averaging the result works well for showing the overall effect, it is striking that again the data sets can be clearly separated into two different groups:

1. cells who require complete depletion of ICAM-1 on the substrate to go with the flow

2. cells who require complete depletion of VCAM-1 on the substrate to go against the flow

This explanation becomes more clear when looking at figure 4.14 where the former case is depicted in the yFMI analysis on top, and the latter at the bottom. It can clearly

be said that one of the driving mechanisms behind the different turnover points of the same cell type to the same environment lies within the individual integrin composition caused by the different donors of the blood. Furthermore the effect for the shift in yFMI is the relative amount of cells going up or downward, not the change in the yFMI itself, whose differences seem negligible (fig 4.9). This implies that the individual cell choses to go either up or downard and then operates at a given directionality, a choice which is dependent on the composition of the substrate and whose outcome on the global level is determined by probability. The cues given after this directional choice make the cell operate at a maximum given directional motility rather than competing directional cues competing against each other and reducing effective directionality. It can clearly be said that one of the driving mechanisms behind the different reactions of the same cell type to the same environment lies within the individual integrin composition caused by the different donors of the blood.

Looking at figure 4.9 again, it can be proven that, taking polarized and non-rolling cells, upstream movement is LFA-1 dependent. This is known, but additionally the data shows that the contrary is not true: Downstream movement does not necessarily require VLA-4 dominant movement: Looking at the yFMIs of cells migrating against the flow, the value for the yFMI does not change too much except for complete absence of ICAM-1. On the other hand, the tendency for cells going with the flow is constantly decreasing without a major jump for the absence of VCAM-1. Also the relative amount of cells proves this: downstream movement happens in non-negligible fractions for pure ICAM-1 substrates under flow, which is not true for upstream movement on surfaces coated only with VCAM-1. These effects also influence the averaged data shown in figure 4.8 where the absolute value of the yFMI for 10μg/mL ICAM-1 is bigger than the absolute value of the yFMI for the same amount of VCAM-1, because the former allows downstream migration while the latter does not allow upstream movement. Nevertheless, on the right part of figure 4.5 it can be seen that ICAM-1 is necessary to trigger upstream movement, as its absence disables any migration against the flow. But ICAM-1 is not only important for the firmly adhesive forms of migration, comparing rolling speeds for mixed substrates with those on pure VCAM-1 substrates as in figure 4.6, we see a noticeable reduction of the rolling speed on the latter, indicating that VLA-4 is not alone responsible for this type of movement. This might appear counter-intuitive at first, because LFA-1 is rather associated with firmly adhesive movement than VLA-4. Although the presence of shear stress is a prerequisite to observe rolling at all, the ratio of rolling cells is hardly dependent on it. The amount of rolling cells rises linearly and makes a sudden jump under the absence of ICAM-1 (figure 4.5), again showing that the substrate alone is responsible for signaling the movement type.

Further elaborating on the influence of the substrate on intracellular signaling, the data on diffusion yields several interesting results. As seen, subpopulations do exist within cells but emerge only due to specific molecules on the substrate. To determine the reason for different cellular behaviour one could ask the question if the specific reaction of the cells is 'hardcoded' or made on the fly when the exposure to flow starts. Here also the high variance on the yFMI graphs in combination with the MSD plots might be useful, as shown in figure 4.14 where it is clearly depicted that cells, who tend to rather go against the flow unless their substrate is purely made out of VCAM-1, have a remarkably higher diffusion coefficient than their counterpart, cells who tend to go with the flow unless the substrate consists only of ICAM-1. As a matter of fact, it can be said that the migrational behaviour of the cells under flow can be predicted from their diffusion coefficient determined in the absence of flow. Another proof for the consistency of this statement is that experiments with cells from the same blood bag in different times yield teh same results, both for high and low diffusive cells. Of course this prediction only includes migrational direction, but nevertheless it establishes a set of terms we can relate to each other: 'ICAM-1 dominated behaviour', for migration against the flow, opposed to 'VCAM-1 dominated behaviour' going with the flow. This also implies that the difference in diffusion coefficients stems from either a LFA-1 or VLA-4-dominant cell migration. The final step after this would be to examine the optimal affinity states for cell diffusion. analogous to the measurements described in 3.2.2, manganese can be used as affinity switch and as expected, overall cell mobility drastically decreases upon introduction of Mn_{2+} in same concentrations as above, meaning that too high adhesion diminishes the average area covered by a diffusive cell in a given time. The difference between control and manganese-modified random movement reduces upon reduction of ICAM-1 (as seen in figure 4.15), showing that high diffusion coefficients can be attributed to LFA-1 as mentioned above. Henceforth the data shows that the diffusion coefficient D is connected to the integrin profile of the overall cell population and the decision to move with or against the flow is made before exposure to shear stress.
In the chapter 3.2 the link between speed, adhesion and diffusive behaviour has been elaborated resulting in figure 3.27 connecting adhesion with cell speeds with and without manganese. Although this connection has been tried to establish also for ICAM/VCAM subtrates, it turned out that the interdependencies of affinity state, integrin profile, drugs and substrate composition are too complex to yield any further insight and clearly link any of the beforementioned conditions to specific migrational behavior patterns.

Chapter 5

Ongoing projects and outlook

One of the key features of the approach used in this thesis, testing adhesion molecules on specific artificial substrates, has proven to have the advantage of identifying specific cellular movement patterns with corresponding adhesion molecule compositions. One of the main reasons for this approach was to avoid too many involved acting proteins which would obfuscate the specific cause and effect of particular proteins. Nevertheless, this method is a very heavy *in vitro* approach far from the dynamics and diversity of an actual cell surface in action. Therefore approaches have been made, already in the framework of this thesis, to approach a more *in vivo* model by a stepwise increase of the complexity of the substrate.
In particular, three steps have been taken towards simulating a human endothelium: Infuence of substrate rigidity on lymphocyte movement properties, functionalizing a lipid bilayer with ICAM-1 and cultivating human umbilical vein endothelial cells under flow. Obviously, the purpose of these approaches was again to seed T-cells and quantify their migrational behaviour analogous to the previous experiments described in this thesis. Except the substrate dependent measurements, which were done as a part of this thesis, and assistance in developing the lipid bilayer protocol, the work described in this subchapter has been done by Thomas Sbarrato and therefore this part is presented as outlook, summary and overview without profound introduction to the used methods.

5.1 Influence of substrate rigidity on lymphocyte movement properties

One of the recurring topics in this work is the influence of substrate dependent cues on cellular migration. Since lymphocytes are highly mobile and explore almost any area of the human body, they also encounter different types of tissues, each with different rigidities. Besides the possibility of a guidance aspect provided by tissue stiffness (brain:

0.3-0.5 kPa, collagenous bone: ca. 100 kPa, subendothelial matrix: 0.42-0.87 kPa (*74*)), there might also be an immunological aspect to rigidity since it is known that tumors have stiffer vasculature than healthy tissue surrounding them (*75*).
As already described in 2.2.2 an unsuccesful attempt to perform traction force microscopy was made. Within the timeframe and set of priorities it was not possible to develop an effective protocol that provides an effective way of linking the active components in a way that is functional for the cells to migrate.
Using commercially available PDMS substrates without incorporated fluorescent beads it is not possible to perform a force mapping over the cellular surface, although more general questions can be addressed like the influence on substrate rigidity on overall migration. The initial aim although, was to examine if the measured migrational data significantly changes dependent on substrate thickness. Comparing, for example, cell speeds on ICAM-1 substrates published in (*68*), to cell speeds in this work, the difference is striking. Interestingly, the aforementioned study uses PDMS - gel as a substrate opposed to our much more rigid IBIDI flow chambers. Using the soft substrates and the tools provided by traction force microscopy, the aim would have been to test cellular force transduction to the surface under various stiffnesses and adhesion molecule densities to possibly map out different states of affinity and adhesion.
The approach was to adapt the sample preparation as described in 2.4.1 from IBIDI flow chambers to polyacrylamide gels of various rigidity. Fluorescent protein A and ICAM-1 was used to prove the successful adsorption of each functional layer of protein on the surface and both layers could be adsorbed in sufficient density as seen with fluorescence microscopy. Nevertheless no cell adhesion was observed in any case leading to the assumption that either protein A or, more probably, ICAM-1 lose their functionality as a consequence of the linking protocols tried. Therefore, the succesful performance of traction force microscopy (which required fluorescent beads included in our custom made gels) was not possible within the frame of this thesis, whereas the same, slightly adapted, functionalization protocol worked well on the stock PDMS gels (which do not allow traction force microscopy due to lack of beads). Nevertheless experiments on the IBIDI PDMS gels were performed to determine the possible influence of different substrate rigidities on cell migration properties.
Starting with MSD/t analysis, the initial problem was the comparability of data obtained on different dates. Due to the limited timeframe and initial problems applying the developed protocol, only one data set could be obtaiend where all the rigidities were tested on the same day. Looking at this data set, the MSD/t-plot revealed abnormalities in diffusional behaviour and had to be discarded. Also looking at other incomplete data sets did not reveal a comprehensible correlation between substrate rigidity and diffu-

sion coefficient or persistence time. Looking at more specific parameters like cell speed (fig5.1) the lack of a connection between substrate and measured parameters becomes even more evident since there is neither a significant increase nor decrease in speed within the range of measured rigidities.

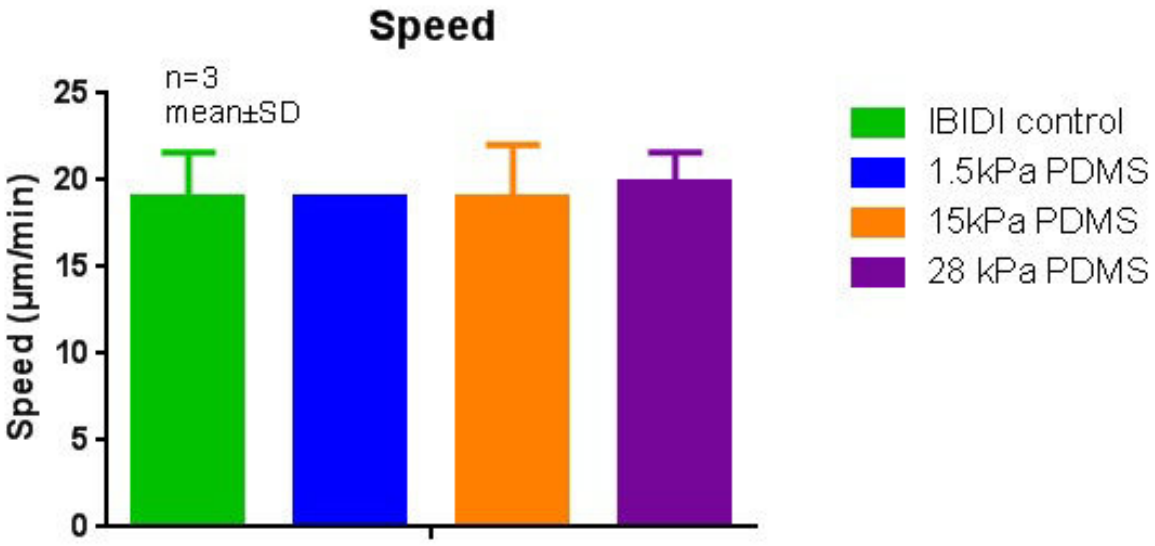

Figure 5.1: Lymphocyte speed as a function of substrate rigidity in absence of shear stress

Figure 5.1 shows that there is no influence of measured substrate rigidity on cell speed. According to the website of IBIDI (http://ibidi.com/applications/technical-aspects-of-microscopy/cell-culture-surfaces/), the Young's modulus of most plastics used in cell culture lies in the range of 1GPa, therefore also a 10^5-fold increase in substrate rigidity has no effects on cell speed.

5.2 Quantification of T-cell migration and qualitative description of the HUVEC adhesion molecule profile

In using human umbilical vein endothelial cells (HUVEC) as a substrate for T-cell migration, a very close approach to *in vivo* conditions has been taken. The advantage of this system is that in using endothelial cells, the authentic migrational properties of lymphocytes are reproduced in the best way possible under given laboratory conditions, although it has to be said that it is also nearly impossible to recognize and control all involved components regarding intercellular signaling. Therefore and important part

of this work has been to study and modify the adhesion molecule profile of the HUVEC as good as possible using mainly two tools: Alignment of the cells under flow and simulating an inflammatory response by using the cytokine (?) TNF-α. HUVEC increase expression of ICAM-1 when inflamed to increase local agglomeration of T-cells and induce extravasation. What we additionally see in 5.3 is that HUVEC also increase ICAM-1 expression under flow.

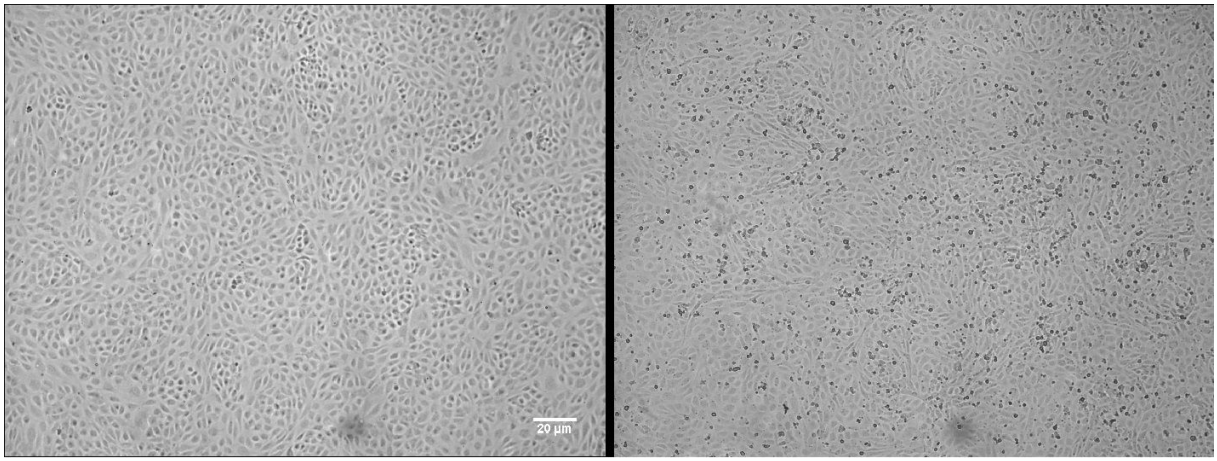

Figure 5.2: aligned human umbilical vein endothelial cell layer (on the left), non-aligned HUVEC with adhering and functionally migrating cells (on the right)

Figure 5.2 gives an overview how the substrate consistent of unaligned HUVEC looks like, with and without T-cells on top. As already mentioned, the integrin expression changes when exposing the cells to flow. The HUVEC in this chapter were generally aligned (exposed to flow in an IBIDI flow chamber analogous to the previously described experiments) for 4 days at 16 dyn/cm^2 at 37°C 5% CO2. Comparing them to non-aligned cells clearly points out the strong increase in expressed ICAM-1 (figure 5.3).

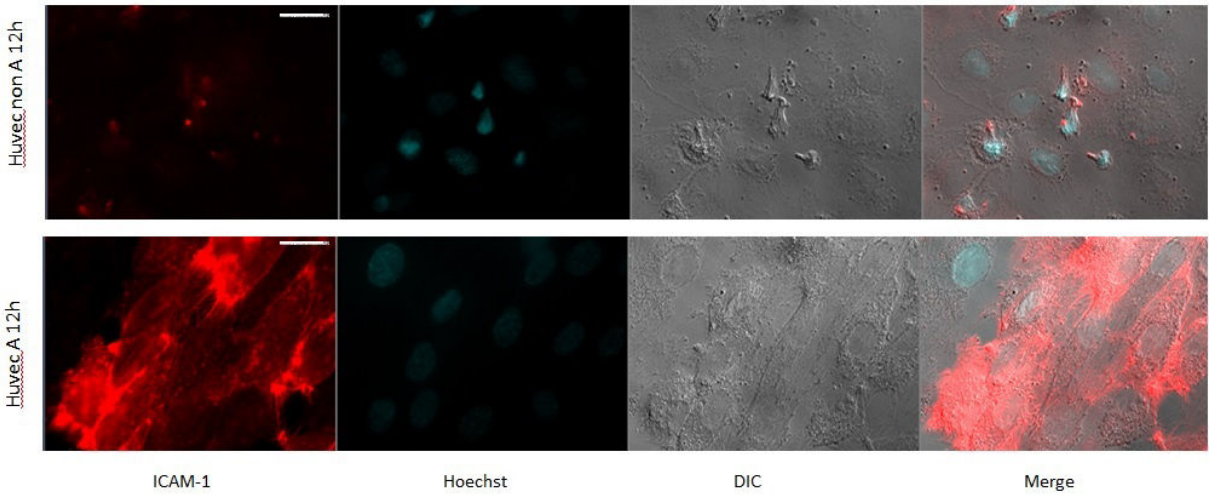

Figure 5.3: Non-aligned human umbilical vein endothelial cell layer (top) and aligned (bottom). Anti-Fc-ICAM-PE was used for the ICAM-1 staining, Hoechst for the nucleus. Scale bar = 20μm

After this qualitative characterization of ICAM-1 expression, cells are seeded as described in 2.7 and their migrational properties analysed

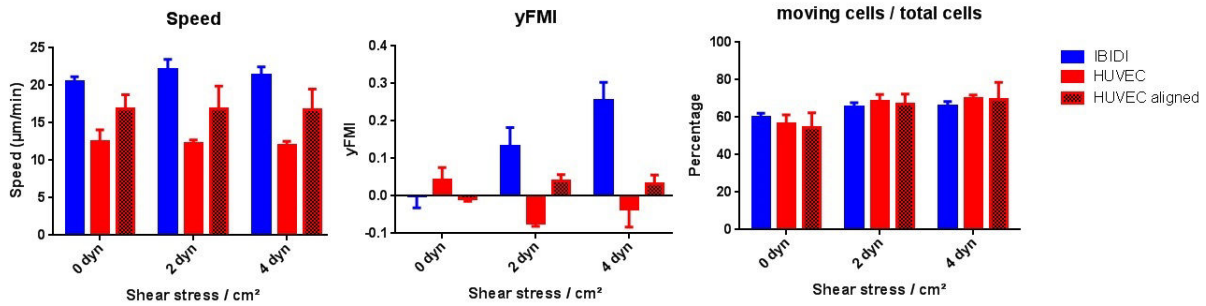

Figure 5.4: Speed, yFMI and ratio of tracked cells/total cells counted dependent on substrate (10μg/ml ICAM-1 on IBIDI on the left, unaligned HUVEC in the middle and aligned HUVED on the right) and shear stress

We see in figure 5.4 that T-cell speed is significantly lower on unaligned, and a little faster on aligned HUVEC. A change in velocity caused only by the observed increase in ICAM-1 expression seems very unprobable and would contradict all previous observations showing that adhesion and speed are independent. It has to be stated that we only measured ICAM-1 expression, not looking at the other components of the different signaling and adhesion molecule profile of the two cell lines, which might be the cause for the change. We again find consistent speeds independent of applied shear force. Also looking at the yFMI-values do not see a pronounced reaction to applied shear stress as

we do see on IBIDI, again this can be explained by different modes of migration induced by additional adhesion molecules and signaling. In context of previously described data artefacts it has nevertheless to be stated, that T-cells do not show leashed cell behaviour, meaning that their mode of migration is not perturbed by overrepresented high affinity integrins. Nevertheless we see that the ratio of migrating and functional cells is in the same range for both control and endothelial cell substrates, proving the comparability of all experiments. To resume, it can be said that T-cell migration characteristics show differences to the substrates tested in this thesis. This was expected as it was one of our key methods to test adhesion molecules in a minimal model to avoid interdependencies. Nevertheless we showed the feasability of our fluorescence quantification model and obtained comparable data regarding T-cell migration.
It has to be said that the results shown are significant, although they have to be complemented by more throrough research on the substrate composition. Whereas The IBIDI control experiment shows results comparable to the previously shown experiments in this thesis, the deviations in speed and yFMI observed on the endothelial cells require further examination to explain the results. We already proved, that on pure ICAM-1 substrates, T-cell speed is independent of adhesion molecule density. Knowing that the adhesion molecule profile of living endothelial cells consists of more than only ICAM-1 the different values for speed on (non-)aligned cells do not contradict our findings, but point out that other signaling mechanisms and adhesion molecules are involved. Nevertheless cell speed is once more independent of applied shear stress. Besides this reasons, only the mobility of the ligand could lead to a decrease in speed, a scenario, that will be covered later on.

5.3 Quantification of T-cell migration on reconstituted mobile ICAM-1 on a functional lipid bilayer

To bridge the gap between the experiments in an IBIDI flow chamber (see 3.2) and on HUVEC (see 5.2, ICAM-1 was adsorbed on a lipid bilayer (sample preparation described in 2.4.2). The advantages of this system lie within it's big approach towards *in vivo* conditions by embedding the used adhesion molecule on a surface that ressembles the endothelium much more in terms of dynamics, viscosity and composition. Nevertheless the use of only ICAM-1 as sole ligand and previous comparable experiments and data in 3.2 makes it easy to separate the specific influences of integrin-adhesion molecule interaction from the newly introduced variable of ligand mobility on cell migration. Most of all, this experimental setup should give insight in the unknown mechanisms that make the cells switch from migration against the flow (IBIDI) to their barely pro-

nounced response to flow seen in figure 5.4. Together with the observed reduction in speed between different substrates, this could be a consequence of the diffusive properties of the ligand which would provide less traction and force transduction for a binding integrin.

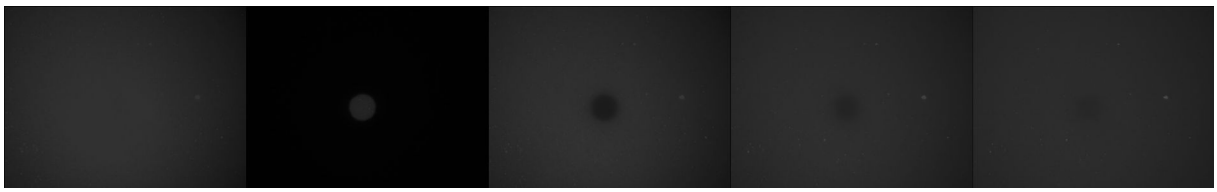

Figure 5.5: FRAP experiment on fluorescently labelled diffusing ICAM-1 on lipid bilayer.From left to right: fluorescence signal before photobleaching-closing the diaphragm and photobleaching the circular area for 10s-reflection images 0; 2 and 5 min after bleaching impulse.

To test if the mobility of the adsorbed ICAM-1 is preserved, a FRAP (fluorescence recovery after photo bleaching) experiments were made (figure 5.5): The ICAM-1 was labelled with the same fluorescent antibody used in the previous experiments and a reflection image is taken to obtain the initial overall intensity. Afterwards the diaphragm is closed and a small area of the sample is illuminated with high intensity for 10s. If the adhesion molecule is able to diffuse along the surface of the bilayer, stochastic movement should mix photobleached with non-bleached fluorophores again and the darker area should refill with non-bleached antibodies again. Measuring the overall intensity again after 0; 2 and 5 minutes, one can see that the distribution of functional, non-bleached fluorophores has equilibrated again by diffusion, which is a proof for the mobility of the layer.

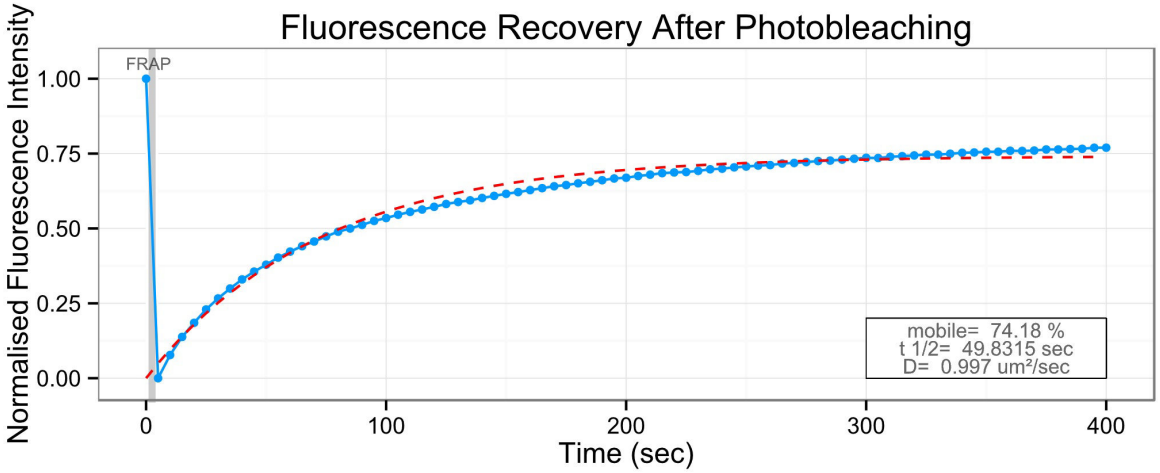

Figure 5.6: Plot of FRAP data including fit and fitted values for $t_{1/2}$, D and the percentage of mobile ligands

Obtaining the fluorescence signal of the spot recovering from photobleaching over time and plotting those values normalized by the initial intensity before bleaching results in figure 5.6. An exponential fit then delivers the time $t_{1/2}$ after which half of the initial intensity has recovered. This value then can be used to determine the diffusion coefficient D of the fluorescent ligand and therefore the lipid bilayer by measuring the radius of the bleached spot and using formula (*76*)

$$D = 0.224\frac{R^2}{t_{1/2}} \tag{5.1}$$

The obtained values are shown in figure 5.6, the additional value for the percentage of mobile ligand is determined by the maximum recovery of fluorescence for t»0.

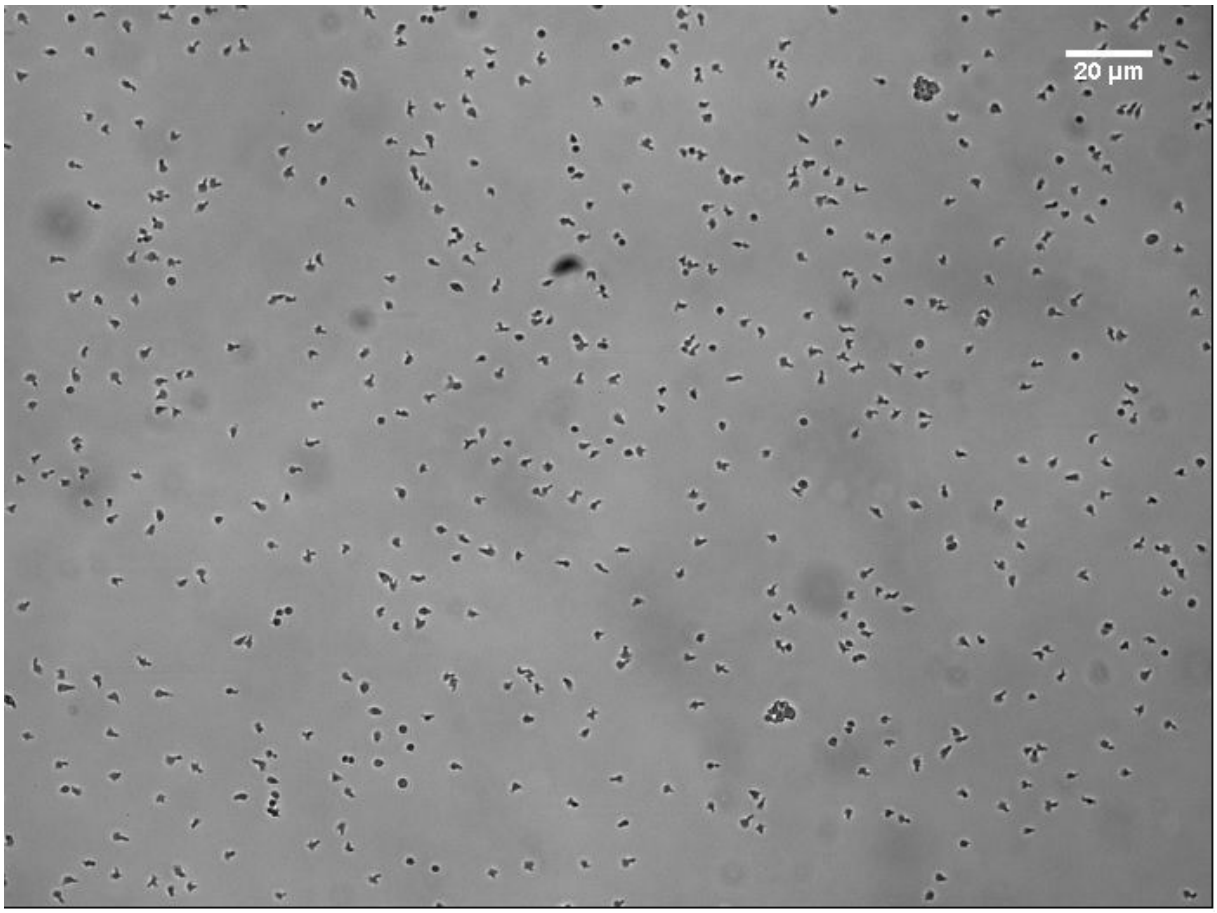

Figure 5.7: T-cells on an ICAM-1 functionalized lipid bilayer under 8 dyn/cm^2.

To test the usability of the protocol used for lipid bilayer reconstitution for cell migration experiments, it is necessary to control if the T-cells are able to adhere, polarize and migrate in usual fashion as one can see in figure5.7.It has to be pointed out that after establishing the bilayer, the same usual procedures for cell seeding and measurement as described in 2.7 and 2.8 were applied, therefore the results can be directly compared to previous flow chamber measurements:

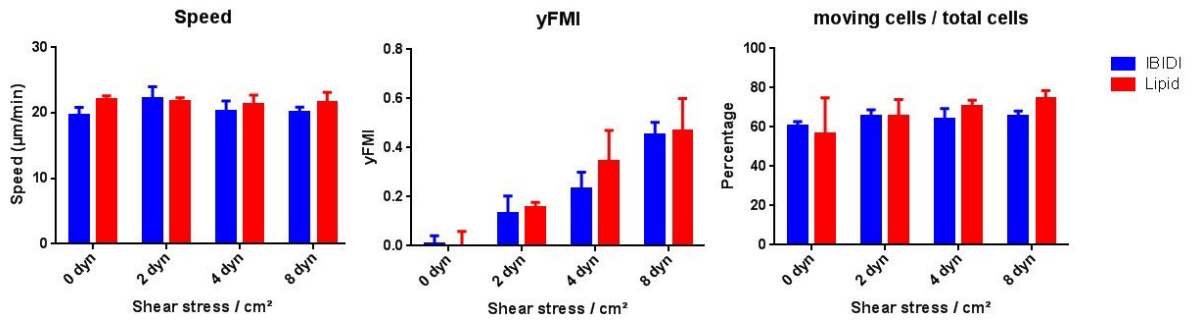

Figure 5.8: Speed, yFMI and ratio of moving cells/total cells for T-cells on ICAM-1 on control IBIDI substrates and on lipid bilayers (N=3)

In figure 5.8 we see again that speed does not change by the application of shear stress, but also that both substrates show reasonably high and similar values for speed. Already we can deduce that the mobility of ICAM-1 does not have any diminishing influence on migrational speed, a theory not so far fetched, as a mobile ligand might tremendously decrease traction on the substrate or complicate ligation. Looking at the yFMI we see the findings in (*23*) confirmed: ICAM-1 only substrates induce cellular migration against the flow. This holds true also for diffusing substrates. Although no quantification of the ICAM-1 on the bilayer has been done, it might be estimated that the concentration is beneath IBIDI control level, if one extrapolates from chapter 3.2 where an increase in yFMI came with a decrease in surface density. Although this is just one possible explanation. If one considers the theory described in 3.3 that lower density substrates help to reorient and align the cells agains the flow by providing more mobility due to less attachment points, one might argue similarily in this case: On the IBIDI flow chamber, only the receptor (LFA-1) is mobile within the plasma membrane of the lymphocyte, whereas the ligand (ICAM-1) is immobilized on the surface. On the lipid although, also the ligand is mobile helping cellular alignment even after ligation. In other words, the cell might be able to pull the bound ICAM-1 in a position favorable to flow alignlent while still maintaining enough traction to move at high speeds. Also adhesion is preserved, as can be seen in the last graph in 5.8, where the amount of moving cells is independent of shear stress and is also similar on both substrates.

Chapter 6

Conclusions

Undisputedly, cell adhesion and migration play a key role in a wide variety of biological processed on as fundamental as proliferation, differentiation, tissue organisation and immune response. For lymphocytes, both characteristics are the foundation of their mode of operation. Therefore understanding the underlying mechanisms and components of migration is a prerequisite for understanding the homing of T-cells and their role in inflammation processes in the context of the human immune system.
The factors influencing migration are in a complex interdependent relationship including mechanical and biochemical cues and act both intra- as well as extracellular, therefore a holistic approach is not sufficient to identify the contribution of single involved components within the cellular motility machinery.
Within the framework of this thesis, we picked the two most important molecules for planar T-cell migration, the integrins LFA-1 and VLA-4, and their ligands ICAM-1 and VCAM-1, and analyzed their contributions and effect on quantifyable characteristics of motility as well as their underlying mechanisms. These two integrin-ligand complexes are the main responsible factors in inducing firm adhesion, directed migration, homing and extravasation, therefore they can be linked to autoimmune diseases like vasculitis, Crohn's disease, etc.. Using flow chambers coated with surface molecules of defined concentrations and mixtures, we are able to reduce any unknown influence on cell behaviour to clearly connect specific characteristics of cell migration to the contribution of ICAM-1 and VCAM-1 in their presented ratios.
To guarantee that the adhesion molecule concentrations used on the flow chambers match the expression levels of the endothelium, a quantification protocol based on fluorescence microscopy was developed, giving a quick estimation of surface density per area as an effect of incubated concentration in volume. After successful development, used concentrations were chosen to cover the expression range between uninflamed and inflamed endothelial cells.
Important attributes of cell motility like speed, directionality and adhesion were quan-

tified in relation to changed ICAM-1 surface density under flow. This enabled to directly link a change in migrational behaviour to one modified component. After obtaining significant data, the expression level and/or affinity of the cellular integrins was altered to gain information about their influence on movement properties, leading to the orbservations that
On ICAM-1 substrates:

1. Cell speed is independent of adhesion:
   As soon as cells are able to properly utilize their motility machinery, integrin expression levels, affinity, shear stress or ligand concentrations do not influence migrational speed.

2. first experiments prove that cell speed is also independent of substrate rigidity.

3. Diffusion coefficients might be more determined by substrate rigidity than by ligand density/

4. Highly increased adhesion (by integrin expression or affinity) results in an attached uropod drastically limiting migration. This suggests activating previously inactive integrins in the uropod.

Although manipulating integrin states and therefore intracellular signalling, none of the findings described above contradicts the passive guidance mechanism relying on uropod orientation proposed in (*22*), cells with attached trailing edge still align themselves using their defunct uropod. Also the independence of speed and adhesion seems to be in contradiction to previous findings (*72*), where a an optimum adhesive point for a peak speed was found. It has to be said although, that these observations were made based on fibronectin substrates, which engage different integrins than in the system used in this thesis.
As soon as additional VCAM-1 is introduced, the complexity of measured phenomena increases.
On ICAM-1/VCAM-1 mictures:

1. subpopulations of cells emerge. These subpopulations have different phenotypes and movement behaviours.

2. rolling with the flow, inert and crawling with the flow are introduced as additional modes of migration.

3. Phenotypes as well as movement modes are dependent on substrate composition and flow.

4. The distribution of these subpopulations and their response to the ligand mixture is variable and depends on the condition and integrin profile of the cells, this might change with blood sample.

5. Diffusive behaviour allows predictions of migration mode under flow.

The characteristic advantage of the approach used in this thesis, artificial substrates with only a small amount of involved components, is also a drawback in understanding the holistic effects of adhesion and cell-substrate signalling on T-cell movement. Whereas the roles and effects of ICAM-1 and VCAM-1 could be identified more clearly, a complexification of the substrate by introducing new parameters has to be the next logical step. The used approaches, lipid bilayers with reconstituted ICAM-1, and cell motility experiments on HUVEC, are promising paths to go. Nevertheless they require further experiments to close the gap between the movement behaviour discrepancies of T-cells on the endothelium and artificial minimal substrates. Besides that, also sample preparation on flow chambers has already been improved: The current developement of protocols,methods of protein printing to generate mechanotactic gradients and gradients of chemotactic cues in surface and volume would be the next logical step based on the findings of this work to deepen the knowledge on the link between intracellular signalling, adhesion and lymphocyte migration.

Bibliography

(*1*) Kenneth M Murphy. *Janeway's immunobiology*. Garland Science, 2012.

(*2*) N. Hogg et al. "The role of the integrin LFA-1 in T-lymphocyte migration". In: *Immunol Rev* 218 (2007), pp. 135–146.

(*3*) M. Sixt and T. Lämmermann. "Mechanical modes of "amoeboid" cell migration". In: *Curr Opin Cell Biol* 21 (2009), pp. 636–644.

(*4*) M. Vicente-Manzanares, C.K. Choi, and A.R. Horwitz. "Integrins in cell migration - the actin connection". In: *J.Cell.Sci.* 122 (2009), pp. 1473–1473.

(*5*) M. (ed.) Shimaoka, W. Fu, and B.-H. Luo. "Integrin and cell adhesion molecules: Methods and protocols". In: *Methods in molecular biology* 757 (2011), pp. 81–99.

(*6*) N. Hogg et al. "A talin-dependent LFA-1 focal zone is formed by rapidly migrating T lymphocytes". In: *JCB* 170 (2005), pp. 141–151.

(*7*) A. Grakoui et al. "The immunological synapse, a molecular machine controlling T cell activation". In: *Science* 285 (1999), pp. 221–227.

(*8*) T. Springer and T. Schürpf. "Regulation of integrin affinity on cell surfaces". In: *EMBO* 30 (2011), pp. 4712–4727.

(*9*) M. Shimaoka et al. "Structures of the αL I-domain and its complex with ICAM-1 reveal a shape shifting pathway for integrin regulation". In: *Cell* 112 (2003), pp. 99–111.

(*10*) M. Shimaoka et al. "Reversibly locking a protein fold in an active conformation with a disulfide bond: Integrin αL I-domains with high affinity and antagonist activity in vivo". In: *Proc Natl Acad Sci USA* 98 (2001), pp. 6009–6014.

(*11*) Michael L Dustin et al. "Antigen receptor engagement delivers a stop signal to migrating T lymphocytes". In: *Proceedings of the National Academy of Sciences* 94.8 (1997), pp. 3909–3913.

(*12*) Motomu Shimaoka, Junichi Takagi, and Timothy A Springer. "Conformational regulation of integrin structure and function". In: *Annual review of biophysics and biomolecular structure* 31.1 (2002), pp. 485–516.

(*13*) Timothy A Springer et al. "Traffic signals for lymphocyte recirculation and leukocyte emigration: the multistep paradigm". In: *Cell* 76.2 (1994), pp. 301–314.

(*14*) Y. Takada, X. Ye, and S. Simon. "The Integrins". In: *Genome biol* 8 (2007).

(*15*) B.-H. Luo, C. Carman, and T. Springer. "Structural basis of integrin regulation and signaling". In: *Annu. Rev. Immunol.* 25 (2007), pp. 619–647.

(*16*) Feng Ye et al. "Recreation of the terminal events in physiological integrin activation". In: *The Journal of cell biology* 188.1 (2010), pp. 157–173.

(*17*) Klaus Ley et al. "Getting to the site of inflammation: the leukocyte adhesion cascade updated". In: *Nature Reviews Immunology* 7.9 (2007), pp. 678–689.

(*18*) Jianghai Zhu et al. "Structure of a complete integrin ectodomain in a physiologic resting state and activation and deactivation by applied forces". In: *Molecular cell* 32.6 (2008), pp. 849–861.

(*19*) Aidong Qu and Daniel J Leahy. "Crystal structure of the I-domain from the CD11a/CD18 (LFA-1, alpha L beta 2) integrin". In: *Proceedings of the National Academy of Sciences* 92.22 (1995), pp. 10277–10281.

(*20*) CBRF Berlin et al. "α4 integrins mediate lymphocyte attachment and rolling under physiologic flow". In: *Cell* 80.3 (1995), pp. 413–422.

(*21*) Sanford J Shattil. "Integrins and Src: dynamic duo of adhesion signaling". In: *Trends in cell biology* 15.8 (2005), pp. 399–403.

(*22*) Marie-Pierre Valignat et al. "Lymphocytes can self-steer passively with wind vane uropods". In: *Nature communications* 5 (2014).

(*23*) Marie-Pierre Valignat et al. "T lymphocytes orient against the direction of fluid flow during LFA-1-mediated migration". In: *Biophysical journal* 104.2 (2013), pp. 322–331.

(*24*) Mia Phillipson et al. "Intraluminal crawling of neutrophils to emigration sites: a molecularly distinct process from adhesion in the recruitment cascade". In: *The Journal of experimental medicine* 203.12 (2006), pp. 2569–2575.

(*25*) Guy Cinamon et al. "Chemoattractant signals and β2 integrin occupancy at apical endothelial contacts combine with shear stress signals to promote transendothelial neutrophil migration". In: *The Journal of Immunology* 173.12 (2004), pp. 7282–7291.

(*26*) Britta Engelhardt and Hartwig Wolburg. "Mini-review: Transendothelial migration of leukocytes: through the front door or around the side of the house?" In: *European journal of immunology* 34.11 (2004), pp. 2955–2963.

(*27*) Christopher V Carman and Timothy A Springer. "A transmigratory cup in leukocyte diapedesis both through individual vascular endothelial cells and between them". In: *The Journal of cell biology* 167.2 (2004), pp. 377–388.

(*28*) Oliver Steiner et al. "Differential roles for endothelial ICAM-1, ICAM-2, and VCAM-1 in shear-resistant T cell arrest, polarization, and directed crawling on blood–brain barrier endothelium". In: *The Journal of Immunology* 185.8 (2010), pp. 4846–4855.

(*29*) Ingo Bartholomäus et al. "Effector T cell interactions with meningeal vascular structures in nascent autoimmune CNS lesions". In: *Nature* 462.7269 (2009), pp. 94–98.

(*30*) Ziv Shulman et al. "Lymphocyte crawling and transendothelial migration require chemokine triggering of high-affinity LFA-1 integrin". In: *Immunity* 30.3 (2009), pp. 384–396.

(*31*) Mia Phillipson et al. "Vav1 is essential for mechanotactic crawling and migration of neutrophils out of the inflamed microvasculature". In: *The Journal of Immunology* 182.11 (2009), pp. 6870–6878.

(*32*) Laurent Golé et al. "A quorum-sensing factor in vegetative Dictyostelium Discoideum cells revealed by quantitative migration analysis". In: *PloS one* 6.11 (2011), e26901.

(*33*) Michael L Dustin and Timothy A Springer. "Lymphocyte function-associated antigen-1 (LFA-1) interaction with intercellular adhesion molecule-1 (ICAM-1) is one of at least three mechanisms for lymphocyte adhesion to cultured endothelial cells." In: *The Journal of Cell Biology* 107.1 (1988), pp. 321–331.

(*34*) Yoji Shimizu et al. "Lymphocyte interactions with endothelial cells". In: *Immunology today* 13.3 (1992), pp. 106–112.

(*35*) Loic Dupré et al. "T lymphocyte migration: an action movie starring the actin and associated actors". In: *Frontiers in immunology* 6 (2015).

(*36*) Sachiko Tsukita, Shigenobu Yonemura, and Shoichiro Tsukita. "ERM (ezrin/radixin/moesin) family: from cytoskeleton to signal transduction". In: *Current opinion in cell biology* 9.1 (1997), pp. 70–75.

(*37*) Neetha Parameswaran and Neetu Gupta. "Re-defining ERM function in lymphocyte activation and migration". In: *Immunological reviews* 256.1 (2013), pp. 63–79.

(*38*) Sean P Palecek et al. "Integrin-ligand binding properties govern cell migration speed through cell-substratum adhesiveness". In: *Nature* 385.6616 (1997), pp. 537–540.

(*39*) Miguel R Campanero et al. "ICAM-3 regulates lymphocyte morphology and integrin-mediated T cell interaction with endothelial cell and extracellular matrix ligands." In: *The Journal of cell biology* 127.3 (1994), pp. 867–878.

(*40*) Thomas P Stossel. "On the crawling of animal cells". In: *Science* 260.5111 (1993), pp. 1086–1094.

(*41*) Mark S Bretscher. "Moving membrane up to the front of migrating cells". In: *Cell* 85.4 (1996), pp. 465–467.

(*42*) TJ Mitchison and LP Cramer. "Actin-based cell motility and cell locomotion". In: *Cell* 84.3 (1996), pp. 371–379.

(*43*) Mark J Dayel and R Dyche Mullins. "Activation of Arp2/3 complex: addition of the first subunit of the new filament by a WASP protein triggers rapid ATP hydrolysis on Arp2". In: *PLoS Biol* 2.4 (2004), e91.

(*44*) Laurent Blanchoin et al. "Actin dynamics, architecture, and mechanics in cell motility". In: *Physiological reviews* 94.1 (2014), pp. 235–263.

(*45*) Guillaume T Charras et al. "Reassembly of contractile actin cortex in cell blebs". In: *The Journal of cell biology* 175.3 (2006), pp. 477–490.

(*46*) Tim Lämmermann et al. "Rapid leukocyte migration by integrin-independent flowing and squeezing". In: *Nature* 453.7191 (2008), pp. 51–55.

(*47*) Kinneret Keren et al. "Mechanism of shape determination in motile cells". In: *Nature* 453.7194 (2008), pp. 475–480.

(*48*) Douglas A Lauffenburger and Alan F Horwitz. "Cell migration: a physically integrated molecular process". In: *Cell* 84.3 (1996), pp. 359–369.

(*49*) Eugenia Manevich et al. "Talin 1 and paxillin facilitate distinct steps in rapid VLA-4-mediated adhesion strengthening to vascular cell adhesion molecule 1". In: *Journal of Biological Chemistry* 282.35 (2007), pp. 25338–25348.

(*50*) Paula Stanley et al. "Intermediate-affinity LFA-1 binds α-actinin-1 to control migration at the leading edge of the T cell". In: *The EMBO journal* 27.1 (2008), pp. 62–75.

(*51*) Zala Jevnikar, Nataša Obermajer, and Janko Kos. "LFA-1 fine-tuning by cathepsin X". In: *IUBMB life* 63.9 (2011), pp. 686–693.

(*52*) Peter Friedl et al. "CD4+ T lymphocytes migrating in three-dimensional collagen lattices lack focal adhesions and utilize β1 integrin-independent strategies for polarization, interaction with collagen fibers and locomotion". In: *European journal of immunology* 28.8 (1998), pp. 2331–2343.

(*53*) Miguel Angel Del Pozo et al. "ICAMs redistributed by chemokines to cellular uropods as a mechanism for recruitment of T lymphocytes". In: *The Journal of cell biology* 137.2 (1997), pp. 493–508.

(*54*) Stuart Ratner, Wilbert S Sherrod, and Darcy Lichlyter. "Microtubule retraction into the uropod and its role in T cell polarization and motility." In: *The Journal of Immunology* 159.3 (1997), pp. 1063–1067.

(*55*) Stephen E Malawista and Anne de Boisfleury Chevance. "Random locomotion and chemotaxis of human blood polymorphonuclear leukocytes (PMN) in the presence of EDTA: PMN in close quarters require neither leukocyte integrins nor external divalent cations". In: *Proceedings of the National Academy of Sciences* 94.21 (1997), pp. 11577–11582.

(*56*) Jordan Jacobelli et al. "Myosin-IIA and ICAM-1 regulate the interchange between two distinct modes of T cell migration". In: *The Journal of Immunology* 182.4 (2009), pp. 2041–2050.

(*57*) Zhonghua Lin et al. "In vivo antigen-driven plasmablast enrichment in combination with antigen-specific cell sorting to facilitate the isolation of rare monoclonal antibodies from human B cells." In: *Nature protocols* 9.7 (2014), pp. 1563–1577.

(*58*) Arthur D Edelstein et al. "Advanced methods of microscope control using μManager software". In: *Journal of biological methods* 1.2 (2014).

(*59*) Laurent Limozin and Kheya Sengupta. "Quantitative Reflection Interference Contrast Microscopy (RICM) in Soft Matter and Cell Adhesion". In: *ChemPhysChem* 10.16 (2009), pp. 2752–2768. ISSN: 1439-7641. DOI: 10.1002/cphc.200900601. URL: http://dx.doi.org/10.1002/cphc.200900601.

(*60*) Stacey A Maskarinec et al. "Quantifying cellular traction forces in three dimensions". In: *Proceedings of the National Academy of Sciences* 106.52 (2009), pp. 22108–22113.

(*61*) A. Einstein. "Investigations on the Theory of the Brownian Movement". In: (1956).

(*62*) David Selmeczi et al. "Cell motility as persistent random motion: theories from experiments". In: *Biophysical journal* 89.2 (2005), pp. 912–931.

(*63*) Paolo Maiuri et al. "Actin flows mediate a universal coupling between cell speed and cell persistence". In: *Cell* 161.2 (2015), pp. 374–386.

(*64*) Reinhold Fürth. "Die brownsche bewegung bei berücksichtigung einer persistenz der bewegungsrichtung. mit anwendungen auf die bewegung lebender infusorien". In: *Zeitschrift für Physik A Hadrons and Nuclei* 2.3 (1920), pp. 244–256.

(*65*) Paul Langevin. "Sur la théorie du mouvement brownien". In: *CR Acad. Sci. Paris* 146.530-533 (1908), p. 530.

(*66*) George E Uhlenbeck and Leonard S Ornstein. "On the theory of the Brownian motion". In: *Physical review* 36.5 (1930), p. 823.

(*67*) Laurent Golé et al. "A quorum-sensing factor in vegetative Dictyostelium Discoideum cells revealed by quantitative migration analysis". In: *PloS one* 6.11 (2011), e26901.

(*68*) George A Dominguez, Nicholas R Anderson, and Daniel A Hammer. "The direction of migration of T-lymphocytes under flow depends upon which adhesion receptors are engaged". In: *Integrative Biology* 7.3 (2015), pp. 345–355.

(*69*) Nathan S Astrof et al. "Importance of force linkage in mechanochemistry of adhesion receptors". In: *Biochemistry* 45.50 (2006), pp. 15020–15028.

(*70*) Andrew Smith et al. "The role of the integrin LFA-1 in T-lymphocyte migration". In: *Immunological reviews* 218.1 (2007), pp. 135–146.

(*71*) Qing Ma et al. "Activation-induced conformational changes in the I domain region of lymphocyte function-associated antigen 1". In: *Journal of Biological Chemistry* 277.12 (2002), pp. 10638–10641.

(*72*) Sean P Palecek et al. "Integrin-ligand binding properties govern cell migration speed through cell-substratum adhesiveness". In: *Nature* 385.6616 (1997), pp. 537–540.

(*73*) Alexandre Chigaev and Larry A Sklar. "Aspects of VLA-4 and LFA-1 regulation that may contribute to rolling and firm adhesion". In: *Arrest chemokines* (2015), p. 44.

(*74*) Kimberly M Stroka and Helim Aranda-Espinoza. "Endothelial cell substrate stiffness influences neutrophil transmigration via myosin light chain kinase-dependent cell contraction". In: *Blood* 118.6 (2011), pp. 1632–1640.

(*75*) V Weaver. "Tissue stiffness and breast cancer invasion." In: *Paper at the Biophysical Society Annual Meeting, Baltimore, MD*. 2011.

(*76*) Daniel Axelrod et al. "Mobility measurement by analysis of fluorescence photobleaching recovery kinetics." In: *Biophysical journal* 16.9 (1976), p. 1055.